STUDY ON FRICTION BASE ISOLATORS FOR SEISMIC CONTROL OF LOW-RISE BUILDINGS

A Thesis
in
The Centre for Building Studies

Presented in Partial Fulfilment of the Requirements
for tne Degree of Master of Applied Science at
Concordia University
Montreal, Quebec, Canada

September 1993

ISBN 0-315-90913-7

Canada

Abstract

STUDY ON FRICTION BASE ISOLATORS

FOR

SEISMIC CONTROL OF LOW-RISE BUILDINGS

Rashmi Pall

This research studies and compares the performances of a friction base isolated structure with and without resilient constraints. Response to sinusoidal ground motion and to real earthquakes was studied, and the benefits of resilient constraints are demonstrated. It was observed that the performance of friction base isolators with springs varies with the type of ground motion. For sinusoidal ground motion, the response is very sensitive to the relationship between the natural frequency of the spring/mass system and the frequency of the ground motion, while for actual seismic motions the optimum values of the coefficient of friction and the spring constant vary with the type of earthquake, thus it is important to carry out analyses for site specific ground motion.

Results are reported for friction base isolators, with different combinations of slip surfaces and springs, tested on a shake table.

ACKNOWLEDGEMENTS

The author would like to thank Professor Cedric Marsh for his valuable advice, guidance and supervision which helped immensely in this report.

Additional thanks are due to Mr. Joseph Zilka, Mr. Hans Obermeir, and Mr. Danny Roy, lab technicians, for their time.

This research would not have been possible without the encouragement and guidance from my parents. Additional thanks are due to my brother for the emotional support provided.

The financial support provided by the National Sciences and Engineering Research Council of Canada is much appreciated.

TABLE OF CONTENTS

Page

LIST OF FIGURES

LIST OF TABLES

LIST OF SYMBOLS

A	Windward area of building
A_5	Cross-sectional area of truss element #5
d	Breadth of Building
Δ	Deflection
E_s	Modulus of Elasticity
η	$\mu g/\ddot{x}_{gm}$
F	Friction force
f	Frequency of ground excitation
F_s	Spring force
f_s	Spring natural frequency
g	Gravity acceleration
k_s	Spring stiffness
k_{TOT}	Total spring stiffness
L_s	Length of spring
M	Mass
μ	Coefficient of friction
μ_{cr}	Critical coefficient of friction
μ_d	Dynamic coefficient of friction
μ_s	Static coefficient of friction
ω	Angular frequency of ground motion
ω_s	Spring angular frequency
p	External pressure
P_s	Slip force
q	Wind pressure

ρ	Density
T	Period of ground motion
t	Time
t_A	Time at which initial motion begins
t_B	Time at which motion ends in that direction
t_f	Time at which sliding ends
t_i	Time step interval
t_o	Initial time of sliding
W	Weight
W_c	Clamping force
x_b	Absolute block displacement
$\dot{x}_b$	Absolute block velocity
$\ddot{x}_b$	Absolute block acceleration
x_{br}	Relative block displacement
$\dot{x}_{br}$	Relative block velocity
$\ddot{x}_{br}$	Relative block acceleration
x_g	Ground displacement
$\dot{x}_g$	Ground velocity
$\ddot{x}_g$	Ground acceleration
$\ddot{x}_{gm}$	Maximum ground acceleration

1. INTRODUCTION

1.1 Background Information

The objective of the current National Building Code of Canada (1990) is to "... provide an acceptable level of public safety, which is achieved by designing to prevent major failure and loss of life. Structures designed in conformance with these provisions should be able to resist moderate earthquakes without significant damage and major earthquakes without collapse."[1] While the code's minimum design provisions were adequate in the past for most buildings, safer approaches are desirable for important buildings, especially those of post-disaster importance. In modern buildings, avoidance of structural collapse alone is not enough as the protection of contents, sensitive instrumentation and records becomes an important consideration.[2]

Learning from the lessons of the Mexico City earthquake, the State of California passed an Assembly Resolution (Appendix A)[3] that all new public owned buildings, such as hospitals, must incorporate the latest aseismic technology, and that existing buildings must be retrofitted to increase their earthquake resistance.

A problem in the earthquake-resistant design of buildings is that their fundamental frequency of vibration may be in the

range where earthquake energy is strongest.[4] This means that the building acts as an amplifier of the ground vibrations and the accelerations experienced increase at each floor level. The degree of amplification can be reduced by introducing damping devices or by making the building rigid. By these means the building's excitation can be limited to that of the ground motion. However, in case of severe seismic activity, this can be sufficient to damage the building's contents.[5] The only way to reduce the accelerations in the building to below the level of ground accelerations, is to disengage the base of the building. In low-rise and medium-rise buildings, the necessary disengagement can be achieved by using base isolators.[6]

The application of the new earthquake-resistant technology of base isolators is now recognized by Canada's National Building Code (1990).[1]

1.2 Base Isolation - Methods Available

Several types of base isolation technique have emerged over the years:

- Rubber base isolators, and high damping rubber isolators: These isolators are made by laminating sheets of natural rubber between thin steel plates (Fig. 1-1a, page 11)[7].

- Lead-rubber bearings:

  This system also uses layers of laminated natural rubber and steel plates, but there is a cylindrical plug of lead in a central hole through the isolator (Fig. 1-1b, page 11)[7].

- Sliding systems with laminated neoprene / steel bearings:

  This isolation system consists of laminated neoprene/steel pads with lead bronze-stainless steel slip plates on top of each bearing (Fig. 1-1c, page 11)[8].

- Resilient friction base isolators:

  This system is composed of layers of teflon sliding rings with a central rubber core. A very flexible rubber cover protects the sliding rings from corrosion and dust (Fig. 1-1d, page 12)[9].

- Sliding resilient-friction base isolators:

  These isolators have two sliding surfaces: the lower surface, ringed with laminated neoprene/steel pads, slides at low levels of seismic excitation, and the upper surface slides at high levels of ground acceleration (Fig. 1-1e, page 12)[10].

- Friction pendulum system:

  This system uses an articulated teflon coated slider resting on a concave spherical hard chrome surface (Fig. 1-1f, page 12)[11].

- Simple friction base isolators:

  These are made of two surfaces, with controlled friction, which slide one over the other (Fig. 1-1g,page 13)[12].

Some of the base isolation systems have been widely used. Table 1-1 lists the systems implemented in buildings in various countries.

Table 1-1 Isolation Systems Implemented[3,12,13,14]

COUNTRY	NO. OF BUILDINGS CONSTRUCTED	ISOLATION SYSTEMS IMPLEMENTED
Japan	67	Low damping rubber base isolators, lead-rubber bearings, high-damping rubber isolators, sliding systems with laminated neoprene / steel bearings.
New Zealand	4	Lead-rubber bearings.
Italy	5 - 10	High-damping rubber isolators.
China	?	Thin layer of specially screened sand on sliding surface.
United States	19	Friction pendulum system, lead-rubber bearings, high-damping rubber isolators, elastomeric isolation bearings.
Canada	1	Friction base isolation.

The performance criteria by which various base isolation systems can be compared are:

a) Ability to support structural dead and live loads at the maximum design displacements.
b) Resistance to wind, temperature and operation loads.
c) Resistance to creep and aging.
d) Ability to isolate a wide spectrum of ground motions.
e) Avoidance of resonance by shifting the natural frequency of the structure away from that of the ground motion for a given region.
f) Energy dissipation capability.
g) Effective performance for earthquakes, foreshocks and aftershocks without needing maintenance, repair or replacement.
h) Relative displacements to be accommodated by ordinary connections for services.
i) Capability to reduce floor accelerations to avoid damage to the contents of the building.
j) Cost effectiveness for implementation.

The relative displacement of rubber pad, lead-rubber bearing, resilient friction base and sliding resilient-friction base isolation systems can be as high as 300 mm.[3,9] This calls for special connections for services which are

expensive. Rubber base isolation systems also have a natural period of vibration of 2 to 3 sec,[3] therefore they are not suitable for use where the frequency of ground excitation is close to the natural frequency of the system.[10] In case of earthquakes similar to 1985 Mexico City Earthquake or 1977 Romania Earthquake, buildings with rubber base isolators would resonate. Moreover, rubber and neoprene undergo stiffness degradation over time and therefore need replacement over the life of the building.[16]

In lead-rubber bearings, the lead plug produces an increase in damping and increases resistance to wind loading. However, there have been problems with the lead working into the rubber and with the lead plugs fracturing thereby reducing the system's effectiveness.[3]

It is claimed that the building with a friction pendulum system nearly returns to its original alignment after the earthquake.[9] However, as the coefficient of friction is very low, the structure may need restraint to resist motion during wind, and displacements during a major earthquake are high.

Some base isolated buildings recently finished in the United States are given in Appendix B.

Simple sliding friction base isolators provide the cheapest solution, but may require constraints to avoid progressive displacements. This report studies the friction base isolation system with and without resilient constraints.

1.3 Friction Base Isolators

Friction base isolators are located horizontally between the foundation and the superstructure of a building to act as a "fuse" and thereby isolate the superstructure from extreme ground motions. Ideally, a frictionless base isolation would allow the foundation to move without exerting any force on the building; the displacement of the ground relative to the superstructure would then be the amplitude of the ground motion, which may be excessive. However, a friction force is required, large enough to resist wind and minor earthquakes but small enough that during a major earthquake slipping occurs. The magnitude of the lateral force that the building experiences is limited to the slip load, which will be chosen such that, for the specified earthquake, the displacement relative to the ground does not exceed an acceptable value.[12] A higher slip load results in lower relative displacements, but higher accelerations.

The relative displacement will lie between zero and the amplitude of the ground motion, unless combined vertical and

horizontal ground motions create a biased action causing a progressive displacement of the structure. Furthermore, if the foundations are slightly sloping due to construction tolerances or subsequent differential settlement, the building may progressively displace under sliding conditions. Additional means to constrain the building are therefore required to avoid the possibility of large displacements.

These means may be provided by ramped or spherical supporting surfaces, resilient restraints, rubber or spring "bumpers",[12] some of which are discussed in Section 1.2.

1.4 Object of Research

In general, it is desirable to minimize both the acceleration transmitted to the superstructure and the displacements of the superstructure relative to the ground. These requirements are contradictory and each can only be achieved at the expense of the other. The object of this research is to establish the optimum design parameters, and to compare the performances of structures supported on flat friction base isolators with and without resilient restraints.

1.5 Scope of Research

a) To establish the most suitable coefficient of friction for friction base isolators without resilient restraints.

b) To establish the relationship between the coefficient of friction and the spring constant for friction base isolators with resilient restraints for optimum response.

c) To compare the results of the analytical studies with the results of the experimental study.

d) To compare the performance of the two systems.

1.6 Thesis Organization

Chapter 2. Literature Review - Friction and Resilience.

The basic concepts of friction and resilience, and the theory of the expected response of friction base isolators with and without resilient restraints are presented.

Chapter 3. Analytical Studies

Computer analyses are reported for a friction base isolated model subjected to simulated ground motion representing sinusoidal ground excitation and actual earthquakes, with and without resilient constraints.

Chapter 4. Experimental Studies

The experimental work is described and the results obtained are compared with the analytical values for sinusoidal ground motion.

Chapter 5. Conclusions

The conclusions made from this study are discussed, and recommendations for future studies on this topic are suggested.

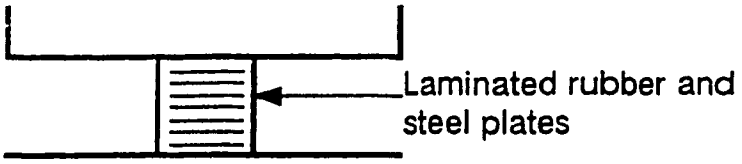

Figure 1-1a Rubber Base Isolator,
High Damping Rubber Isolator

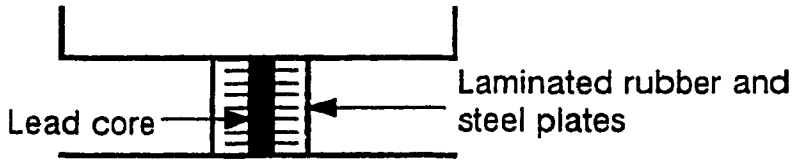

Figure 1-1b Lead-Rubber Bearing

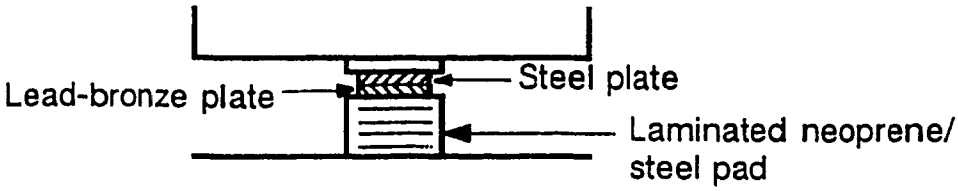

Figure 1-1c Sliding System with Laminated Neoprene/
Steel Bearing

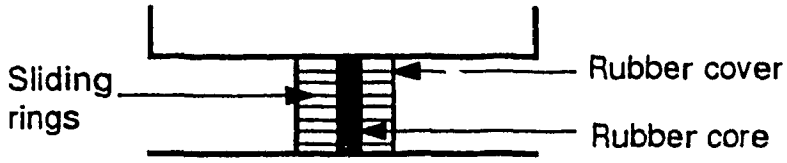

Figure 1-1d Resilient Friction Base Isolator

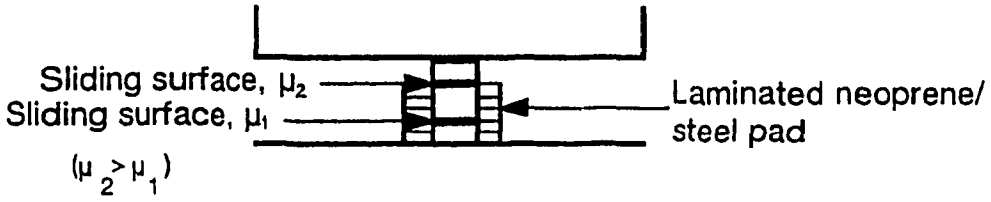

Figure 1-1e Sliding Resilient-Friction Base Isolator

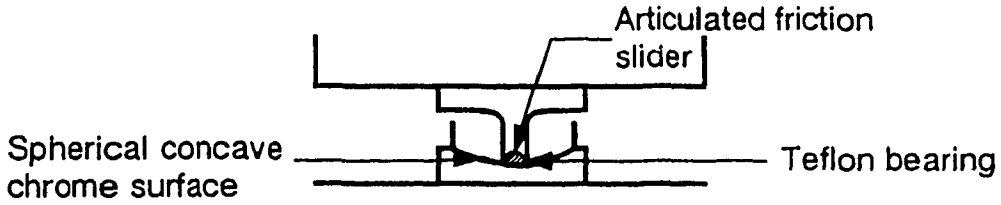

Figure 1-1f Friction Pendulum System

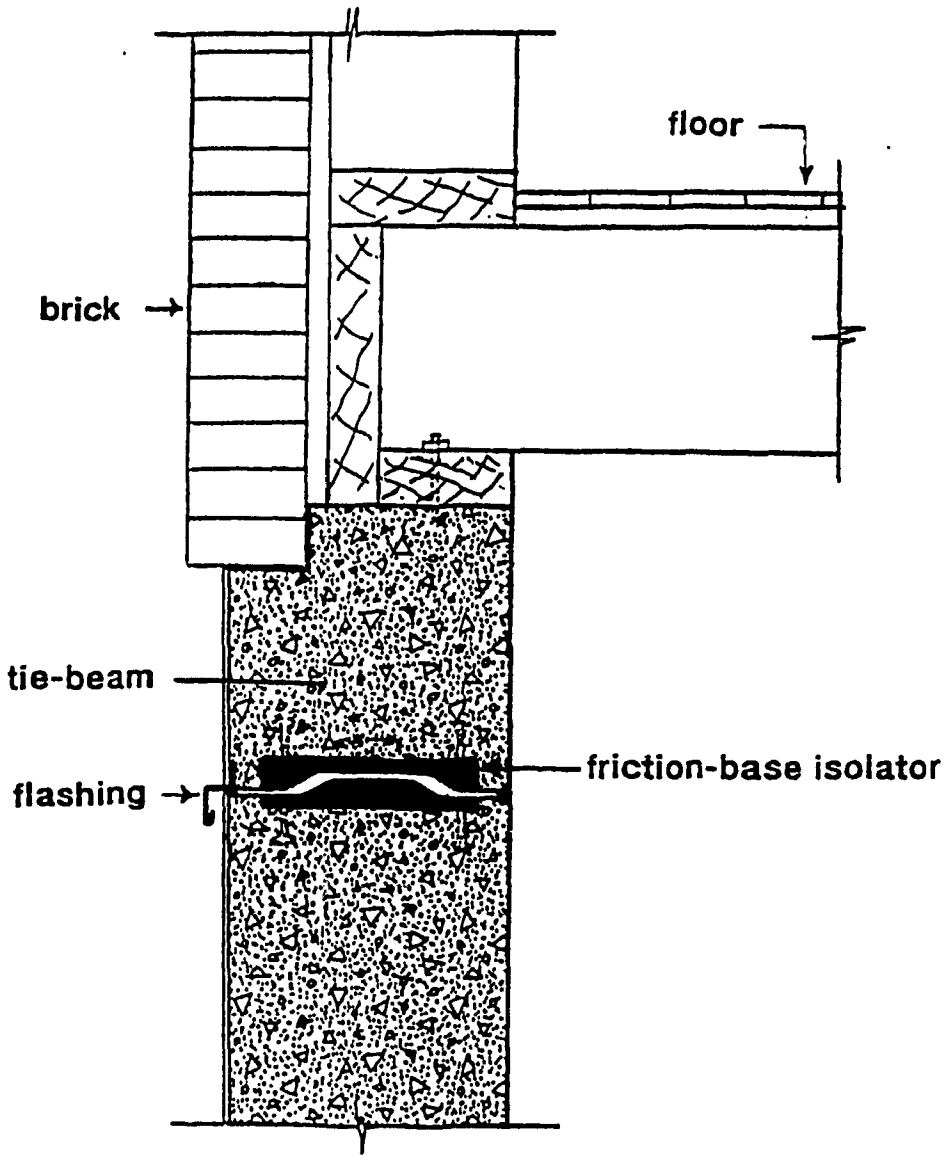

Figure 1-1g. Friction Base Isolator - Section Through Foundation Wall

2. LITERATURE REVIEW - FRICTION AND RESILIENCE

2.1 Friction

2.1.1 Coefficient of Friction

The coefficient of friction, μ, of unlubricated solids depends upon the surface roughness, the strength of bond formed at the contact interface, and the area of true contact between the sliding surfaces which is dependent on the deformation properties of the materials and the surface topographies.[17]

Two similar metals in contact show strong adhesive bonding. When their atoms come in contact, the bond created across the interface is like that existing within the metal. Two dissimilar metals in contact show weak adhesive bonding.[17]

The initial coefficient of friction is called the static coefficient of friction. As soon as motion begins, the value of μ drops. This reduced value is called the dynamic coefficient of friction. During seismic activity, the dynamic coefficient governs.

The coefficient of friction is approximately independent of velocity, thus the value exhibits little sensitivity to variations in frequency content. However, low coefficients of

friction are affected by the frequency of motion.[17]

In friction base isolators, it is desirable that:

- the opposing contact surfaces be of dissimilar materials to avoid bonding;
- the coefficient of friction be reliable and stable over time and over repeated cycles of reversals;
- the static coefficient of friction be somewhat higher than the dynamic coefficient of friction.

2.1.2 Influence of Coefficient of Friction on Motion

If the superstructure of an isolated building is taken to be a rigid body of mass M, friction base isolators will start slipping when:

$$|M\ddot{x}_b| = \mu Mg \tag{2.1}$$

Thus, during sliding the acceleration of the building is:

$$\ddot{x}_b = \pm\mu g \tag{2.2}$$

and, as the acceleration is uniform, the velocity is:

$$\dot{x}_{b(t)} = \pm\mu g(t-t_o) + \dot{x}_{b(t_o)} \tag{2.3}$$

where x_b = displacement

$\dot{x}_b$ = velocity

$\dot{x}_{b(t)}$ = velocity at time t of the building

t = time

t_o = initial time (start of slipping)

Slippage is related to ground acceleration and is independent of the frequency of the ground excitation.

For sinusoidal ground motion:

$$\ddot{x}_g = \ddot{x}_{gm} \sin(2\pi f t) \tag{2.4}$$

where $\ddot{x}_g$ = ground acceleration

$\ddot{x}_{gm}$ = maximum periodic acceleration

f = ground excitation frequency

The condition for slippage to occur is given by $\eta < 1$.

where:

$$\eta = \frac{\mu g}{\ddot{x}_{gm}} \tag{2.5}$$

After slippage has begun, the reversal of the ground acceleration brings the velocities of the ground and the building to a common value at which point an immediate reversal in the direction of slipping may or may not occur. Two conditions termed "slip-slip" and "slip-stick" are identified. Figures 2-1a and 2-1b (pages 24 and 25) illustrate these patterns of behaviour.[19]

The time, t_o, at which sliding commences is found using equations 2.2 and 2.4 where $\ddot{x}_g$ is equal to μg:

$$\pm \mu g = \ddot{x}_{gm} \sin(2\pi f t_o)$$

$$\therefore \qquad t_o = \frac{1}{2\pi f}[\sin^{-1}(\pm\eta) \pm 2n\pi] \quad , \quad n=0,1,2,3,... \tag{2.6}$$

The time, t_f, at which sliding ends is when the ground and structure again have the same velocity. This is found using equations 2.3, and the integration of 2.4 over the interval $(t_f - t_o)$:

$$\pm\mu g(t_f - t_o) = \frac{\ddot{x}_{gm}}{2\pi f}(\cos(2\pi f t_o) - \cos(2\pi f t_f))$$

$$\therefore \qquad \mp\eta\omega(t_f - t_o) = \cos(\omega t_o) - \cos(\omega t_f) \tag{2.7}$$

where $\omega = 2\pi f$ = angular frequency of the ground motion

At this point in the motion, whether the structure moves with the ground or slides in the opposite direction relative to the ground, depends on the value of η. Sliding will continue if the acceleration at time t_f exceeds μg. For the steady state slip-slip behaviour:

$$t_f - t_o = \frac{1}{2f} \tag{2.8}$$

Using equations 2.6, 2.7 and 2.8, slip-slip behaviour, i.e. sliding is continuous, can be shown to occur when:[19]

$$\eta < 0.537 \tag{2.9}$$

and slip-stick behaviour, i.e. superstructure and ground move together without sliding for a measurable time, occurs when:

$$0.537 < \eta \tag{2.10}$$

From equations 2.5 and 2.9, the critical coefficient of friction, μ_{cr}, is then:

$$\mu_{cr} = 0.537 \frac{\ddot{x}_{gm}}{g} \tag{2.11}$$

Assuming that the static coefficient is equal to the dynamic coefficient of friction then for any μ less than or equal to μ_{cr}, "sticking" can occur only at the beginning of the motion.[19] (Should the static value exceed the dynamic value of μ, then, once sliding is initiated, the probability of it continuing is increased.) During sliding, the slope of the lines representing the absolute velocity of the superstructure is $\pm\mu_d g$.

For time-histories representing actual earthquakes, this simplistic treatment can only be used to suggest a coefficient of friction to be matched, say, to the mean ground acceleration.

2.1.3 Wind Loads

2.1.3.1 Sliding

The coefficient of friction must be high enough so that the isolator does not slide during wind storms, that is:

$$pA < W\mu \tag{2.12}$$

$$\therefore \quad \mu > \frac{p}{\rho d} \tag{2.13}$$

where p = factored wind pressure

A = windward area of building

W = ρAd

ρ = mean density of the enclosed volume

d = breadth of building in direction of the wind

Typically a wood stud / brick veneer construction weighs $\rho = 900\ N/m^3$, then for a wind pressure p = 1.3 kPa (Montreal), and a building depth of 15 m, the coefficient of friction must exceed 0.10. In the case of concrete construction, the density may be as high as $2500\ N/m^3$, for which the required minimum coefficient of friction would be 0.04 for a building 15 m in breadth.

2.1.3.2 Overturning and Base Uplift

To avoid overturning of a base isolated structure, before sliding occurs, without need for tension restraints, the overturning moment due to seismic load must not exceed the stabilizing moment due to gravity. If the superstructure is taken to be a rigid body as shown in Figure 2-2 (page 26),

then the seismic overturning moment is Wμh/2 and the restoring moment is Wd/2, thus:

$$W\mu\frac{h}{2} < W\frac{d}{2}$$

$$\therefore \mu < \frac{d}{h} \qquad (2.14)$$

For no uplift to occur, on any base isolator, the required direction of the resultant of the lateral seismic force and the vertical gravity force will depend on the distribution of the isolators in the building plan. For example, for base isolators located only at the corners of the structure, uplift will be avoided if:

$$\mu < \frac{d}{h} \qquad (2.15)$$

For rows of three base isolators, in the direction of the force, uplift will be avoided if:

$$\mu < \frac{2d}{3h} \qquad (2.16)$$

For larger numbers of base isolators in line, the relationship approaches:

$$\mu < \frac{d}{3h} \qquad (2.17)$$

2.2 Resilient Constraints

The incorporation of resilient constraints in friction base isolators may permit the use of a lower coefficient of friction to reduce accelerations without increasing the displacements. Resilient constraints also provide a restoring force and prevent progressive relative displacements.

The stiffness of the constraint to be incorporated in friction base isolators is selected such that the natural frequency of the spring/mass system is lower than the frequency of the expected ground motions, to avoid the risk of resonance.

The natural frequency, f_s, of a spring restrained mass is given by:

$$f_s = \frac{1}{2\pi}\sqrt{\frac{k_s}{M}} \tag{2.18}$$

where k_s = spring stiffness

The natural angular frequency,

$$\omega_s = 2\pi f_s$$

thus:

$$k_s = M\omega_s^2 \tag{2.19}$$

A diagram of a friction base isolated system with resilient constraints is as shown in Figure 2-3 (page 26). For sliding of the superstructure, combined forces due to the acceleration and the elastic restraint must exceed the friction force, thus the condition for sliding to occur is:

$$|M\ddot{x}_b + k_s x_{br}| > M\mu_s g$$

$$\therefore \quad |\ddot{x}_b + \omega_s^2 x_{br}| > \mu_s g \tag{2.20}$$

where x_{br} = the displacement of the body relative to the ground

During sliding, the equation of motion of the building becomes:

$$|\ddot{x}_g + \omega_s^2 x_{br} + \ddot{x}_{br}| = \mu_d g \tag{2.21}$$

For sinusoidal ground motion, the equation is:

$$\omega_s^2 x_{br} + \ddot{x}_{br} \pm \mu g = -\ddot{x}_{gm}\sin(2\pi ft) \tag{2.22}$$

An optimal value of ω_s which will give the minimum relative displacement and minimum absolute acceleration for fixed values of μ, $\ddot{x}_{gm}$ and f cannot be found using this equation of motion because the objectives are in conflict. By differentiating the above equation with respect to x_{br}, the lowest value of x_{br} occurs when $\omega_s = \infty$. Differentiating with respect to $\ddot{x}_{br}$, the lowest value of $\ddot{x}_{br}$ occurs when $\omega_s = 0$. The objective of obtaining the optimum balance between relative

displacement and acceleration cannot be achieved by this method. The practical approach is to plot x_{br} and $\ddot{x}_b$ with respect to μ and ω_s for each type of ground motion. From these curves, a best compromise between μ and ω_s can be established based on the acceptable level of x_{br} and $\ddot{x}_b$.

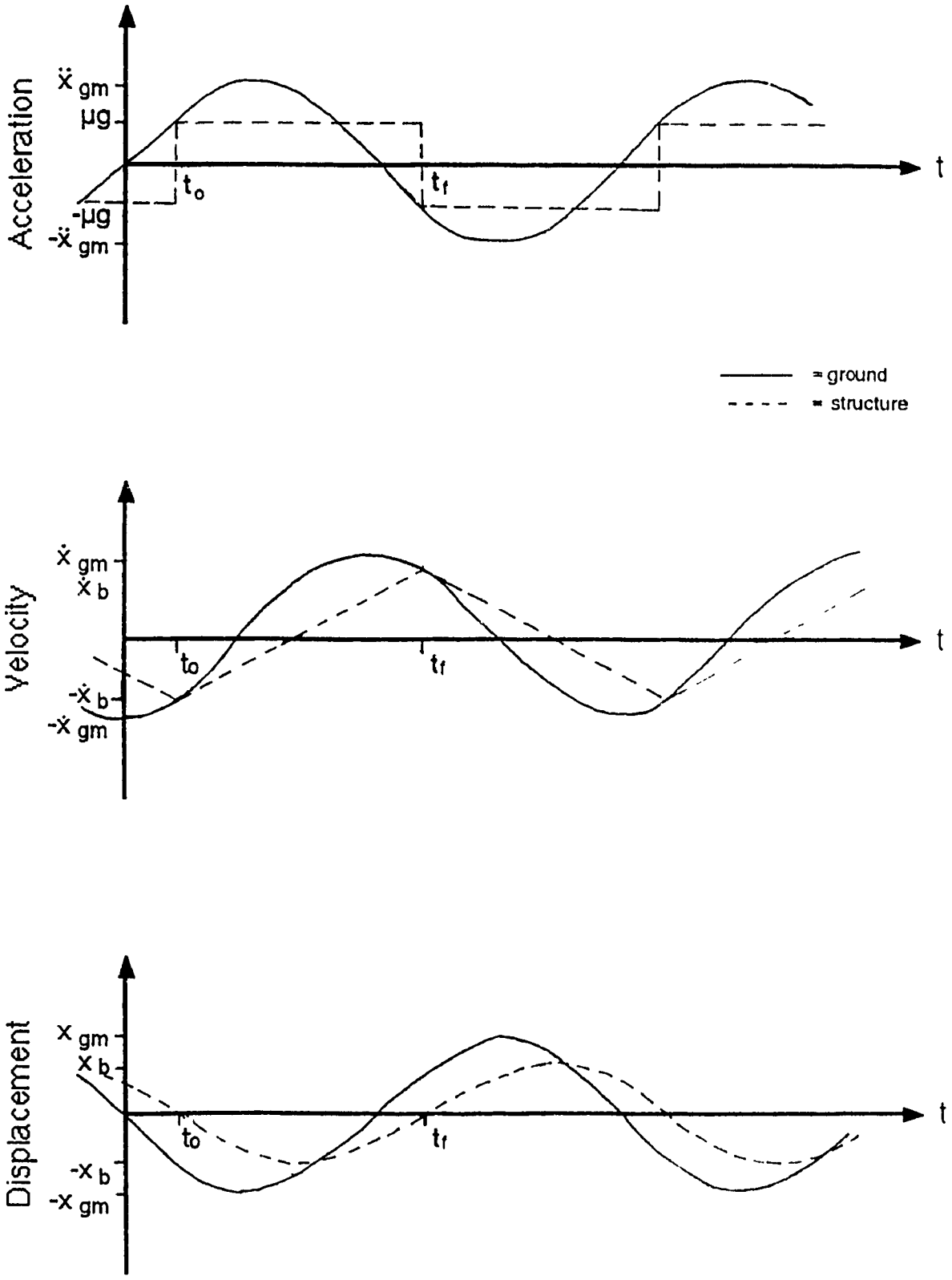

Figure 2-1a Slip-Slip Behavior

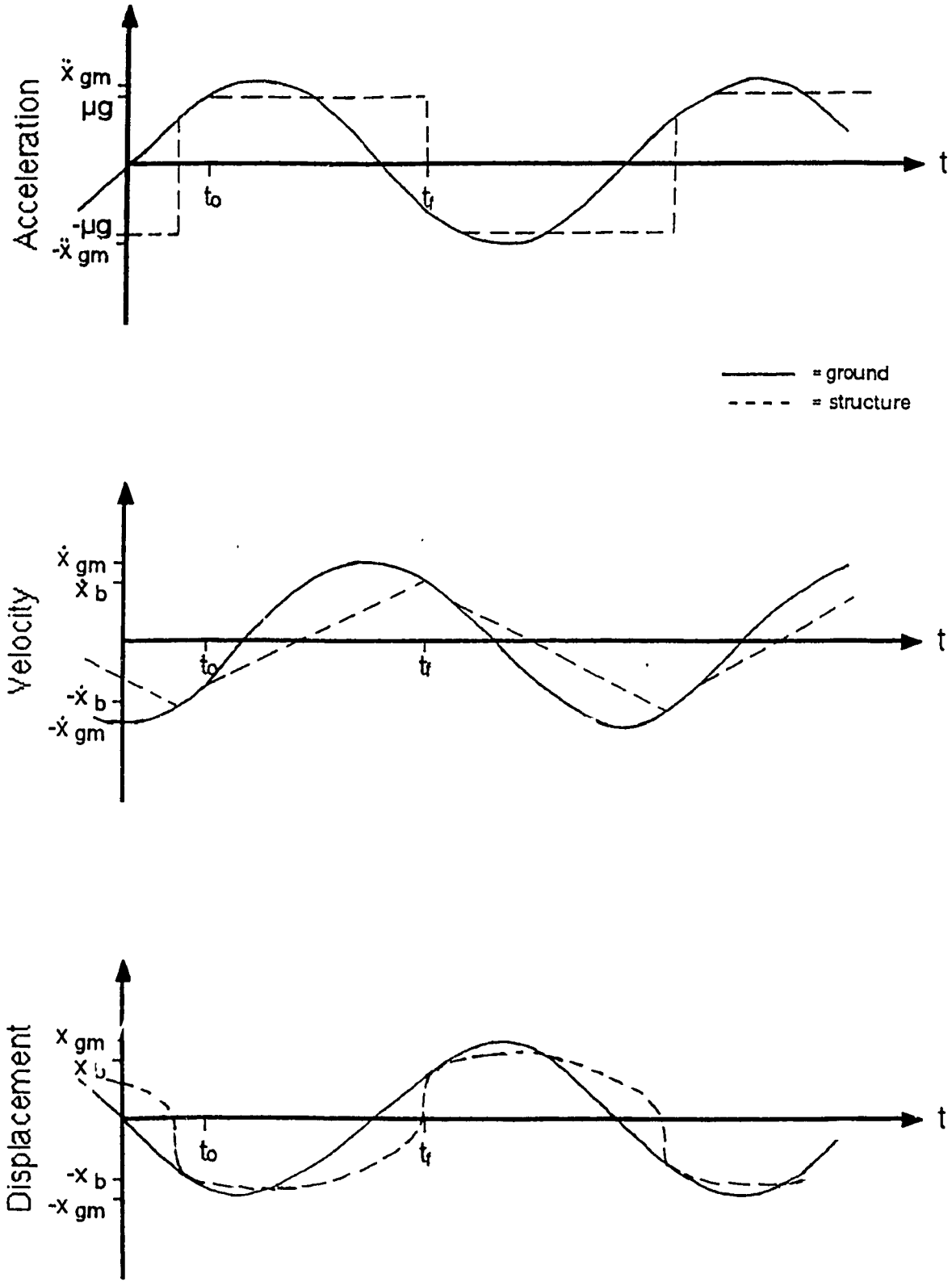

Figure 2-1b Slip-Stick Behavior

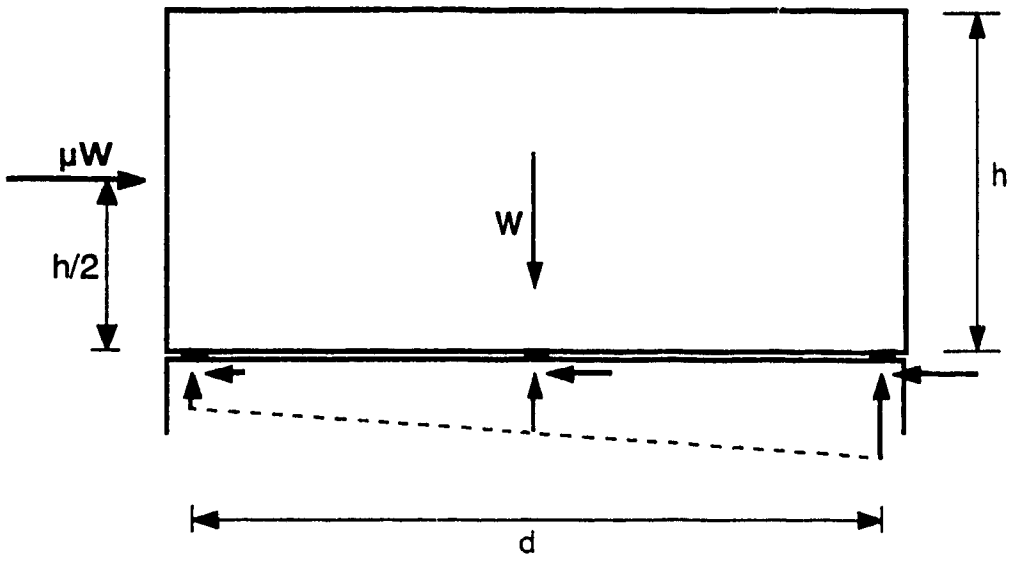

Figure 2-2 Earthquake Loads on a Low-Rise Building

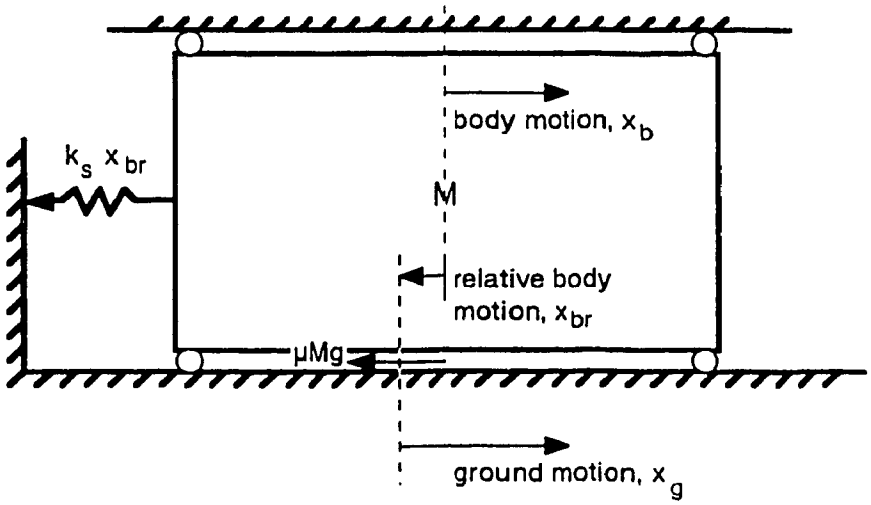

Figure 2-3 System with Friction and Springs

3. COMPUTER ANALYSIS STUDIES OF FRICTION BASE ISOLATORS

3.1 Computer Programs

To establish the influence of different variables on the response of a friction base isolated structure and to determine the best compromise between the coefficient of friction and the spring constant, parametric studies were made. The different variables were: ground motion frequency and peak intensity; coefficient of friction and natural frequency of the spring/mass system.

Assuming that the superstructure, although elastic, behaves as essentially rigid, and nonlinearity occurs only in the friction base isolators, it can be modelled as a single-degree-of-freedom (SDOF) system.

Three computer programs were used in the analyses:

(1) SINMOT

This program, shown in Appendix C, was developed to solve the equation of motion for the relative displacements and absolute accelerations of a body, on friction base isolators with resilient constraints, subjected to sinusoidal ground motion.

During sliding (Equation 2.22, Section 2.2):

$$\omega_s^2 x_{br} + \ddot{x}_{br} \pm \mu g = -\ddot{x}_{gm}\cos(2\pi ft) \tag{2.22}$$

where $\ddot{x}_{br} = \ddot{x}_b - \ddot{x}_g$

The reversal in sign occurs at a point when the ground velocity:

$$\dot{x}_{g(i)} = \frac{\ddot{x}_{gm}}{2\pi f}\sin(2\pi ft) \tag{3.1}$$

and body velocity:

$$\dot{x}_{b(i)} = \ddot{x}_{b(i)}t \tag{3.2}$$

have a common value.

During the first time step, (i.e. i=1)

$$x_{br(1)} = 0$$

and

$$\ddot{x}_{br(1)} = \mu g - \ddot{x}_{gm}$$

In the second time step,

$$x_{br(2)} = \frac{1}{2}\ddot{x}_{br(1)}\Delta t^2$$

For all consecutive time steps,

$$x_{br(i)} = 2x_{br(i-1)} - x_{br(i-2)} + \ddot{x}_{br(i-1)}\Delta t^2 \qquad i = 3,4,5,... \tag{3.3}$$

$$\ddot{x}_{br(i)} = \pm\mu g - \omega_s^2 x_{br(i)} - \ddot{x}_{gm}\cos(2\pi ft) \tag{3.4}$$

(2) DRAIN-2D

This time-history dynamic analysis program was developed at the University of California at Berkeley.[20] Analysis is by the direct stiffness method. Earthquake excitation is defined by time-histories of ground accelerations. Thus, analyses can be done for time-histories of actual earthquakes. Dynamic response is determined by a step-by-step integration with constant acceleration within each time step. The dynamic equilibrium equation at any time, neglecting viscous damping, is:

$$[M]\Delta\ddot{x}_{br} + [K_T]\Delta x_{br} = -M\Delta\ddot{x}_g \tag{3.5}$$

where [M] = mass matrix

$\{\Delta x_{br}\}$ = increment of nodal displacement relative to ground

$[K_T]$ = tangent values of stiffness matrix

$\{\Delta\ddot{x}_{gm}\}$ = increment of ground acceleration

The output from DRAIN-2D gives the forces in the members and the nodal displacements relative to ground. It does not give the absolute nodal accelerations, which are required to compare with the results obtained using SINMOT. A new program,

ACCEL, (Appendix D) was written to access DRAIN-2D's input ground accelerations and the calculated relative accelerations. To compute the absolute nodal accelerations, use was made of the following relationship after each time step interval, t_i:

$$\ddot{x}_b(t_i) = \ddot{x}_{br}(t_i) + \ddot{x}_g(t_i) \tag{3.6}$$

ACCEL also gives the peak absolute nodal accelerations.

For input to DRAIN-2D, the body is first modelled as a single mass restrained by an elasto-plastic truss element which represents the friction base isolators, and an elastic element which represents the resilient restraint. This is called the "simple" model. In the case of pure friction, the stiffness of the elastic element is a assigned zero value (Fig. 3-1, page 49). The elasto-plastic truss element possesses a high elastic stiffness, and yielding in tension and compression represents slippage. The fictitious yield stress is obtained from:

$$\sigma_y = Mg\frac{\mu}{A} \tag{3.7}$$

where A = cross-sectional area of the plastic truss element
A total mass of 2626 kg, the same as the test arrangement in the shake table studies, is used for comparison with experimental results. (No mass is required with the SINMOT program.)

(A model which could be used later to represent actual buildings was also studied. The node and element layout of the model is shown in Figure 3-2 (page 49). Although this model can include elastic response, in these studies it was modelled to behave like a rigid body, by giving elements 1, 2, 3, 4, 6 and 7 a cross-sectional area, A = 0.5 m^2 and a modulus of elasticity, E = 2 x 10^5 MPa, making AE very large. Nodes 1 and 2, and nodes 3 and 4 are constrained to have identical displacements in the horizontal direction. The total mass of the block is lumped at nodes 1 to 4. Friction base isolators are lumped and modelled as truss element # 5 which has elasto-plastic behaviour. This is called the "detailed" model.)

(3) FRICTION

This time-history dynamic analysis program was developed at Concordia University to represent a SDOF friction-damped braced frame.[21] This program can be used for the analysis of the "simple" model in Figure 3-1 of a friction base isolated body with and without resilient restraint. The program differs from DRAIN-2D in that instead of constant acceleration, linearly increasing acceleration is used within each time step.

3.2 Sinusoidal Ground Motion

Since the shake table operates only on a sinusoidal motion, analyses were conducted using this motion to compare the analytic studies with experimental results.

When a sine form acceleration is used, with initial zero acceleration, displacement of the ground increases progressively in one direction because the velocity always remains positive (Fig. 3-3, page 50). By starting with the acceleration at the maximum value, i.e. a cosine form ground acceleration (Fig. 3-4, page 50), the velocity changes sign, and gives a constant mean displacement. Thus, cosine excitation of the following form was used in this study:

$$\ddot{x}_g = \ddot{x}_{gm}\cos(2\pi ft) \tag{3.8}$$

With the cosine form for the acceleration, i.e. with the values of $\ddot{x}_{gm}$ and x = 0 at t = 0, the ground displacement is in one direction only and thus biases the motion of the body as seen in Figure 3-5 (page 51). For simplicity of study, it is better to have body displacement curves where the peak positive and negative displacements are the same. In order to obtain such a displacement curve, the initial point must be changed.

The consequence of the bias is illustrated in Figure 3-6 (page 51). If initial motion begins at time, t_A, where:

$$t_A = t_B - \frac{T}{2}$$

$$t_A = \frac{1}{\omega}\cos^{-1}\left(\frac{-\mu g}{\ddot{x}_{gm}}\right) - \frac{T}{2} \qquad (3.9)$$

then the bias is eliminated as seen in Figure 3-7 (page 52). Therefore, if time t_A is taken to be the initial time at which motion begins, the ground acceleration, $\ddot{x}_{gA}$, corresponding to t_A should be the initial ground acceleration (Fig.3-8, page52)

$$\ddot{x}_{g_A} = \ddot{x}_{gm}\cos(\omega t_A) \qquad (3.10)$$

This approach of eliminating the bias caused by the initial conditions of the cosine ground excitation is good for use in SINMOT where the ground accelerations are input in the form of an equation. However, it is tedious to input time-histories in DRAIN-2D or FRICTION starting with different values of acceleration for different combinations of μ and $\ddot{x}_{gm}$.

To permit the same input for all cases, a modified sinusoidal time-history with linearly increasing peak ground accelerations for five cycles of equal periods and then twenty cycles of constant peak ground accelerations was used to bring the block oscillations to a steady amplitude about the initial position. This approach eliminates wandering when the initial slip starts in the introductory five cycles, and the oscillations are stabilized by the time the final sinusoidal time-history commences. The time-histories for the sinusoidal

curve were represented by inputting four coordinates for every quarter cycle.

3.3 Friction Without Resilient Constraint

3.3.1 Sinusoidal Ground Motion

3.3.1.1 General Parametric Studies

In case of a pure friction base isolated body, the stiffness (and thus ω_s) of the elastic restraint is zero. Analyses were done, using SINMOT, for peak ground motion intensities 0.2g to 0.4g and frequencies 2 Hz, 5 Hz and 10 Hz. The coefficient of friction, μ, was varied from 0.0 to 0.4. The relative displacements of the body for different frequencies of excitation are shown in Figures 3-9, 3-10 and 3-11 (pages 53, 54, 55). It can be observed that for a given μ and f, the relative displacements increase as the peak ground accelerations increase. As μ increases for a given peak ground acceleration and frequency, the relative displacements decrease. At μ = 0 the maximum relative displacement is equal to the ground displacement. The relative displacement is zero for $\mu > \ddot{x}_{gm}/g$.

Figure 3-12 (page 56) shows that for a given ground excitation frequency, the body accelerations, $\ddot{x}_b$, increase linearly with μ until $\ddot{x}_b = \mu g$, as the accelerations

experienced by the body during sliding are limited to the coefficient of friction.

3.3.1.2 Slip-Slip and Slip-Stick Behaviour

As shown in Section 2.1.2, slip-slip behaviour occurs when:

$$\mu \leq 0.537 \frac{\ddot{x}_{gm}}{g} \tag{2.17}$$

For the case of $\mu = 0.25$, three conditions were studied:

- Slip-stick ($\mu_{cr} < \mu$)
- Critical ($\mu_{cr} = \mu$)
- Slip-slip ($\mu_{cr} > \mu$)

For $\ddot{x}_{gm} = 0.4g$, μ_{cr} is 0.215. As this is less than 0.25, slip-stick will occur. The curves for $\ddot{x}_b$, $\dot{x}_b$ and x_b were plotted with respect to time in Figure 3-13 (page 57). It can be seen in the figure where sticking occurs.

For $\ddot{x}_{gm} = 0.47g$, μ_{cr} is 0.25 which is the value provided. The computer results are plotted in Figure 3-14 (page 58). The response is a slip-slip motion.

For $\ddot{x}_{gm} = 0.6g$, μ_{cr} is 0.32 which is well into the slip-slip domain, as seen in Figure 3-15 (page 59).

The above results confirm that computer analysis by SINMOT reproduces the behaviour predicted by the basic theory.

3.3.1.3 Verification Using DRAIN-2D

Analyses were also made using DRAIN-2D. The responses obtained using the "simple" and the "detailed" models in DRAIN-2D are the same while the results of DRAIN-2D are within 3% of those obtained from SINMOT program for the "simple" model. (The computation time for "simple" and "detailed" model using DRAIN-2D were about 2 and 5 seconds, respectively. The computation time for SINMOT, using the "simple" model, was less than 1 second.)

Figure 3-16 (page 60) illustrates the body response with modified sinusoidal ground excitation for $\mu = 0.2$ and $\ddot{x}_{gm} = 0.4g$ (i.e. slip-slip behaviour).

3.3.2 Performance with Time-Histories of Actual Earthquakes

The use of sinusoidal ground motions makes it possible to study the influence of various parameters on the response. In reality, actual earthquakes are random excitations and it is necessary to carry out parametric studies for time-histories of actual earthquakes. Earthquake records of the same intensity but with different frequency contents will give

different relative displacements. The following three types of earthquake records were used for the ground motion:

- El Centro, California, 1940 (N-S component)
- Olympia, California, 1949
- Newmark-Blume-Kapur (N.B.K.) artificial earthquake.[22]

Time-histories of the El Centro earthquake (north-south components) are shown in Figure 3-17 (page 61). The peak ground acceleration is 0.33g, the peak ground velocity is 0.35 m/s and the peak ground displacement is 0.21 m. This is one of the severest earthquake motions for which accurate data is available. The predominant frequency (frequency at which the input energy is the greatest) of the El Centro earthquake is 2.6 Hz.

Although the Olympia earthquake record (Fig. 3-18, page 62) is not as severe as the El Centro earthquake record, the effect of the Olympia earthquake was also studied because of its special characteristics on firm soils. The predominant frequency content of this earthquake is 2.9 Hz.

Since earthquakes are erratic in nature, an artificial record generated by Newmark, Blume, Kapur, which is an average of many earthquake records, was also used. Time-history of

N.B.K. is shown in Figure 3-19 (page 62), and it has a wide range of frequency contents. It is more severe than the El Centro record.

Using the computer program, FRICTION, the earthquake records of El Centro, Olympia and N.B.K. were scaled to give peak ground accelerations, $\ddot{x}_{gm}$, of 0.2g, 0.3g, 0.4g, 0.5g and 0.6g, and the coefficient of friction, μ, was varied from 0.0 to 0.6. The integration time step was 0.01 sec.

The relative displacements of the body, x_{bt}, for different earthquake records are shown in Figures 3-20, 3-21 and 3-22 (pages 63, 64 and 65). It is observed that for any given $\ddot{x}_{gm}$ and μ, the maximum relative displacements are highest for N.B.K. and lowest for Olympia. For example, at $\ddot{x}_{gm} = 0.4g$ and $\mu = 0.1$, the relative displacements are 178, 107 and 33 mm for N.B.K., El Centro and Olympia, respectively.

It is seen that the three different earthquakes, even though of the same peak ground accelerations, result in different values of displacements due to their different frequency contents.

It is also observed that the use of the actual earthquake time-histories does not cause any wandering of the body in one direction as is the case with the unmodified sinusoidal motion.

The analyses were also carried out using the computer program DRAIN-2D. The results are within 0.5%, a difference that is attributed to the use of linear acceleration in each time step in FRICTION and constant acceleration in DRAIN-2D. (For El Centro earthquake, the computation time for analysis with FRICTION was two seconds compared to five seconds for DRAIN-2D).

3.3.3 Discussion

In pure friction base isolators, an increase in the coefficient of friction leads to a decrease in the relative displacements and an increase in absolute accelerations of the body for all types of ground motion. For a typical earthquake expected in the Montreal region, the peak ground acceleration is 0.2g. A coefficient of friction of $\mu = 0.1$ (the minimum for wind resistance of wood stud / brick veneer structures) will halve the maximum acceleration of the body. The relative displacements, while they vary with the frequency contents of the earthquakes, are significantly less than the amplitude of the ground motion. For an intensity of $\ddot{x}_{gm}$=0.2g and μ of 0.1, the maximum relative displacements are only 13%, 31% and 11% of the amplitude of the ground displacement for El Centro, Olympia and N.B.K. earthquakes, respectively (Table 3-1).

Table 3-1 Comparison of Relative Displacements for $\ddot{x}_{gm} = 0.2g$

EARTHQUAKE	$\mu = 0$	$\mu = 0.1$
El Centro x_{br}, m (% of amplitude of ground motion)	0.120 (100%)	0.016 (13.3%)
Olympia x_{br}, m (% of amplitude of ground motion)	0.026 (100%)	0.008 (30.8%)
N.B.K. x_{br}, m (% of amplitude of ground motion)	0.193 (100%)	0.021 (10.9%)

3.4 Friction with Resilient Constraint

3.4.1 Performance with Sinusoidal Ground Motion

To establish the values for μ and k which give the best compromise between x_{br} and $\ddot{x}_b$, parametric studies were conducted using sinusoidal ground motion to excite a model with friction base isolators and resilient constraints.

The values used in the study were: ground frequencies of 2 Hz, 5 Hz and 10 Hz for peak ground accelerations of 0.2g, 0.3g and 0.4g, with the coefficient of friction varying from 0.0 to 0.4 and the spring/mass natural frequency varying from 0.0 to 1.0 Hz.

Figures 3-23 to 3-31 (pages 66 to 74) show the relative displacements and absolute accelerations of the body for varying values of μ and f_s for different ground motions, obtained with the SINMOT program.

It can be observed that an increase in spring stiffness, thereby increasing f_s, results in an increase in the absolute accelerations which is higher at lower coefficients of friction (Fig. 3-23 to 3-31, pages 66 to 74). Similarly, the influence of springs on relative displacements is greater at low coefficients of friction. For ground frequencies of 2 Hz and 5 Hz (Fig. 3-23 to 3-28, pages 66 to 71), it is seen that a natural frequency of the spring/mass system of 0.2 Hz gives

the lowest relative displacement, with only a small increase in acceleration.

As the natural frequency of the spring/mass system is further increased, for a ground frequency of 2 Hz, the relative displacement increases, as it approaches the frequency of the ground motion, and at f_s = 1 Hz, it is well in excess of the absolute ground displacement (Fig. 3-23 to 3-25, pages 66 to 68). This illustrates that while resilient constraint is essential to prevent wandering, it may not necessarily result in reduced displacement.

For a ground frequency of 10 Hz (Fig. 3-29 to 3-31, pages 72 to 74), natural frequency of the spring/mass system of 0.8 Hz gives the lowest relative displacements.

The conflicting demands of low body acceleration and low relative displacement, together with the variations in the response with the frequency of the ground motion, require a compromise to be made. From the curves of Figures 3-23 to 3-31, the best relationship between μ and ω_s can be established based on the minimum value permitted for μ and on acceptable values of x_{br} and $\ddot{x}_b$.

The values of the natural frequency which give the lowest relative displacement are given in Table 3-2. (The

coefficient of friction of $\mu = 0.10$ is again chosen for wind resistance of wood stud / brick veneer structures.)

Table 3-2 Response Comparison for Sinusoidal Time-Histories

$\ddot{x}_{gm}$ & f	NATURAL FREQUENCY, Hz	μ	x_{br}, m	$\ddot{x}_b$	*PERMANENT OFFSET, m
0.2g, 2 Hz	$f_s = 0$	0.1	.0078	0.10g	0.00081
	$f_s = 0.2$	0.1	.0077	0.10g	0.00065
0.3g, 2 Hz	$f_s = 0$	0.1	.0145	0.10g	0.00137
	$f_s = 0.2$	0.1	.0142	0.10g	0.00109
0.4g, 2 Hz	$f_s = 0$	0.1	.0230	0.10g	0.00181
	$f_s = 0.2$	0.1	.0227	0.10g	0.00139
0.2g, 5 Hz	$f_s = 0$	0.1	.0014	0.10g	0.00007
	$f_s = 0.2$	0.1	.0014	0.10g	0.00005
0.3g, 5 Hz	$f_s = 0$	0.1	.0023	0.10g	0.00022
	$f_s = 0.2$	0.1	.0023	0.10g	0.00017
0.4g, 5 Hz	$f_s = 0$	0.1	.0036	0.10g	0.00033
	$f_s = 0.2$	0.1	.0031	0.10g	0.00025
0.2g, 10 Hz	$f_s = 0$	0.1	.0004	0.10g	0.00002
	$f_s = 0.8$	0.1	.0003	0.10g	0.00001
0.3g, 10 Hz	$f_s = 0$	0.1	.0007	0.10g	0.00003
	$f_s = 0.8$	0.1	.0006	0.10g	0.00002
0.4g, 10 Hz	$f_s = 0$	0.1	.0009	0.10g	0.00005
	$f_s = 0.8$	0.1	.0008	0.10g	0.00004

* The permanent offset is the building's displacement relative to the ground at the end of the motion.

Choosing the best compromise, represented by the values in Table 3-2, results in a small reduction in the relative displacement, when compared to the behaviour with pure friction, without noticeably increasing the absolute acceleration.

The introduction of resilience reduced the maximum permanent offset of the body from 0.00181 m to 0.00139 m.

The analyses were also conducted using FRICTION and DRAIN-2D programs. The stiffness of the resilient constraint, k_s, required in these programs but not in SINMOT, ranged from 4.1 to 103.7 N/mm for f_s from 0.2 to 1.0 Hz. (The stiffness of the elasto-plastic element, which represented the friction base isolators, is assigned a high value of 2×10^8 N/mm.) The results of SINMOT are within 3% of those obtained from FRICTION and DRAIN-2D.

3.4.2 Performance with Time-Histories of Actual Earthquakes

To study the influence of the natural frequency of the spring/mass system on the response, the "simple" model was analyzed using FRICTION with the time-histories of the El Centro, Olympia and N.B.K. earthquakes.

The time step was 0.01 second. Parametric studies were made for system natural frequencies from 0 to 3.0 Hz for peak ground accelerations of 0.2g and 0.4g, and coefficients of friction ranging from 0.0 to 0.4.

The analyses were also carried out using DRAIN-2D, which gave results within 0.5% of those from FRICTION. (For El Centro earthquake, the computation time with DRAIN-2D was 8 seconds compared to 3 seconds with FRICTION.)

The results of the parametric studies are shown in Figures 3-32 and 3-37 (pages 75 to 80). It is seen that by introducing springs, the absolute accelerations increase marginally, but that the relative displacements are significantly reduced at coefficients of friction below 0.15, although less so for the N.B.K. earthquake.

For the El Centro and Olympia earthquakes, as the natural frequency of the spring/mass system increases, the relative displacements decrease until the natural frequencies are 1.8 and 2 Hz respectively, beyond which the displacements increase (Fig. 3-32 to 3-35, pages 75 to 78), as the system frequency moves towards the value of the predominant ground frequency i.e. 2.6 and 2.9 Hz, respectively. Due to the random nature of earthquakes, the natural frequency of the spring/mass system which gives the lowest relative displacements is closer

to the predominant ground frequency than for sinusoidal ground motion (Section 3.4.1).

For the N.B.K. earthquake, the natural frequency of the spring/mass system of 1.5 Hz gives the lowest relative displacements (Fig. 3-36 and 3-37, pages 79 and 80). Because of the wide range of frequency content of this earthquake, there is not a big difference between the responses for natural frequencies of the spring/mass system from 1 to 3 Hz.

3.4.3 Discussion

Resilient constraints prevent the unrestricted progressive displacement of the building by providing a restoring force. These constraints may also allow the use of a lower coefficient of friction to reduce accelerations of the body without increasing its relative displacements, or, for a given coefficient of friction, reduce the relative displacements even further.

As discussed earlier, optimization for minimum body acceleration and minimum relative displacement places conflicting demands on the coefficient of friction and the spring stiffness. From the parametric studies, the values for μ and k can be chosen to get the best compromise between x_{br} and $\ddot{x}_b$. This will be different for each ground motion. Using

the value of $\mu = 0.1$, previously selected as the most suitable for pure friction isolation, the optimum natural frequencies of the spring/mass system for actual earthquakes are 1.8 Hz for El Centro, 2.0 Hz for Olympia and 1.5 Hz for N.B.K.

The comparisons of the responses for a pure friction system, with $\mu = 0.1$, to the best response with the resilient system for actual earthquakes are taken from Figures 3-32 to 3-37, and are shown in Table 3-3.

Table 3-3 Response Comparison in Actual Earthquakes

EARTHQUAKE $\ddot{x}_{gm}$	NATURAL FREQUENCY, Hz	μ	x_{br}, m	$\ddot{x}_b$	PERMANENT OFFSET, m
El Centro 0.2g	$f_s = 0$	0.1	0.016	0.10g	0.0019
	$f_s = 1.8$	0.1	0.009	0.10g	0.0002
El Centro 0.4g	$f_s = 0$	0.1	0.107	0.10g	0.0038
	$f_s = 1.8$	0.1	0.043	0.10g	0.0008
Olympia 0.2g	$f_s = 0$	0.1	0.008	0.10g	0.0009
	$f_s = 2.0$	0.1	0.005	0.10g	0.0001
Olympia 0.4g	$f_s = 0$	0.1	0.032	0.10g	0.0031
	$f_s = 2.0$	0.1	0.023	0.10g	0.0003
N.B.K. 0.2g	$f_s = 0$	0.1	0.021	0.10g	0.0007
	$f_s = 1.5$	0.1	0.020	0.10g	0.0001
N.B.K. 0.4g	$f_s = 0$	0.1	0.175	0.10g	0.0062
	$f_s = 1.5$	0.1	0.162	0.10g	0.0011

It is seen from the values in Table 3-3 that choosing the best compromise of f_s results in a reduction in the relative displacement, x_{br}. When compared to pure friction, the reduction in displacement for the El Centro and N.B.K. earthquakes at $\ddot{x}_{gm}$=0.4g are 60% and 7%, respectively. No increase in peak acceleration, $\ddot{x}_b$, of the body is shown in this table, as it was less than 4%.

For conditions representing Montreal, a peak ground acceleration of 0.2g and a coefficient of friction of 0.1, the value of f_s which gives the best compromise reduces the maximum relative displacements to only 10% of the amplitude of the ground displacement for the N.B.K. earthquake (Table 3-1).

The introduction of resilience reduced the permanent offset of the body from 0.0062m (for pure friction) to 0.0011m for the N.B.K. earthquake.

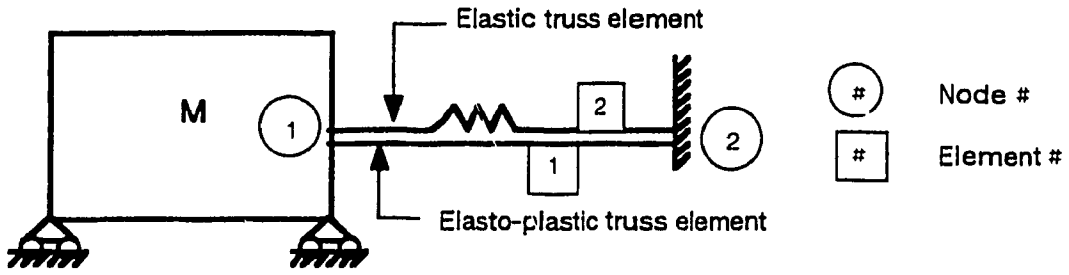

Figure 3-1 "Simple" Model for Analysis in DRAIN-2D

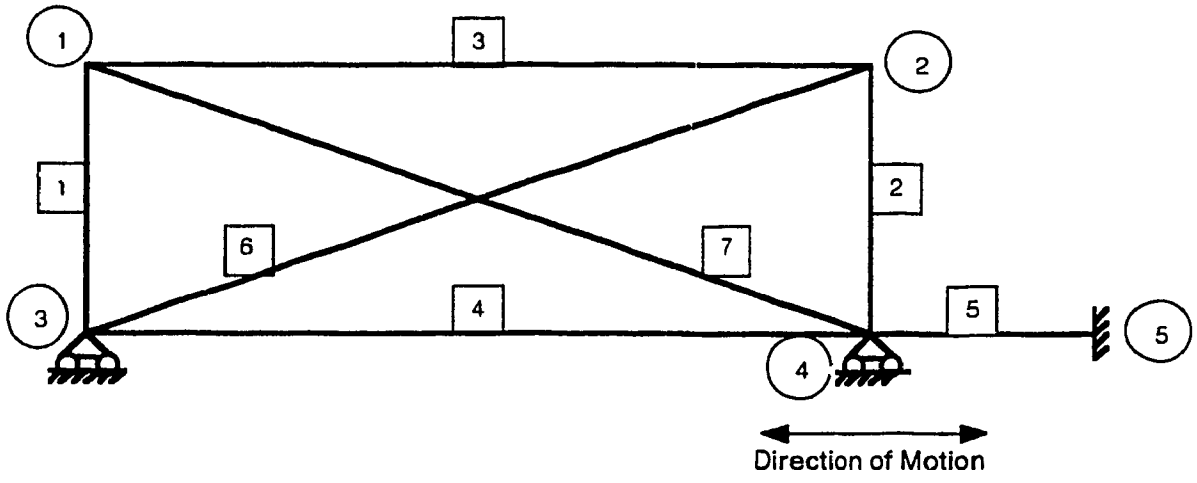

Figure 3-2 Node and Element Layout of "Detailed" Model for Analysis in DRAIN-2D

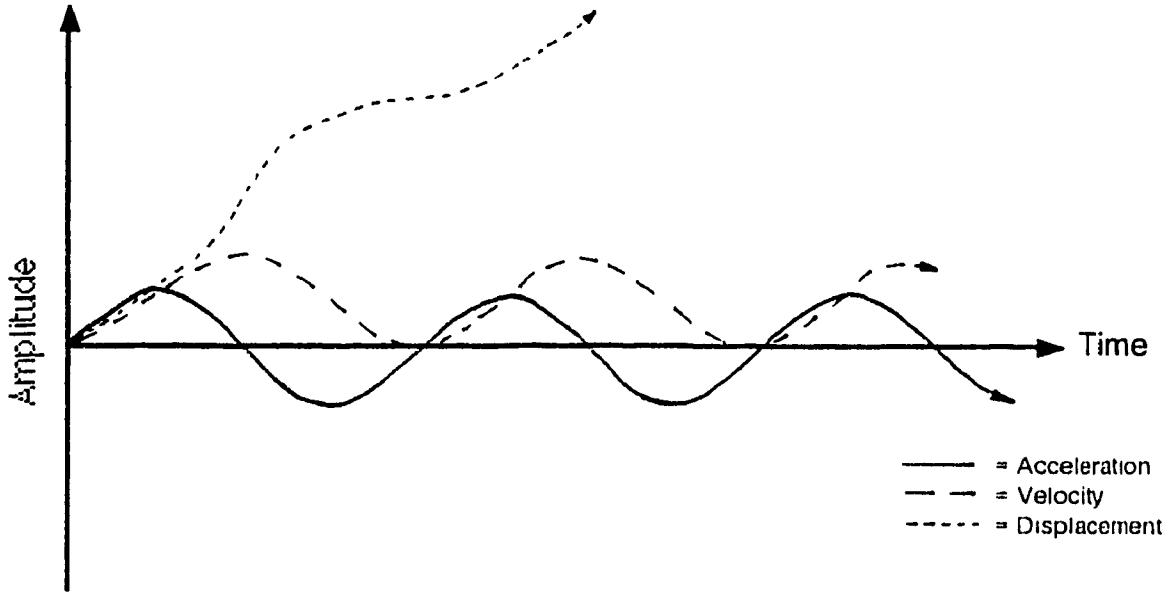

Figure 3-3 Sine Ground Excitation

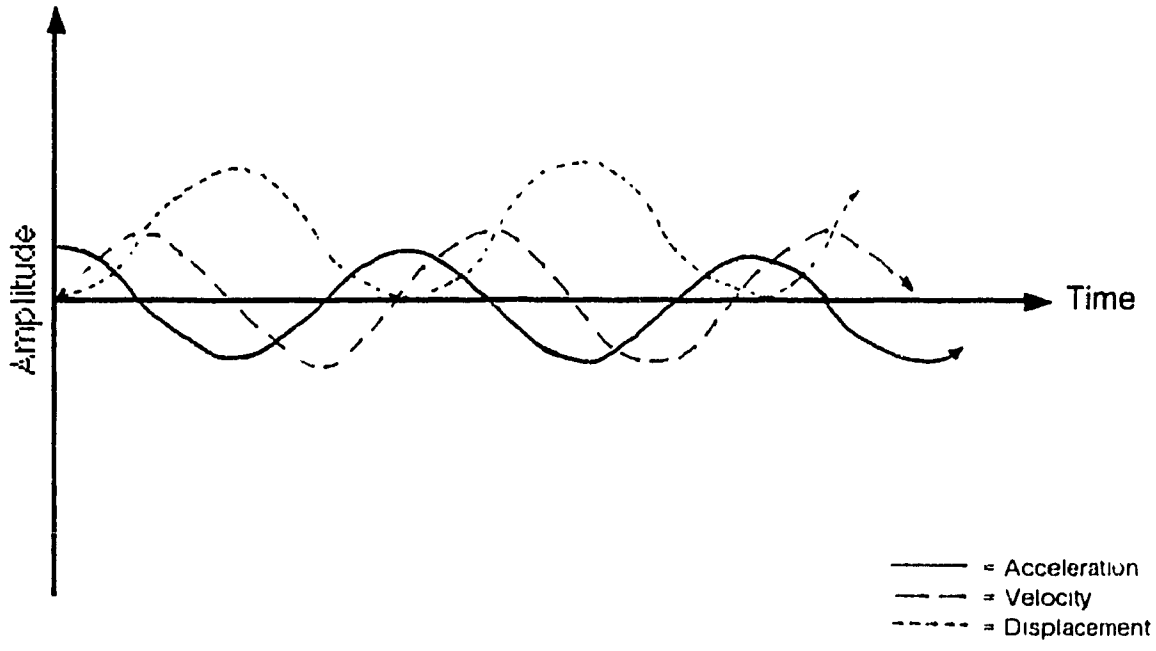

Figure 3-4 Cosine Ground Excitation

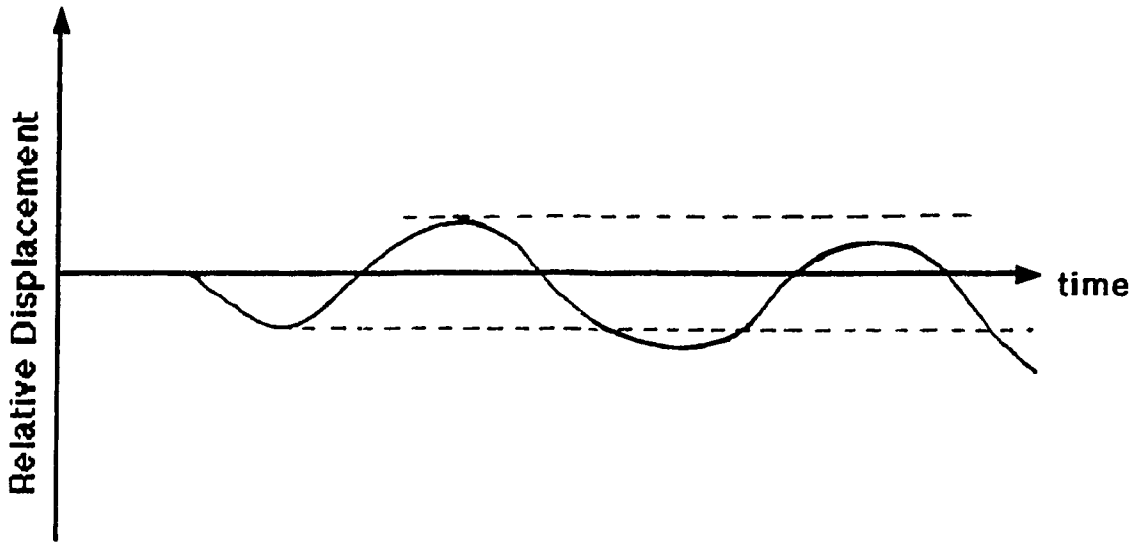

Figure 3-5 Body Displacement to One Side

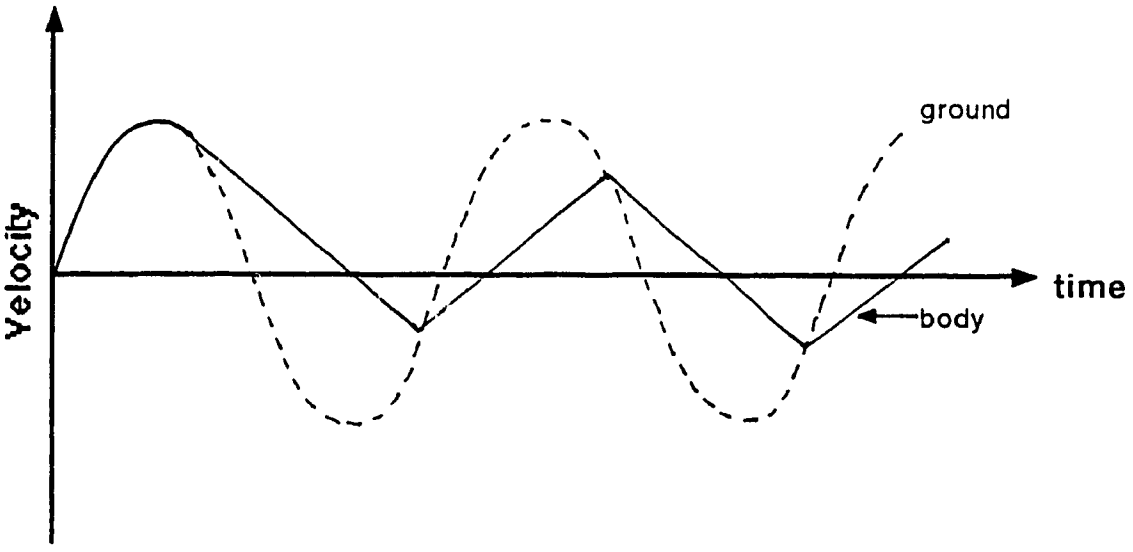

Figure 3-6 Wandering Body Motion

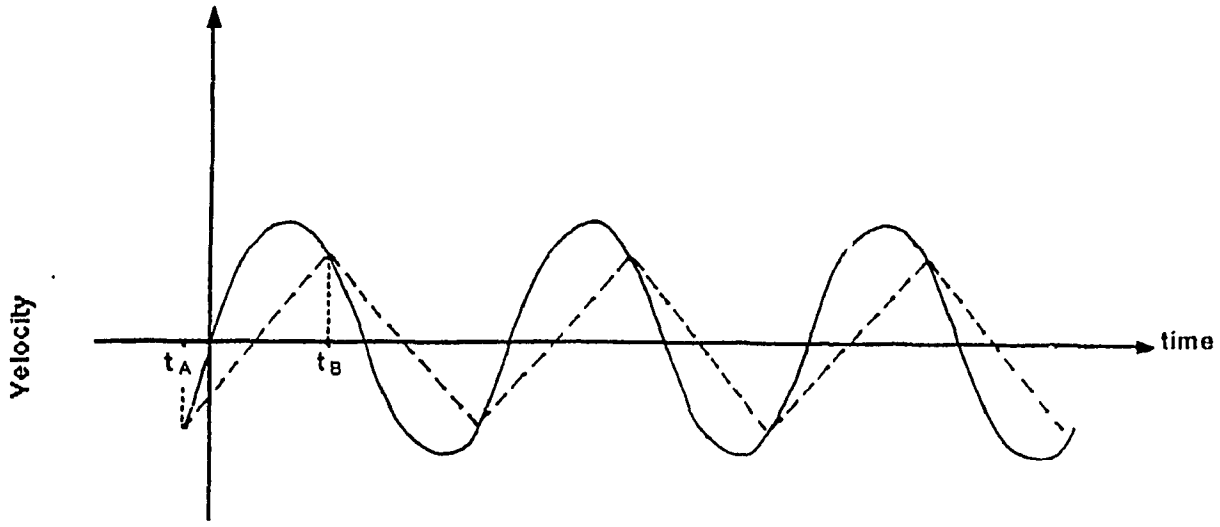

Figure 3-7 Ideal Body Velocity

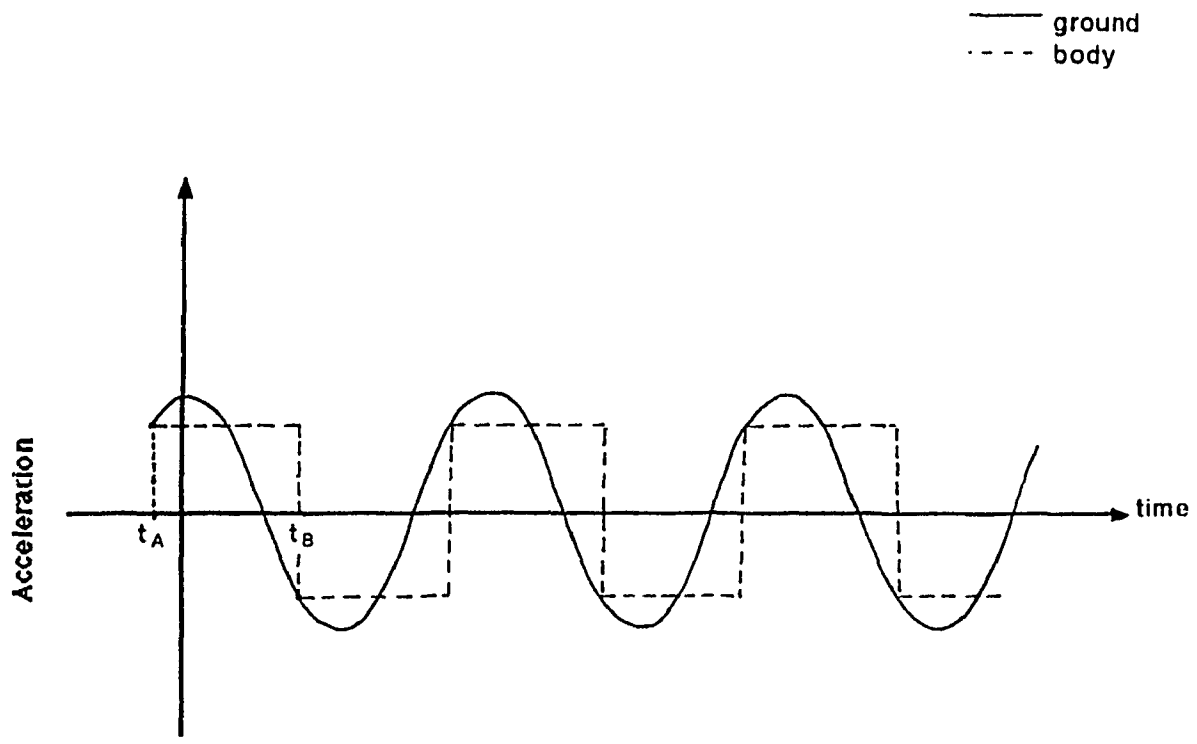

Figure 3-8 Ideal Body Acceleration

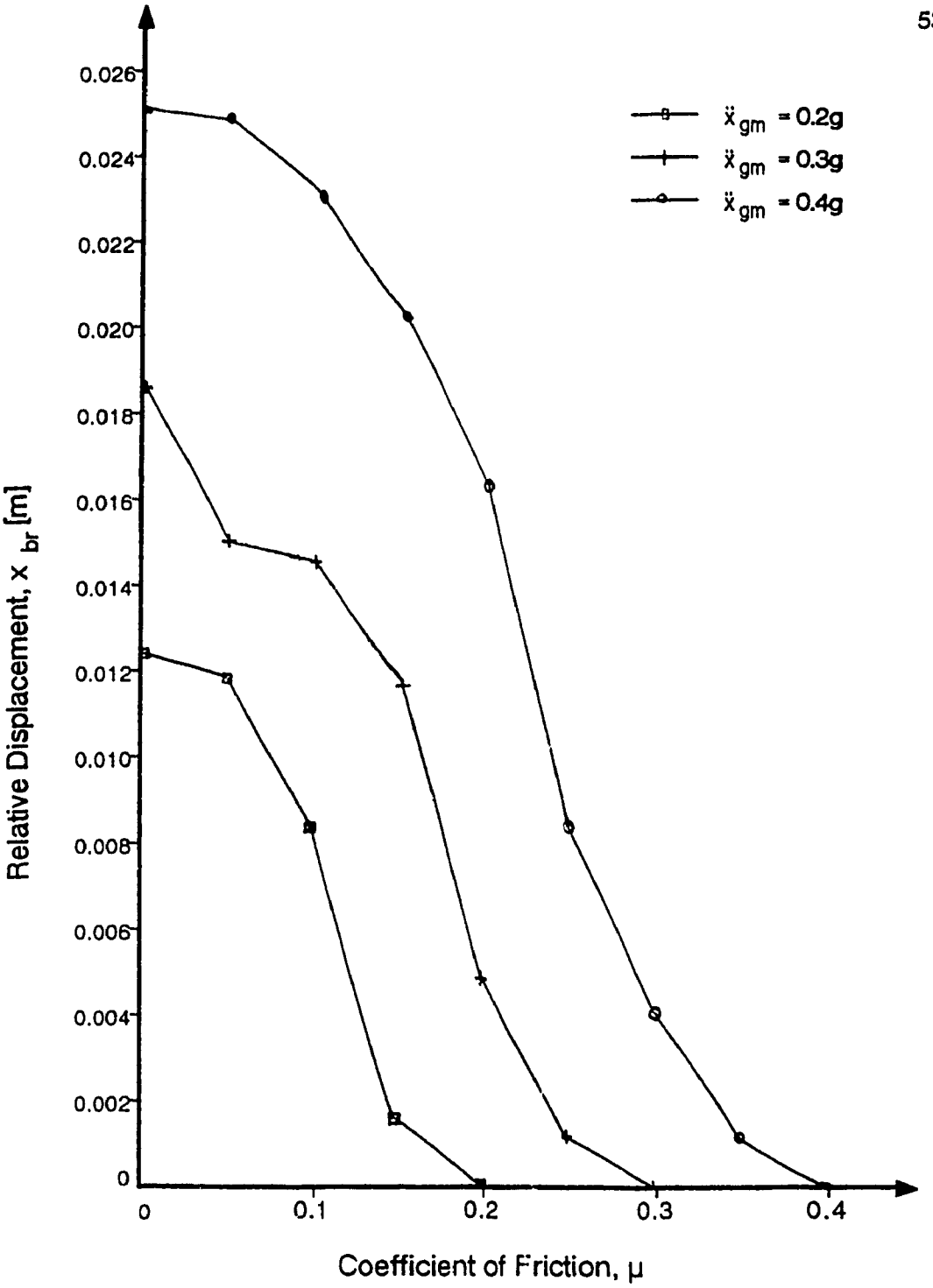

Figure 3-9 Relative Displacements for Pure Friction in Cosine Excitation, f = 2 Hz

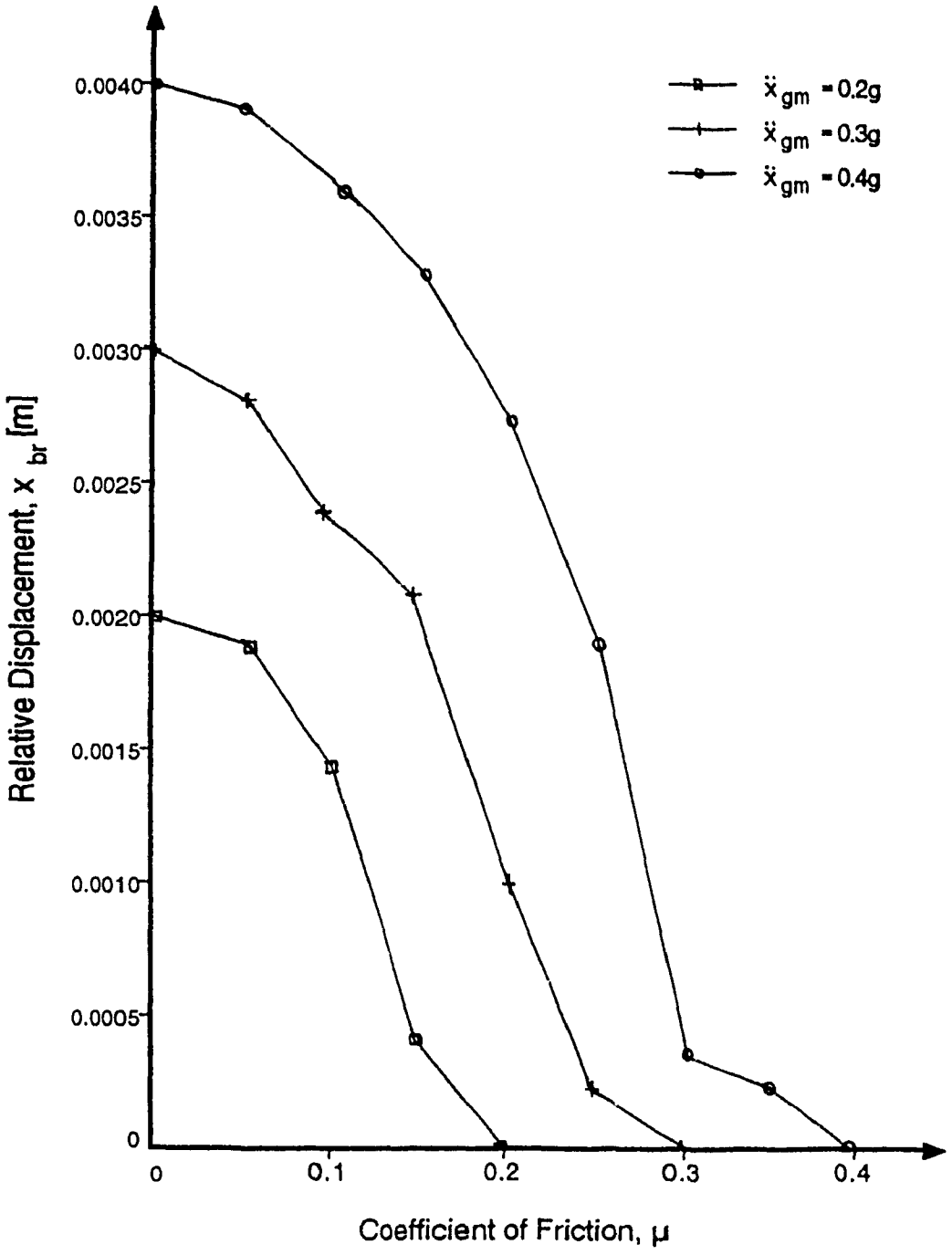

Figure 3-10 Relative Displacements for Pure Friction in Cosine Excitation, f = 5 Hz

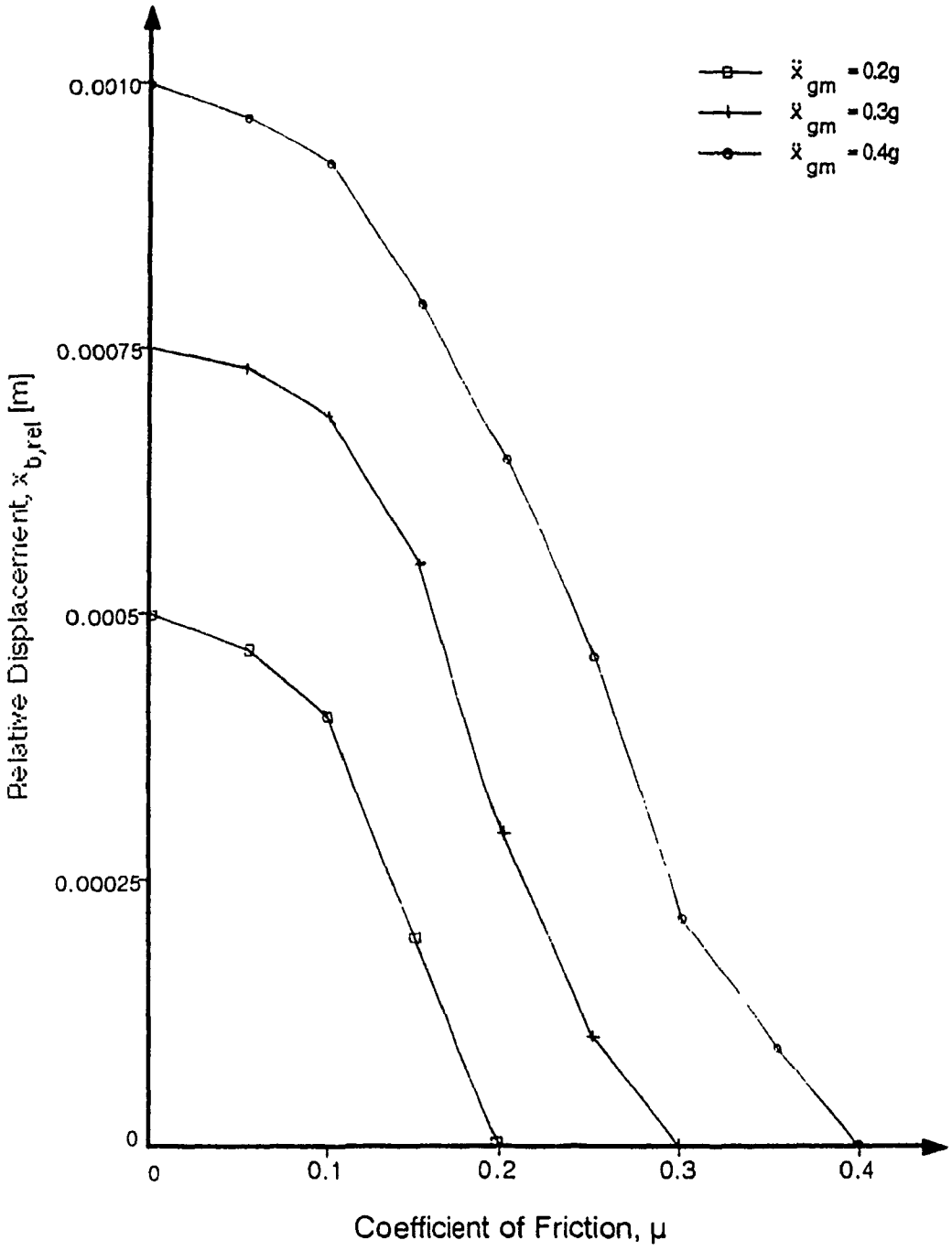

Figure 3-11 Relative Displacements for Pure Friction in Cosine Excitation, f = 10 Hz

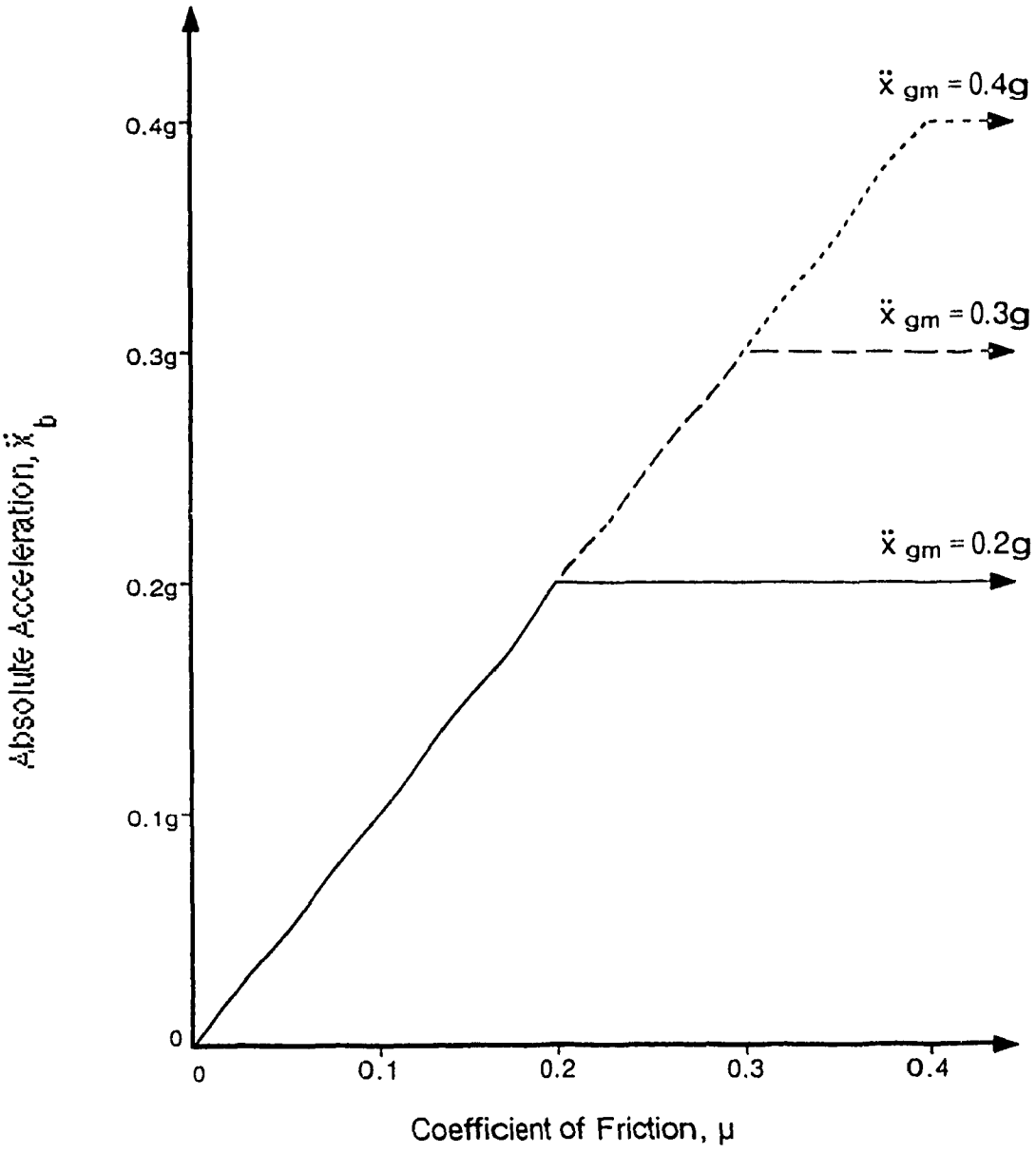

Figure 3-12 Absolute Accelerations for Pure Friction in Cosine Excitation, f = 2 Hz, 5 Hz and 10 Hz

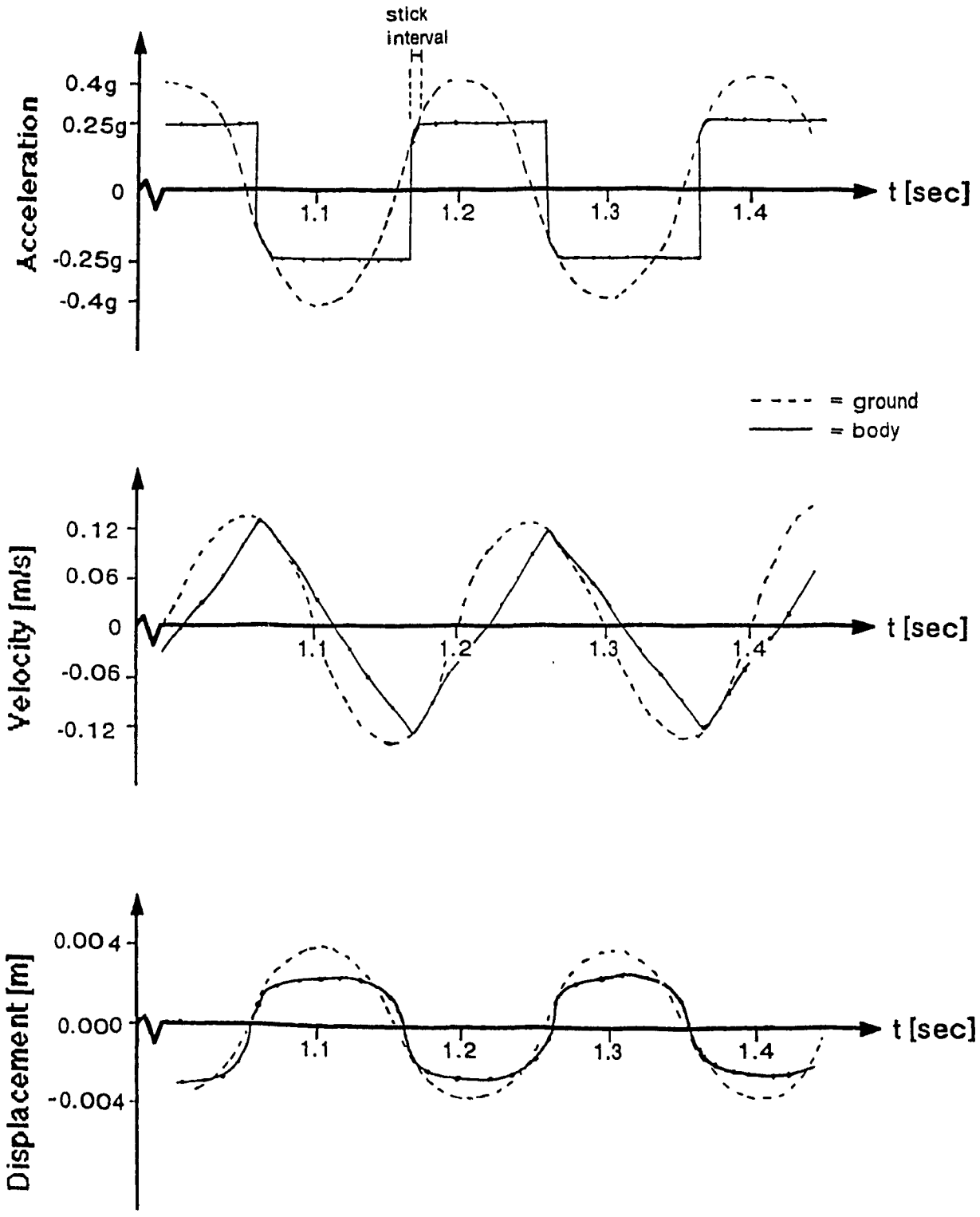

Figure 3-13 Ground Motion and Body Response for $\mu > \mu_{cr}$

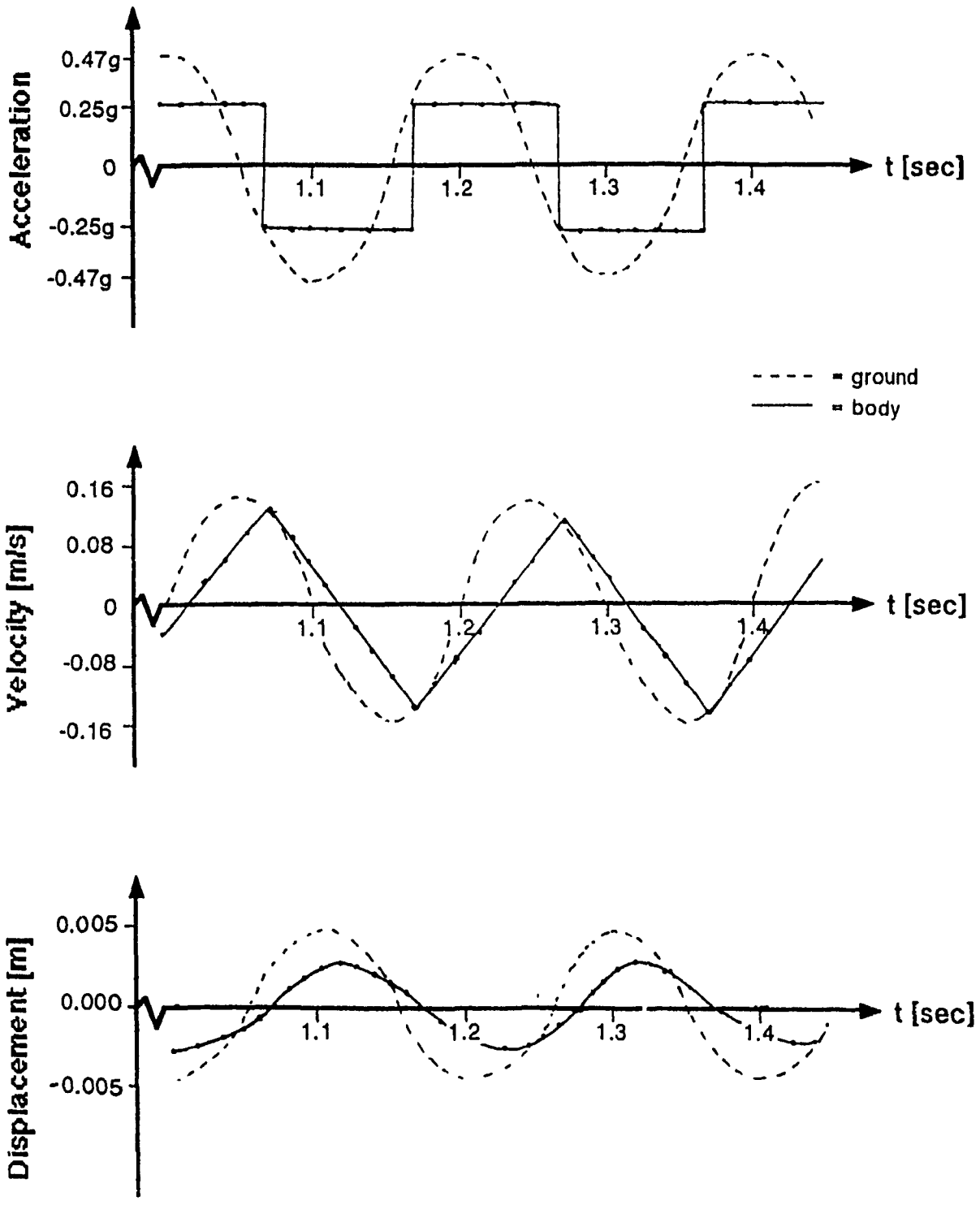

Figure 3-14 Ground Motion and Body Response for $\mu = \mu_{cr}$

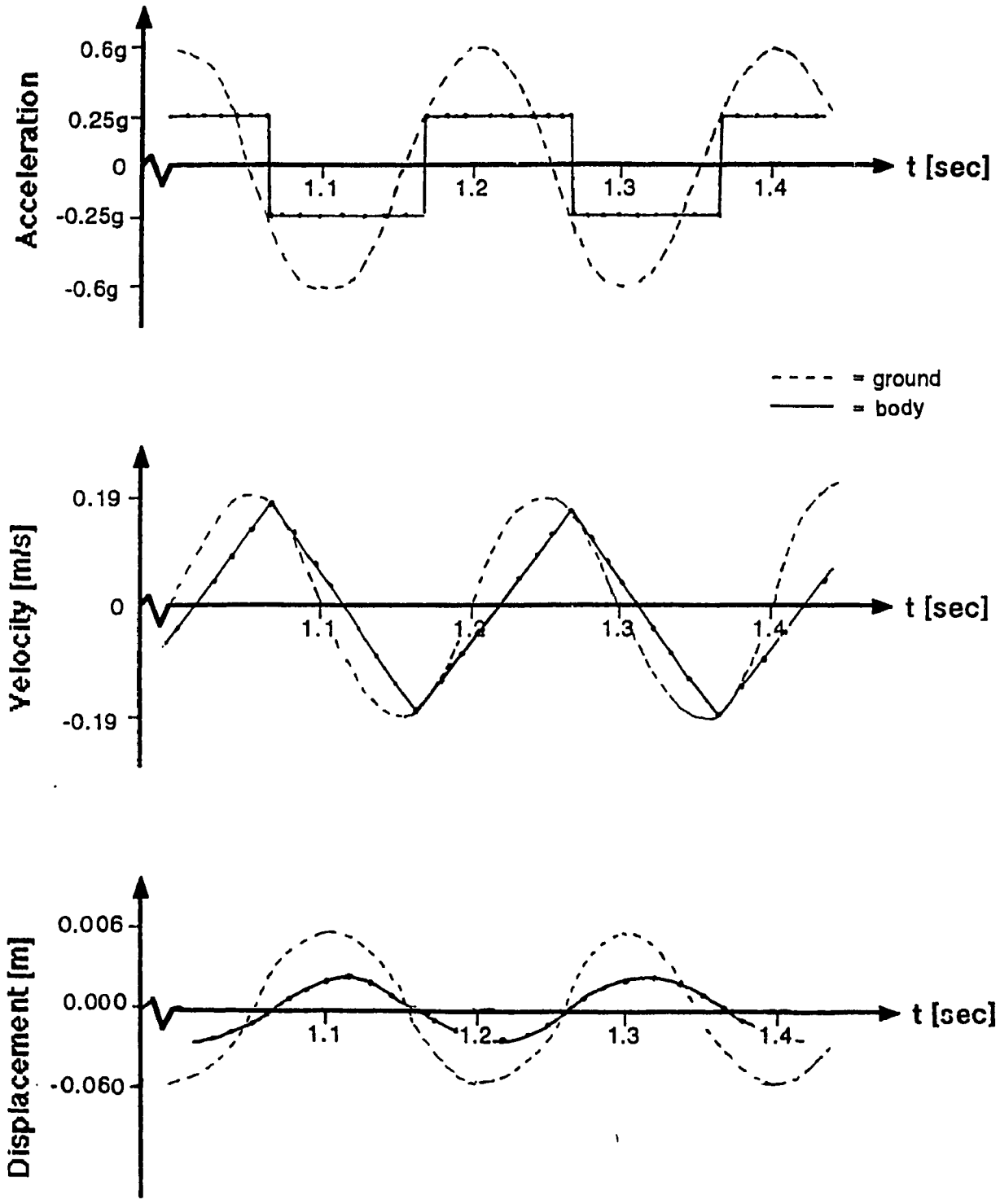

Figure 3-15 Ground Motion and Body Response for $\mu < \mu_{cr}$

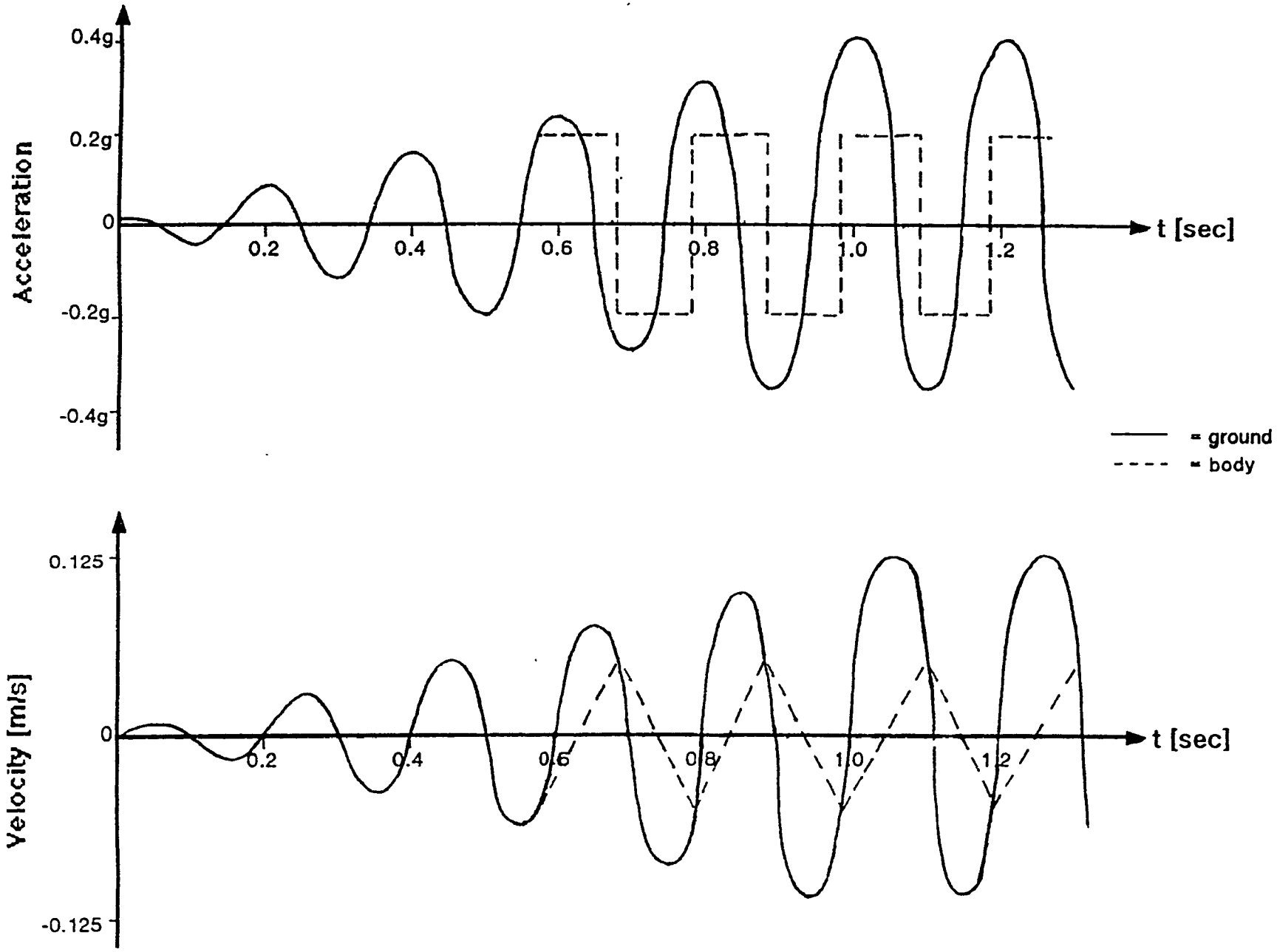

Figure 3-16 Ground Motion and Body Response for Modified Cosine Time-History, $\ddot{x}_{gm} = 0.4g$ and $\mu = 0.2$

Figure 3-17 Ground Acceleration, Velocity and Displacement, El Centro Earthquake[22]

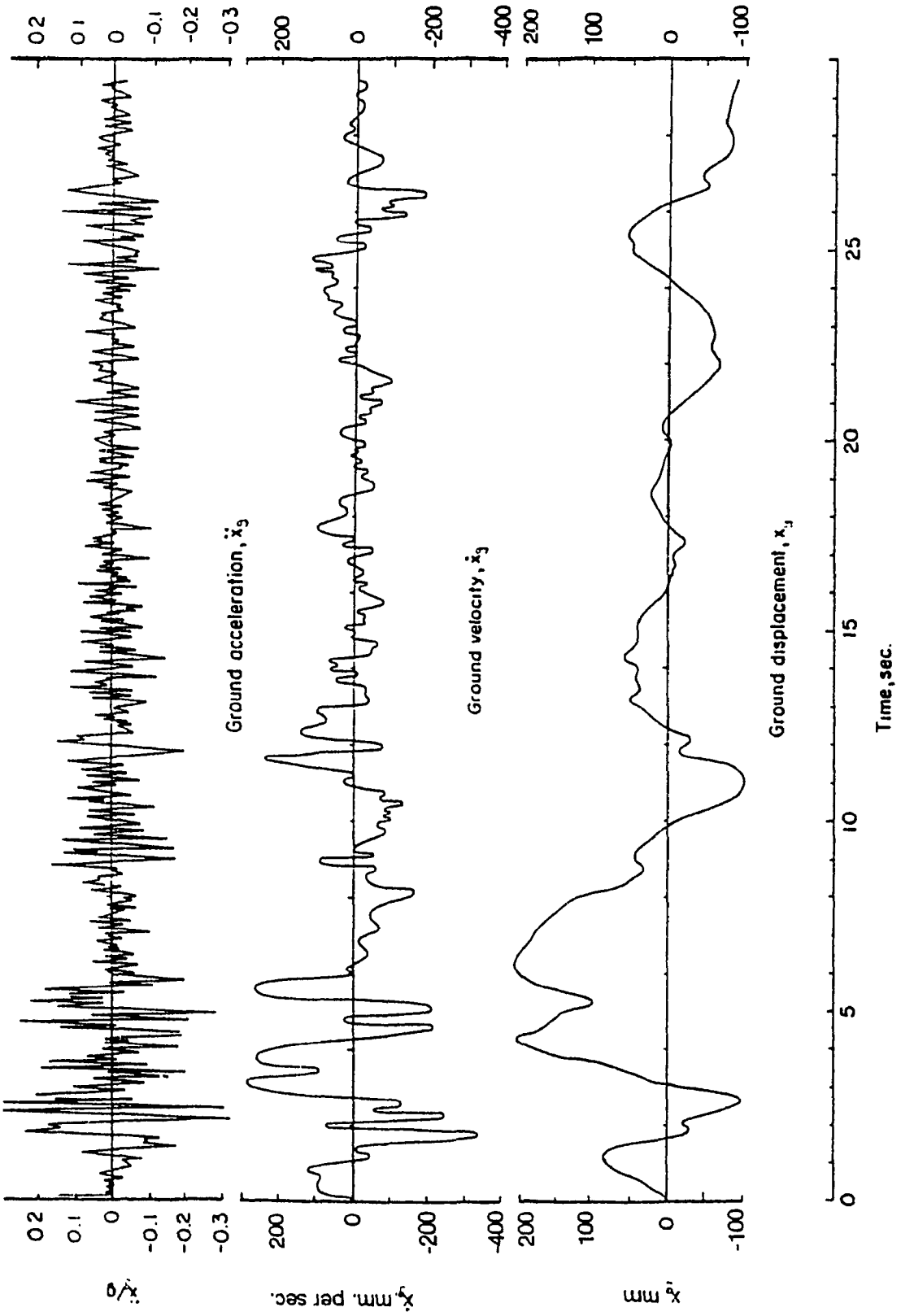

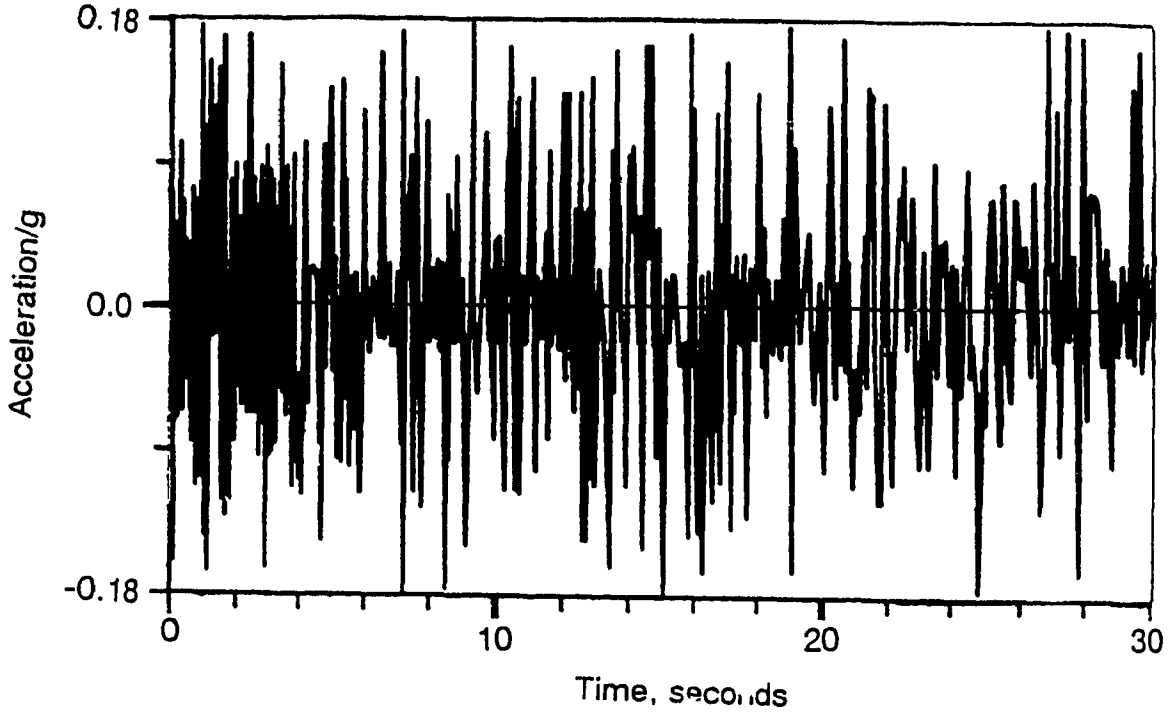

Figure 3-18 Time-Histories of Olympia Earthquake

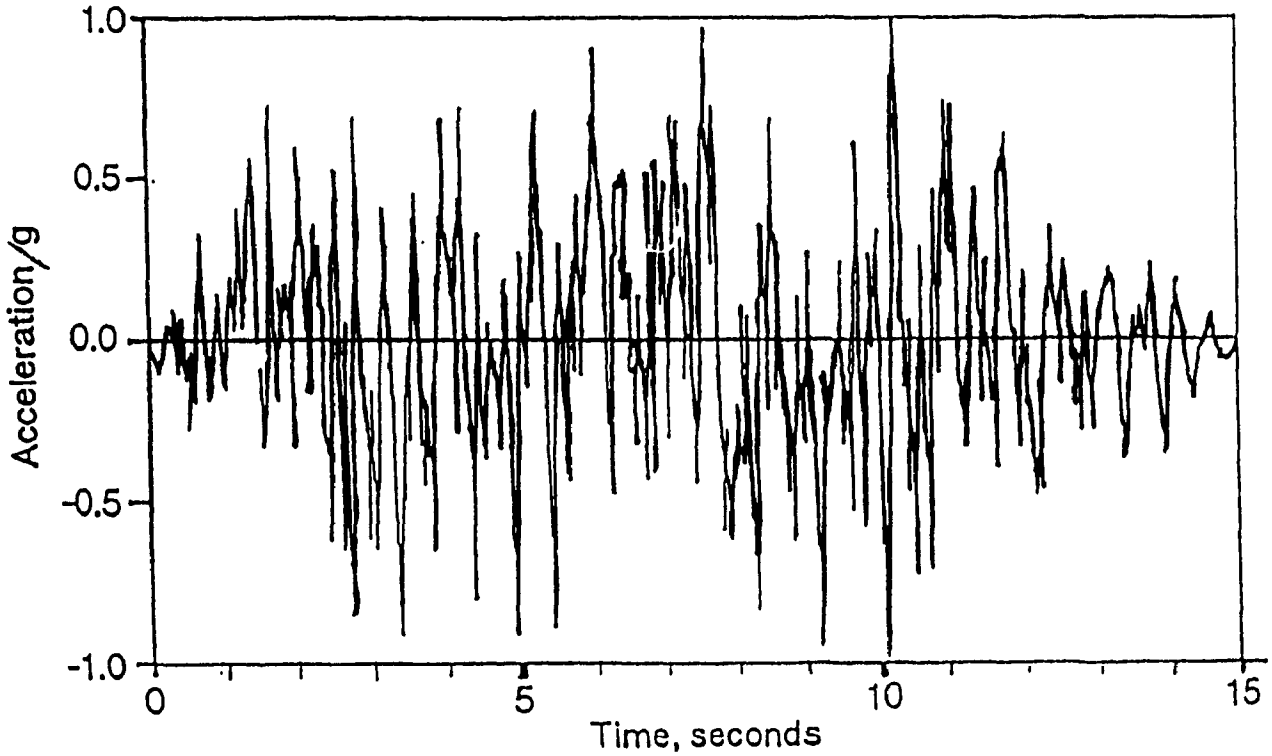

Figure 3-19 Time-Histories of Artificial Earthquake

(Newmark-Blume-Kapur)

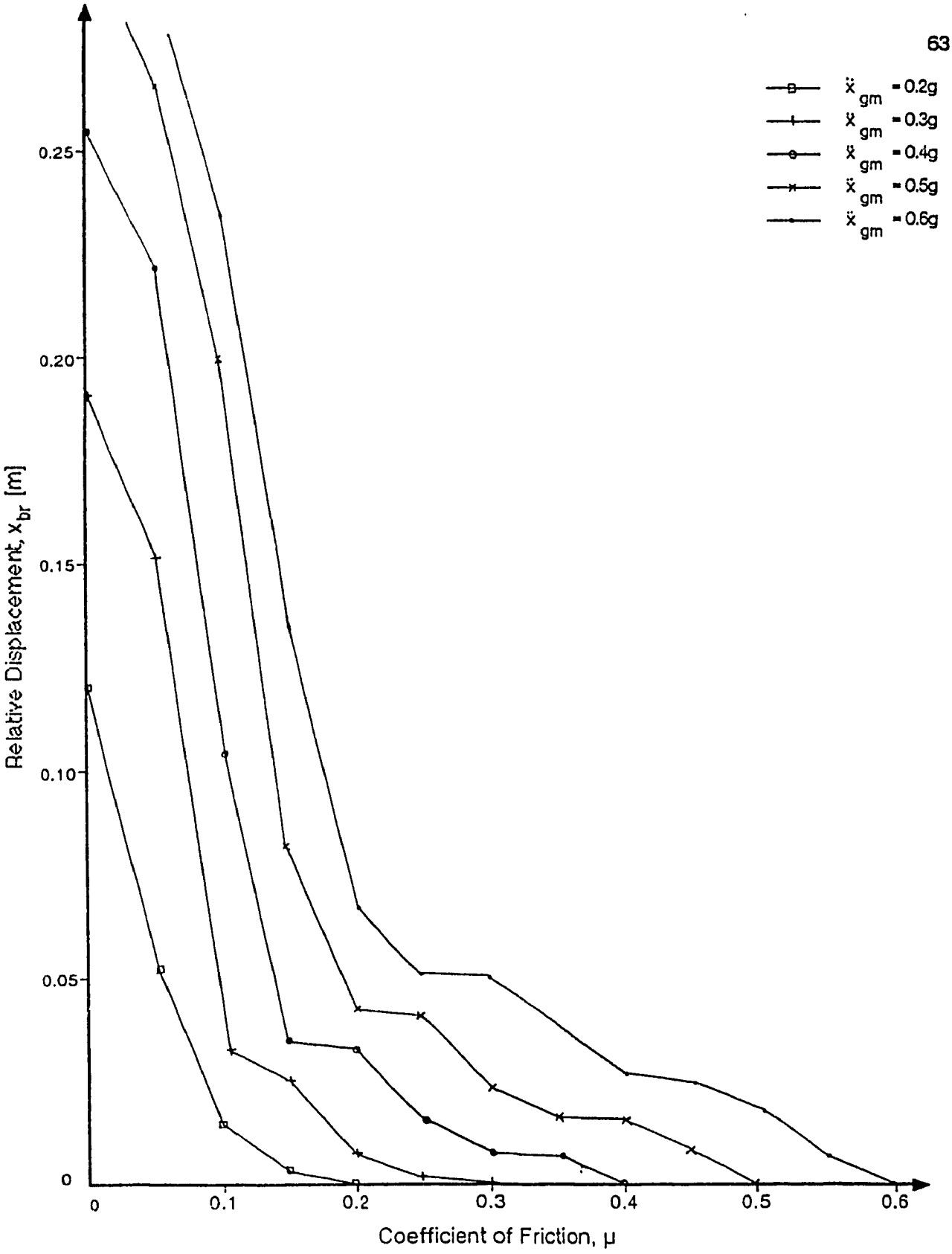

Figure 3-20 Relative Displacements for Pure Friction in El Centro Earthquake

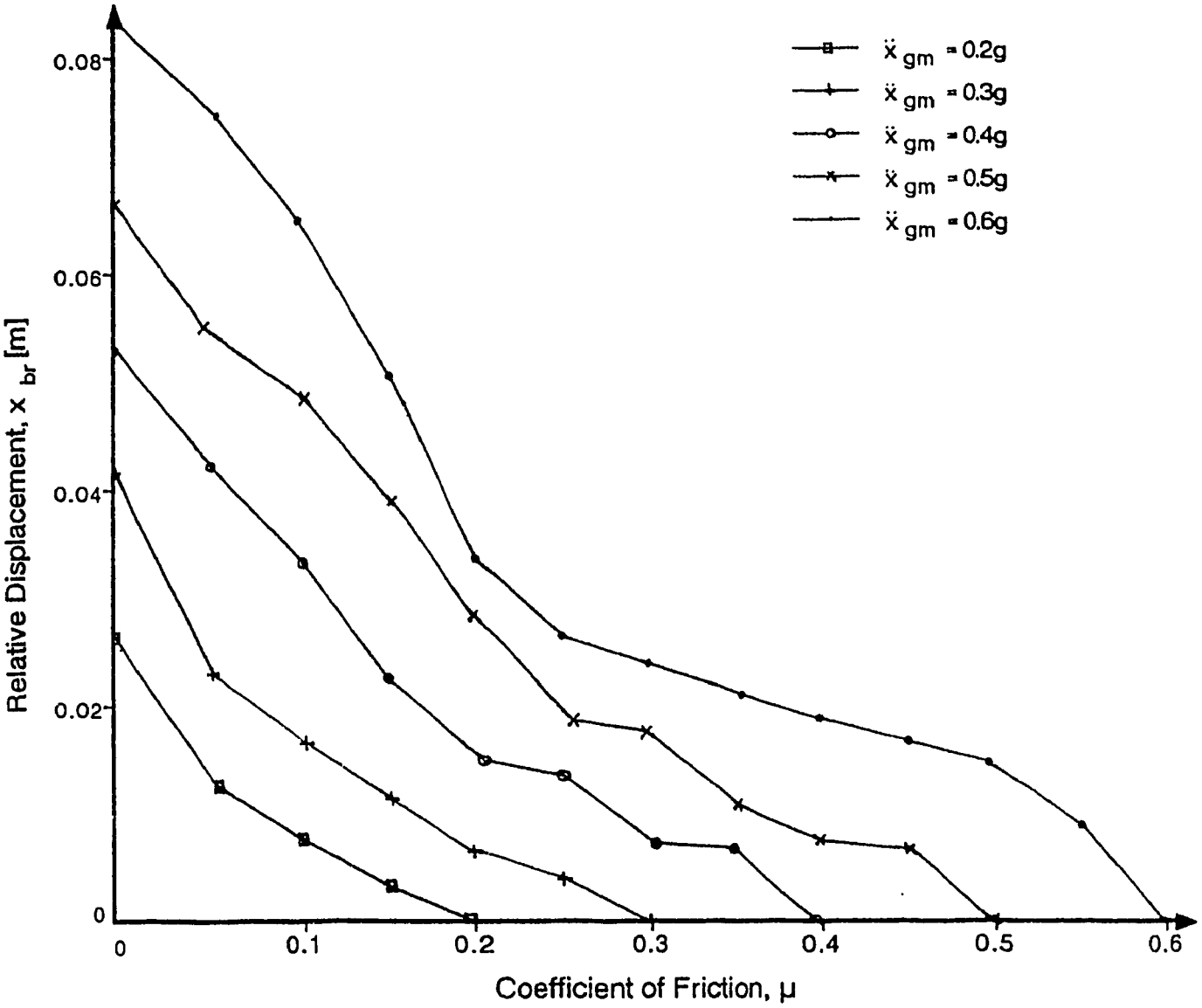

Figure 3-21 Relative Displacements for Pure Friction in Olympia Earthquake

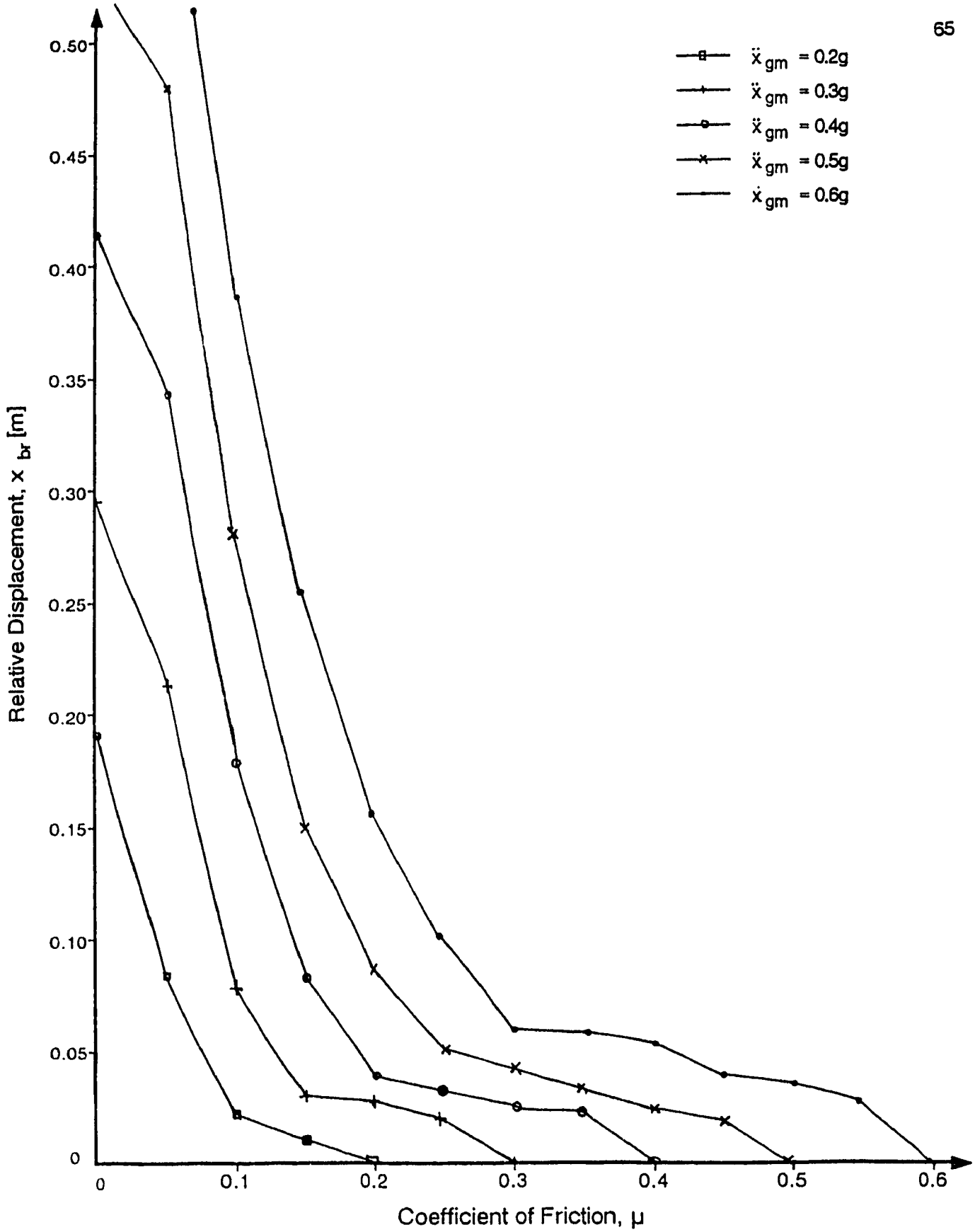

Figure 3-22 Relative Displacements for Pure Friction in N.B.K. Earthquake

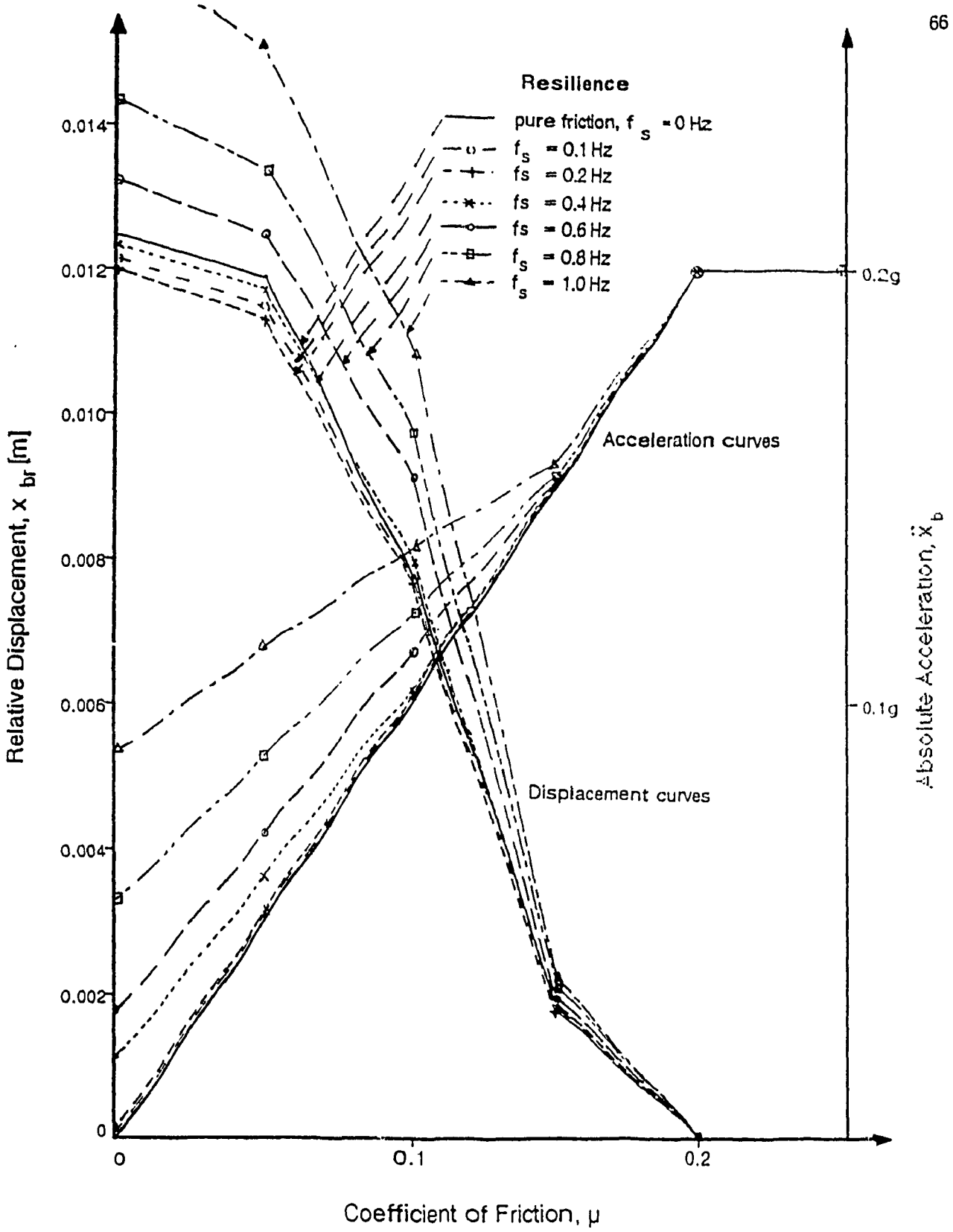

Figure 3-23 Body Response to Sinusoidal Ground Motion
f = 2 Hz and $\ddot{x}_{gm}$ = 0.2g

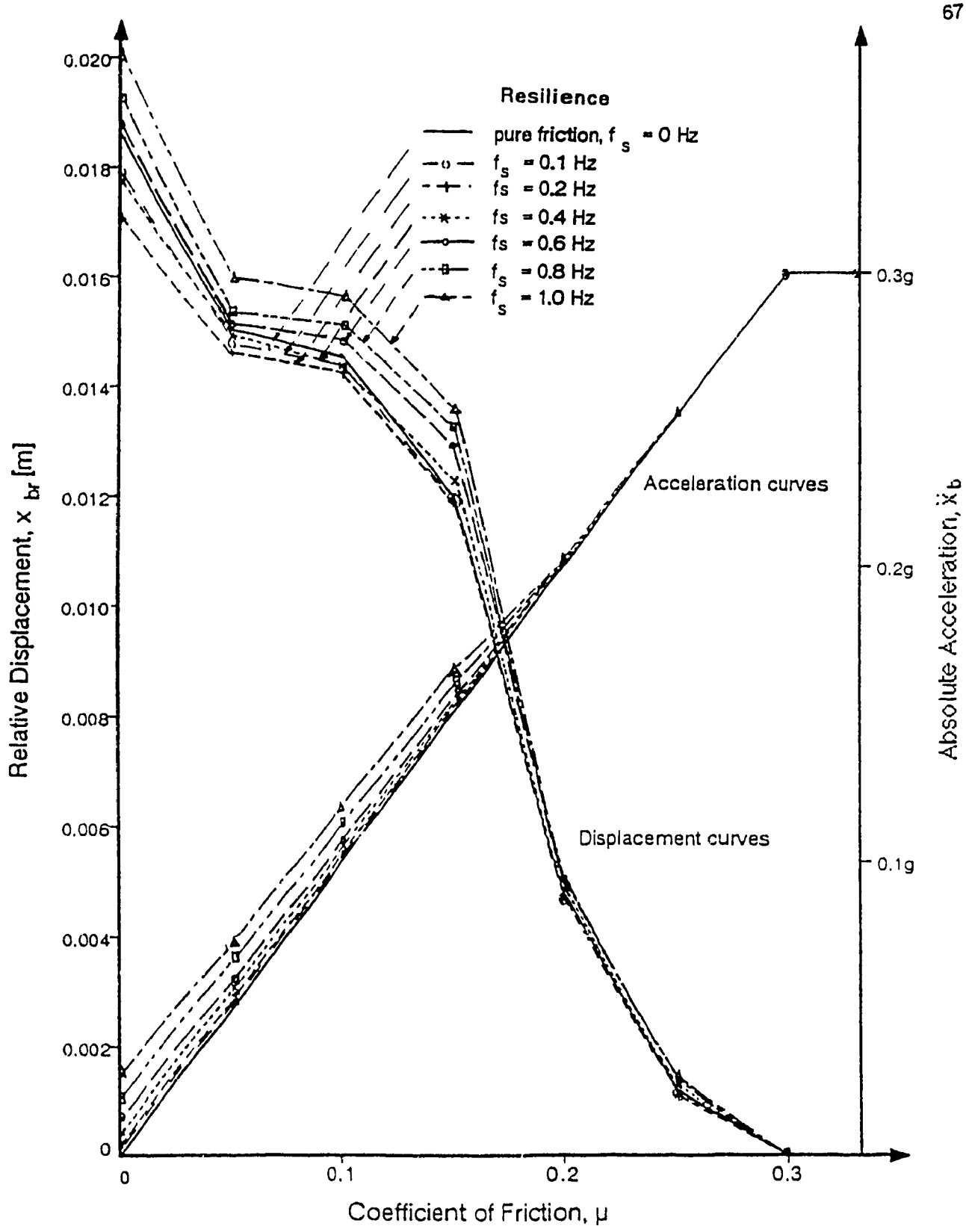

Figure 3-24 Body Response to Sinusoidal Ground Motion, f = 2 Hz and $\ddot{x}_{gm}$ = 0.3g

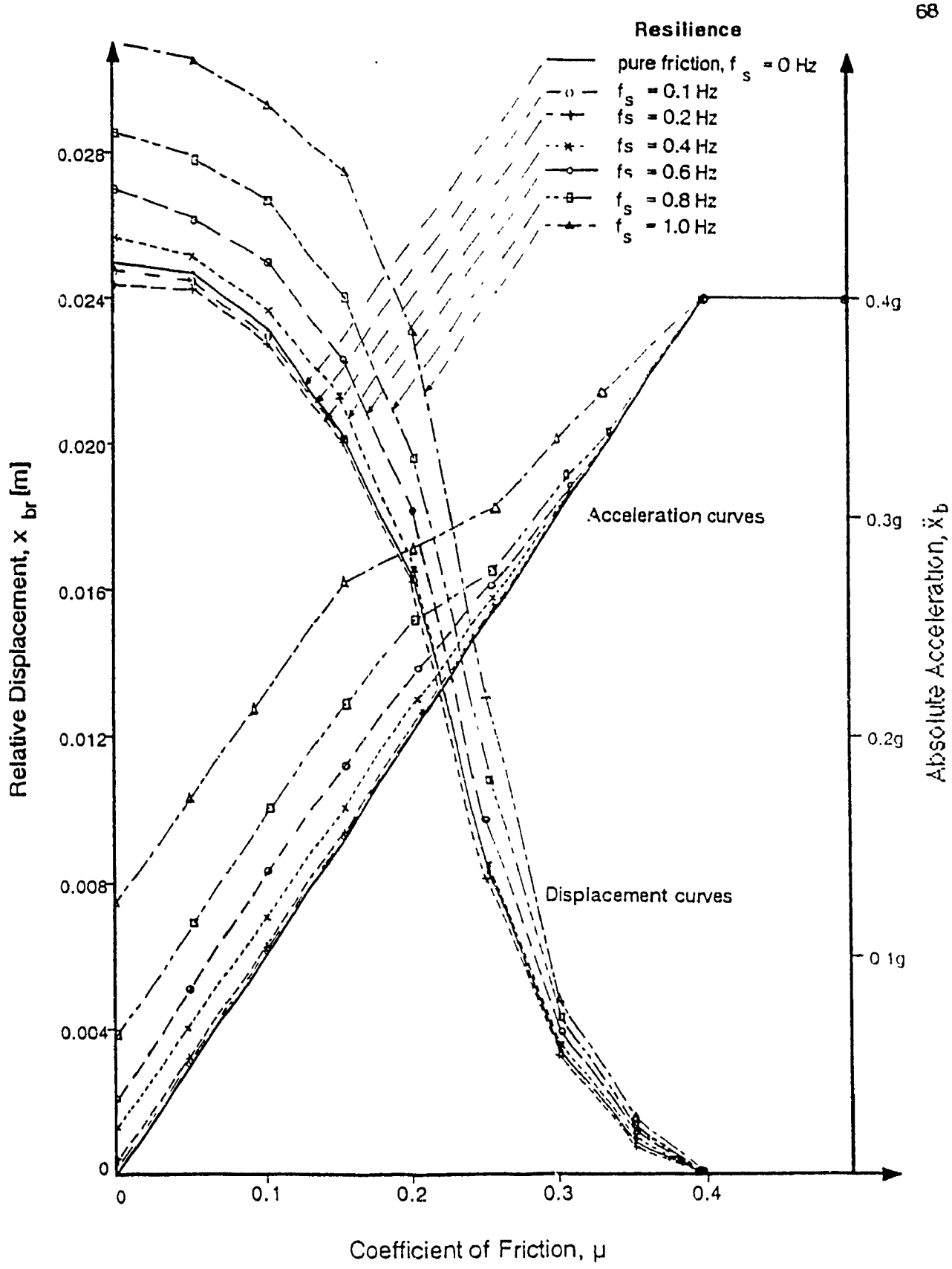

Figure 3-25 Body Response to Sinusoidal Ground Motion, f = 2 Hz and $\ddot{x}_{gm}$ = 0.4g

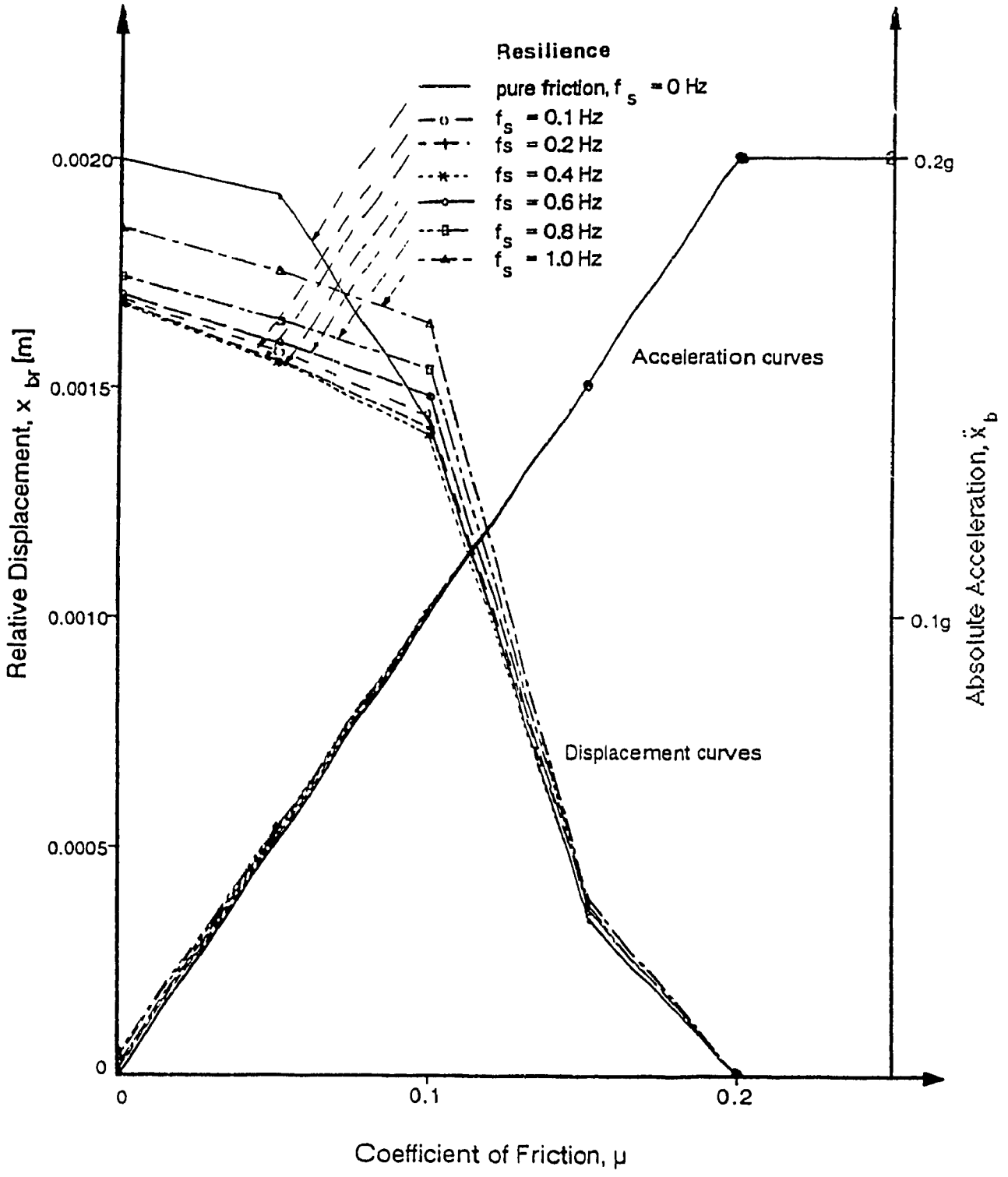

Figure 3-26 Body Response to Sinusoidal Ground Motion, f = 5 Hz and $\ddot{x}_{gm}$ = 0.2g

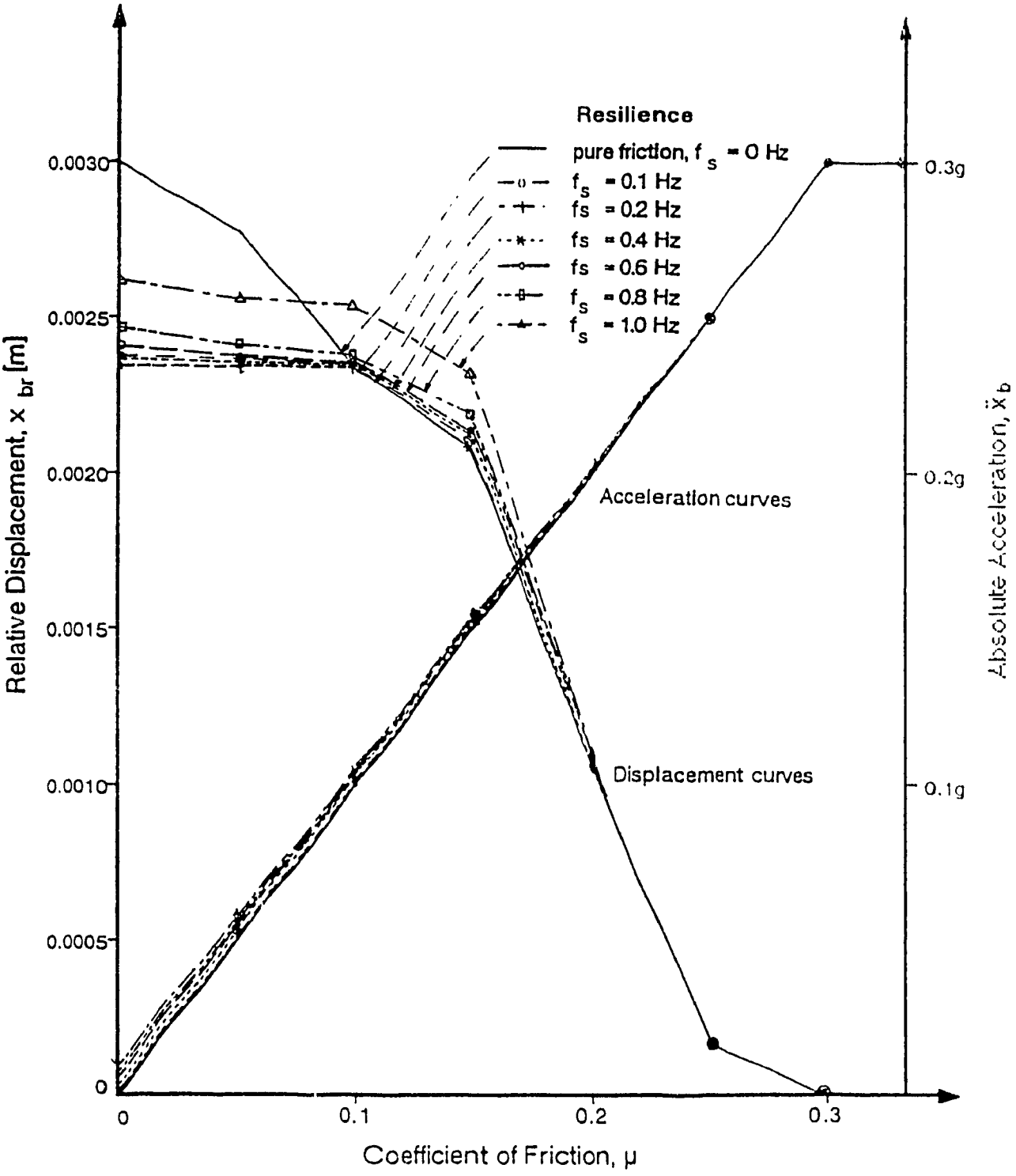

Figure 3-27 Body Response to Sinusoidal Ground Motion, f = 5 Hz and $\ddot{x}_{gm}$ = 0.3g

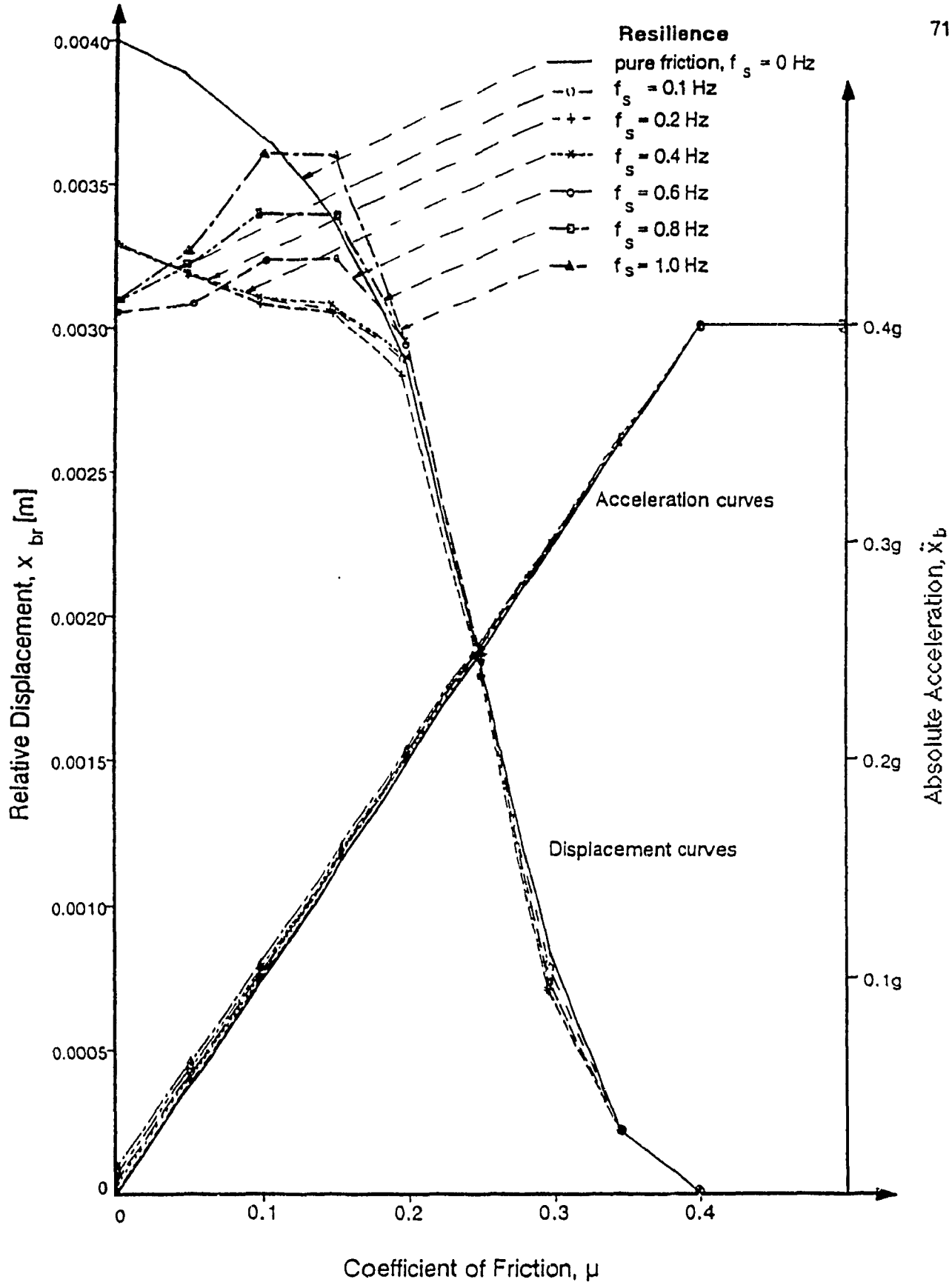

Figure 3-28 Body Response to Sinusoidal Ground Motion, f = 5 Hz and $\ddot{x}_{gm}$ = 0.4g

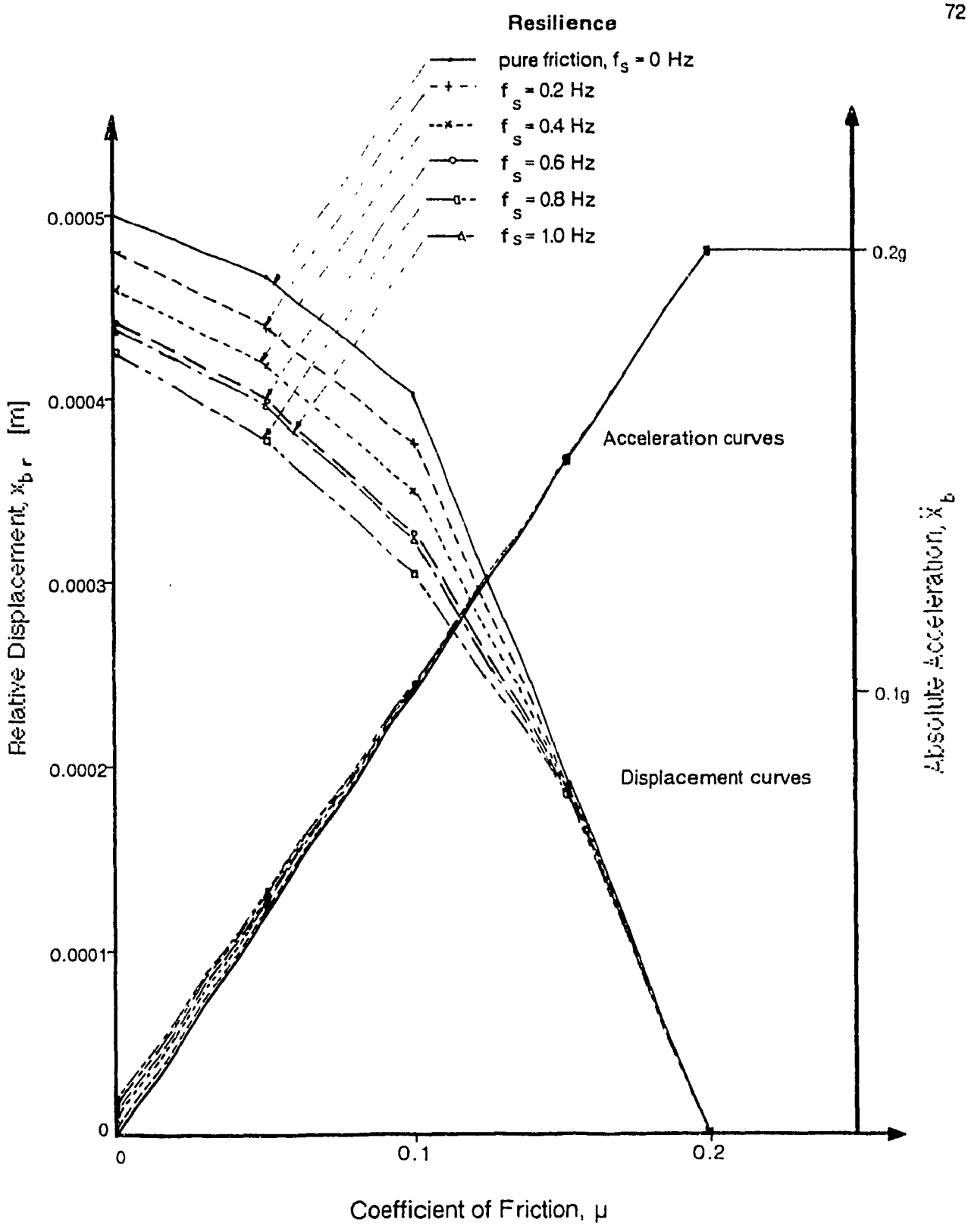

Figure 3-29 Body Response to Sinusoidal Ground Motion, f = 10 Hz and $\ddot{x}_{gm}$ = 0.2g

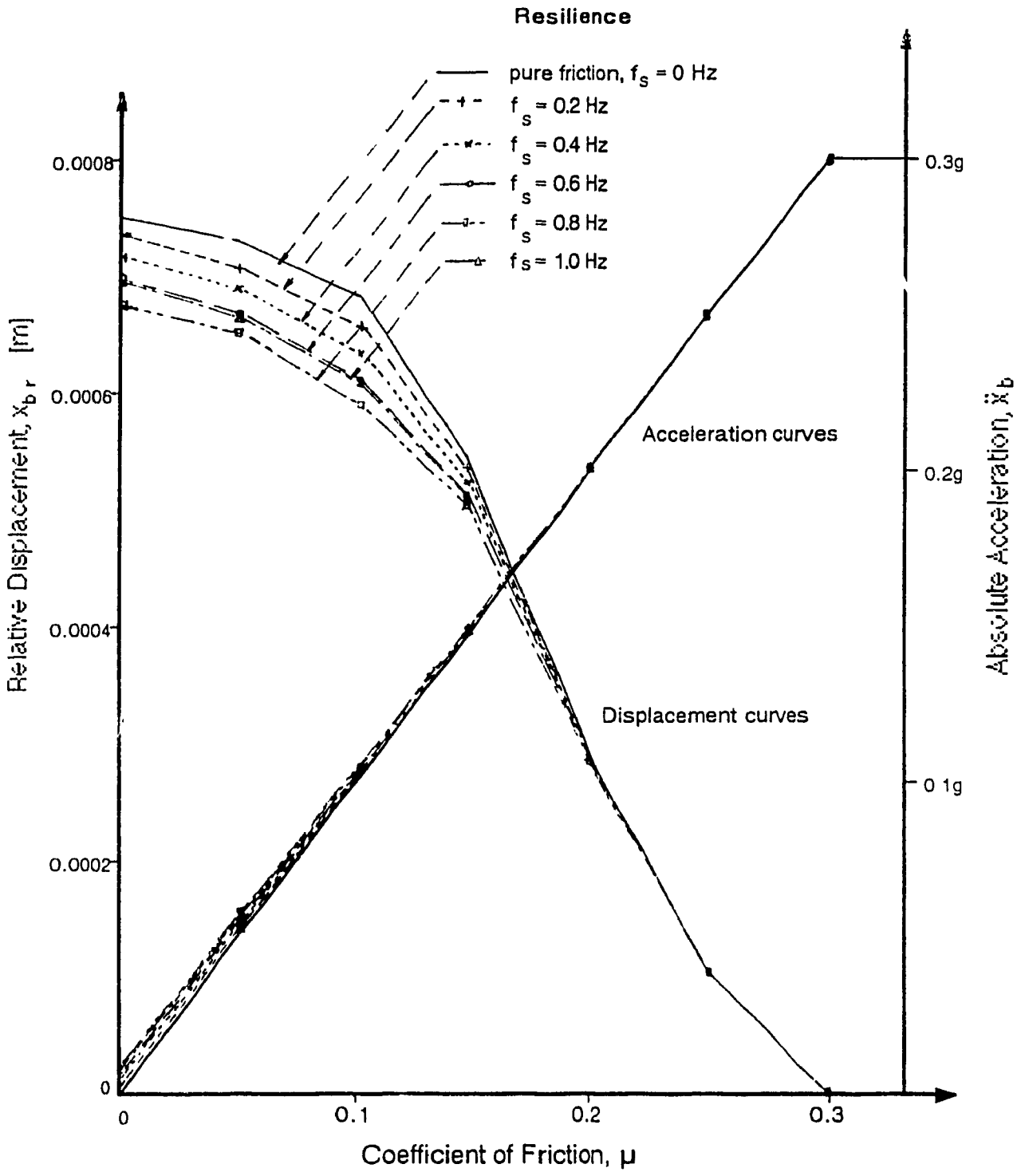

Figure 3-30 Body Response to Sinusoidal Ground Motion
f = 10 Hz, $\ddot{x}_{gm}$ = 0.3g

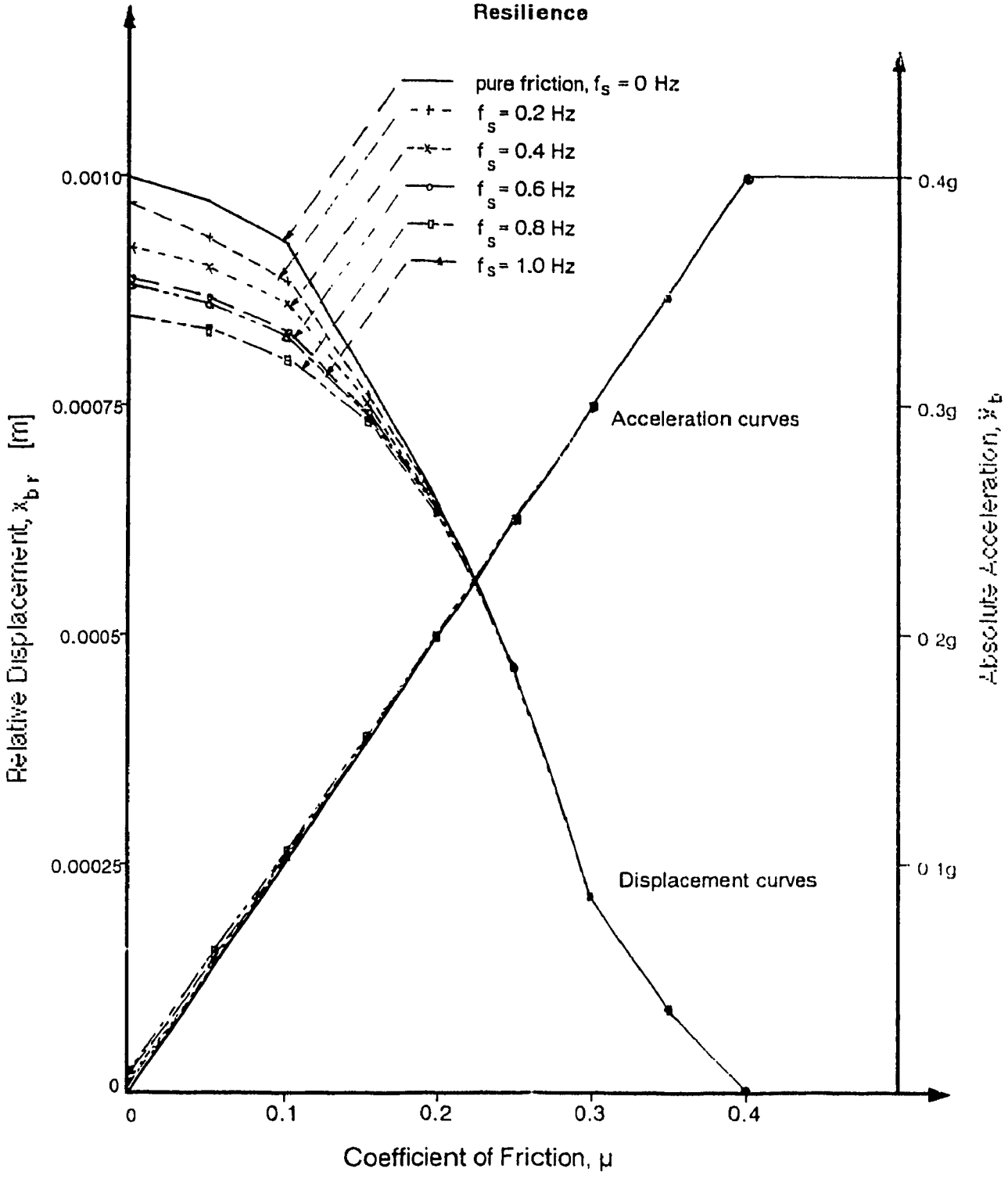

Figure 3-31 Body Response to Sinusoidal Ground Motion, f = 10 Hz and $\ddot{x}_{gm}$ = 0.4g

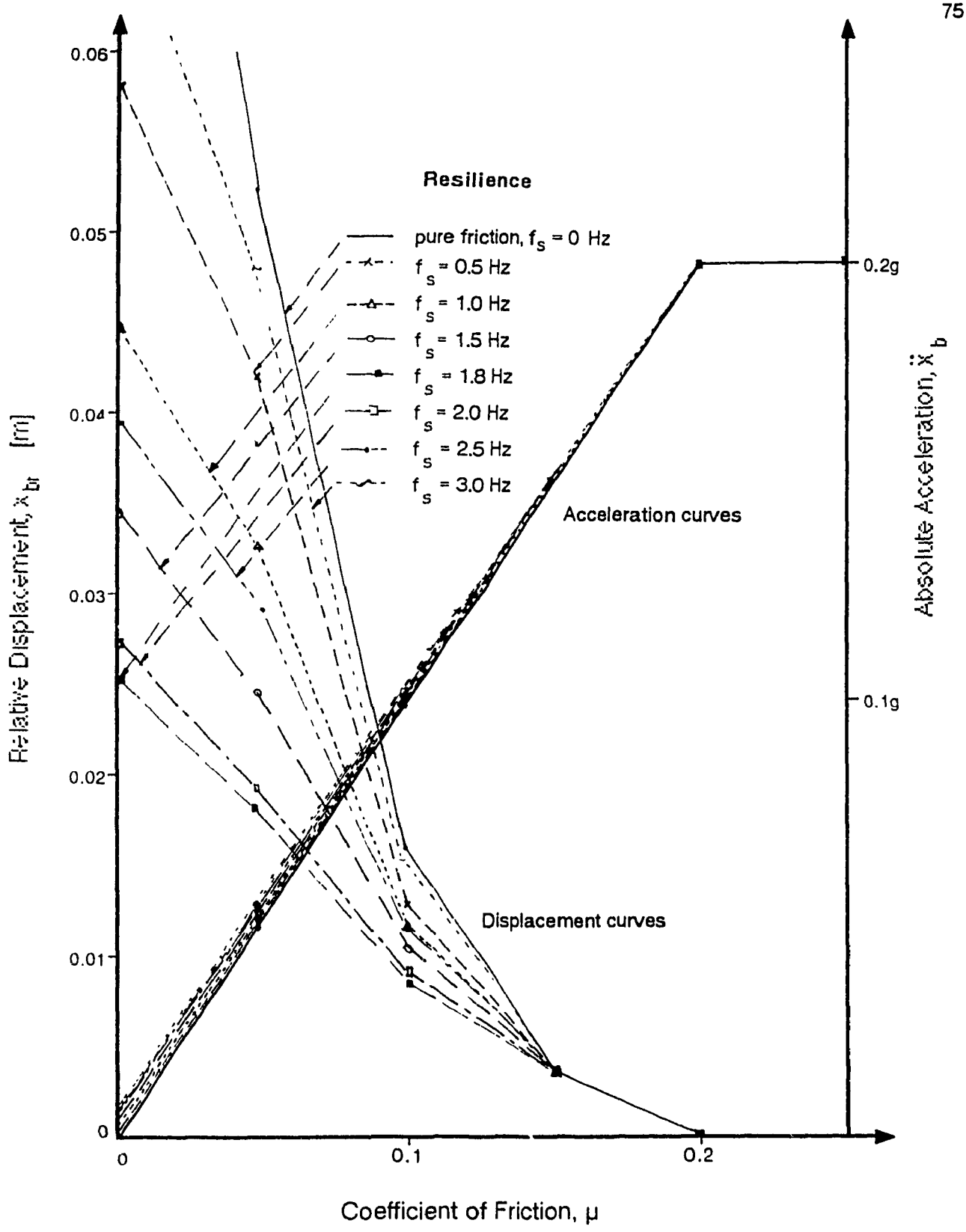

Figure 3-32 Body Response to El Centro Earthquake, $\ddot{x}_{gm}$ = 0.2g

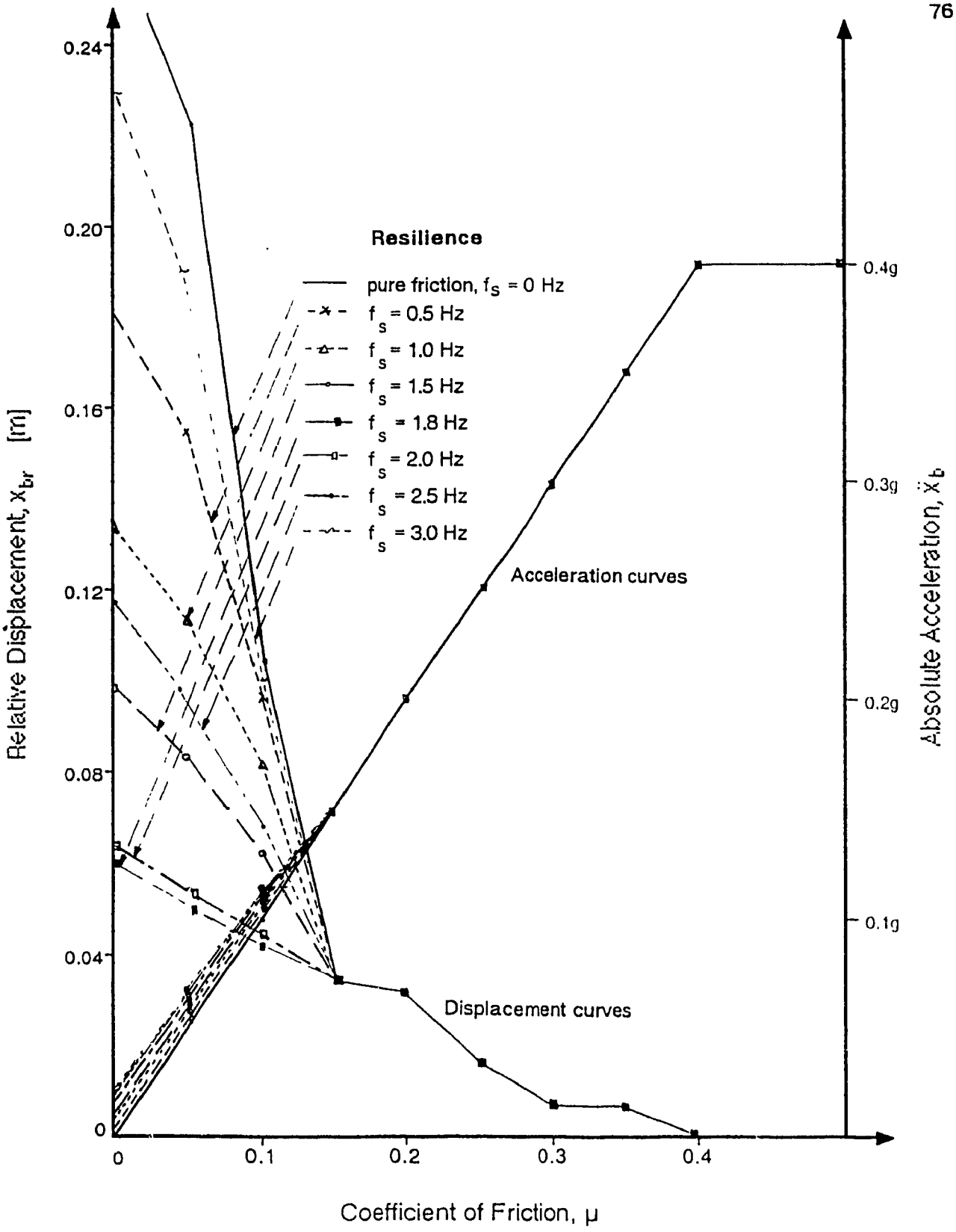

Figure 3-33 Body Response to El Centro Earthquake, $\ddot{x}_{gm} = 0.4g$

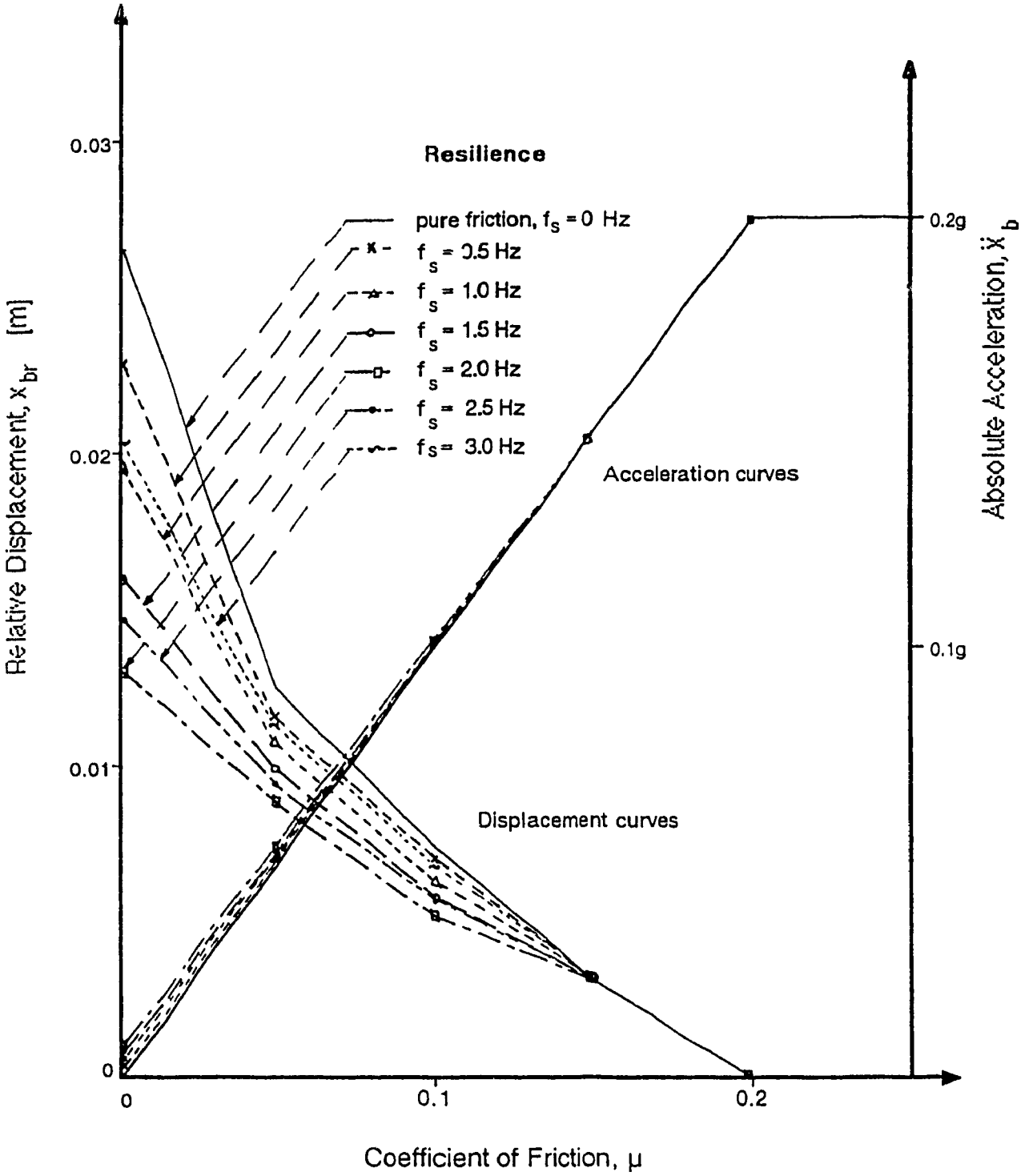

Figure 3-34 Body Response to Olympia Earthquake, $\ddot{x}_{gm}$ = 0.2g

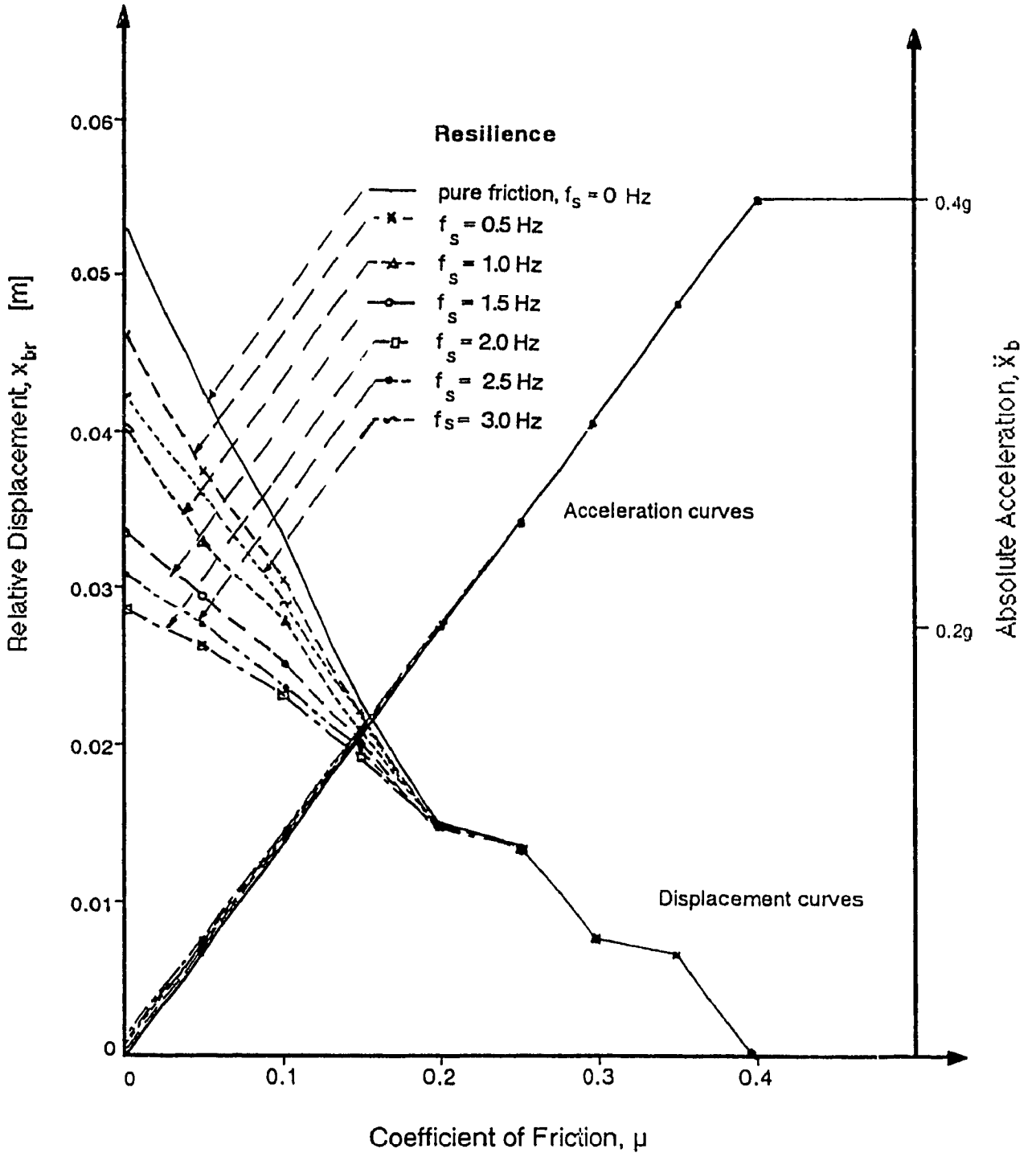

Figure 3-35 Body Response to Olympia Earthquake, $\ddot{x}_{gm} = 0.4g$

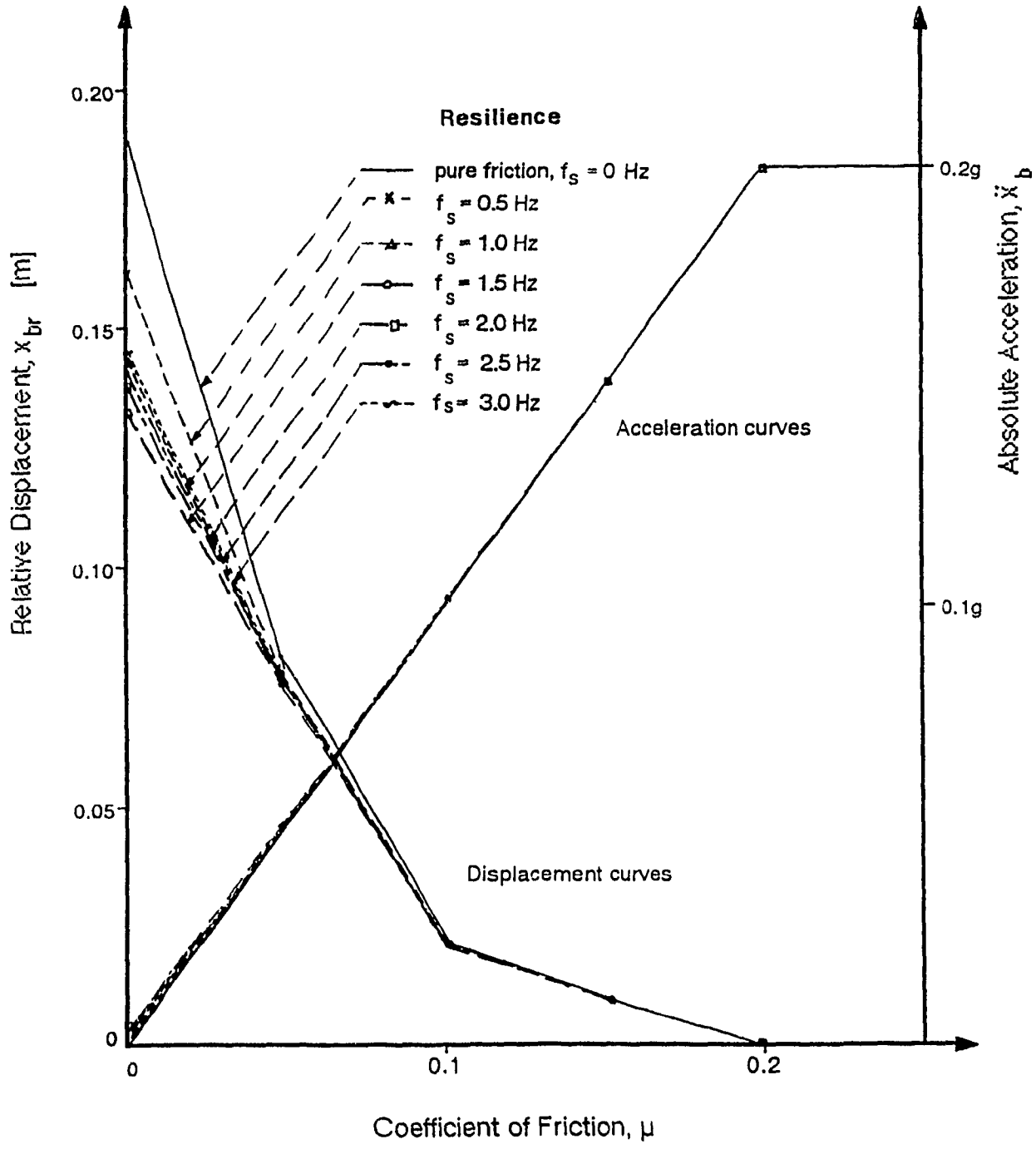

Figure 3-36 Body Response to N.B.K. Earthquake, $\ddot{x}_{gm}$ = 0.2g

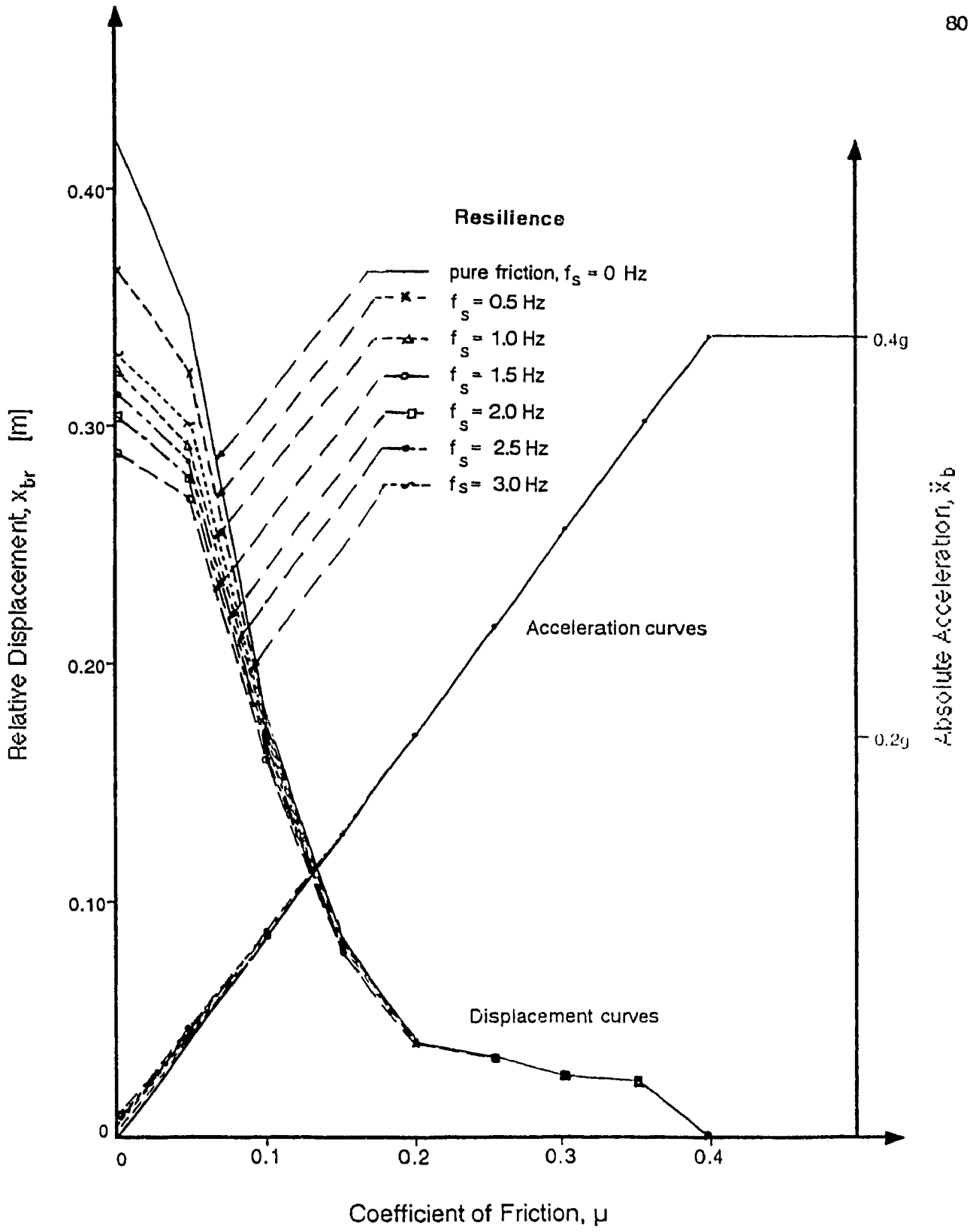

Figure 3-37 Body Response to N.B.K. Earthquake, $\ddot{x}_{gm} = 0.4g$

4. EXPERIMENTAL STUDIES

4.1 Objective of Experimental Studies

Experimental studies were conducted to: (1) determine the static and dynamic coefficients of friction of different contact surfaces; (2) determine the static and dynamic characteristics of the prototype friction base isolators with selected friction surfaces; (3) test friction base isolated models, with and without resilient constraints, on a shake table to check the validity of analytical studies.

4.2 Tests for Coefficient of Friction

4.2.1 Description of Test Assembly

The assembly for these tests is shown in Figure 4-1 (page 93). It consists of one central plate 175 x 125 x 12.7 mm with a slotted hole of 13 x 32 mm, and two cover plates of 200 x 125 x 9.5 mm with 14.3 mm diameter holes. Contact surfaces of these plates were specially treated to offer reliable friction. Before assembling the plates, all contact surfaces were cleaned of dust, oil and grease by using vaporised chlorinated hydrocarbon solvent (chlorothene NU degreaser).

The three plates were clamped together by tightening a 1/2" Ø bolt (ASTM A-325). The relationship between the actual

bolt tension and torque was established by using Hilti's 100 Digital Test Gauge, a bolt tension measuring device, fitted over the bolt. Figure 4-2 (page 94) shows the load calibration curve. The calibrated bolt was torqued to 0.062 kN·m to give a bolt tension of 50 kN.

The friction surface combinations were selected from the following dissimilar materials:

- hard chrome, metallized (H.C.M.)
- stainless steel, metallized (S.S.M.)
- aluminum bronze, metallized (A.B.M.)
- stainless steel plate (S.S.P.)
- teflon sheet (T.S.)
- leaded bronze plate (L.B.P.)

4.2.2 Test Procedure

Instron Universal Testing Machine, Model 1125 was used as a loading and recording device. This machine incorporates an electronic load weighing system with load cells that use strain gauges to measure tensile or compressive loads. A tension-compression load cell of 100 kN capacity was used for these tests.

The test assembly was mechanically attached to the load cell. Compressive and tensile loads were applied by the moving cross head. In order to measure accurate relative displacements between the plates of the test assembly, the Instron strain gauge extensometer was used and connected directly to the servo chart drive system which gave continuous load/displacement record. Specimens were tested for about 20 cycles of reversals.

4.2.3 Test Results

From the load/displacement curves (hysteresis loops), the static and dynamic slip loads were obtained. The coefficient of friction is given by:

$$\mu = \frac{P_s}{2W_c} \tag{4.1}$$

where P_s = slip force

W_c = clamping force

2 represents the two slip surfaces in the test configuration.

The coefficients of friction for different surface combinations are shown in Table 4-1. For the surfaces tested there is little difference between the static coefficient, μ_s, and the dynamic coefficient, μ_d. The hysteretic loop for a surface of H.C.M. sliding on A.B.M. (listed in Section 4.2.1)

is shown in Figure 4-3 (page 94).

Table 4-1 Coefficient of Friction - Test Results

FRICTION SURFACES	STATIC COEF., μ_s	DYNAMIC COEF., μ_d
1 H.C.M., S.S.M.		
test 1	0.24	0.23
test 2	0.25	0.24
2 S.S.M., A.B.M.		
test 1	0.16	0.16
test 2	0.15	0.15
3 H.C.M., A.B.M.		
test 1	0.16	0.16
test 2	0.16	0.16
4 A.B.M., T.S.		
test 1	0.05	0.04
test 2	0.05	0.04
5 S.S.P., L.B.P.		
test 1	0.18	0.14
test 2	0.16	0.13
6 H.C.M., L.B.P.		
test 1	0.24	0.20
7 S.S.P., A.B.M.		
test 1	0.17	0.16
test 2	0.17	0.16
8 S.S.P., A.B.M. machined		
test 1	0.10	0.10
test 2	0.09	0.09
9 H.C.M., A.B.M. machined		
test 1	0.12	0.11
test 2	0.11	0.10
10 H.C.M., A.B.M. machined and oil impregnated		
test 1	0.06	0.06

4.3 In-Situ Tests on Prototype Friction Base Isolators

4.3.1 Test Model

Four friction base isolators, connected to two steel beams carrying a concrete block of 1.5 x 1.5 x 0.42 m, was tested on a shake table (Fig. 4-4, page 95). The bottom halves of the four friction base isolators were fixed to the shake table with the top halves fixed to the steel beams. This assembly of steel beams and concrete block (Fig. 4-5, page 96) has a calculated mass of 2626 kg. To prevent lateral motion of the model during testing, greased rollers were placed against the sides of the steel beams.

4.3.2 Details of Specimen

Friction surface combinations #3 and #4, were selected for tests on prototype friction base isolators. The base metal of the friction base isolators was sand blasted prior to metallizing. In the first specimen, the bottom plate was metallized with aluminum bronze (A.B.M) and the top plate was metallized with hard chrome (H.C.M). In the second specimen, metallized aluminum bronze (A.B.M) was used on the bottom plate with teflon sheet (T.S.) attached to the top plate.

4.3.3 Test Procedure

A Simplex Hydraulic Jack with a Enerpac Pump was used to push the concrete mass on the friction supports. The slip load readings were taken from a Measurements Group P-3500 strain indicator which was connected to the load cell on the jack. The set-up for this test on the shake table is shown in Figure 4-6 (page 97).

Before testing, the slip surfaces were cleaned with Chlorothene NU degreaser.

4.3.4 Test Results

Figure 4-7 (page 98) shows the average force-displacement curve obtained from three tests for the first specimen (H.C.M. - A.B.M.). The slip load divided by the weight of the model gives the coefficient of friction, $\mu = 0.225$. The static and dynamic values were the same.

Figure 4-8 (page 98) shows the average force-displacement curve obtained from three tests for the second specimen (A.B.M. - T.S.). The static and dynamic coefficients of friction, $\mu_s = \mu_d = 0.035$, are very close to those noted in Table 4-1, $\mu_s = 0.05$, $\mu_d = 0.04$, using the Instron Universal Testing Machine. These results are also consistent with previous studies[24] which found the dynamic coefficient of

friction of teflon sliding on metal to be 0.032 for slow sliding.

4.4 Shake Table Tests

4.4.1 Test Equipment and Procedure

The shake table, 4 x 2 m, located in Concordia University's Civil Engineering Structural Laboratory, is supported by Thompson ball bushings riding on 100 mm Ø shafts attached to a frame which is bolted to the structural floor.[25] The table is driven horizontally by a hydraulic actuator controlled by a Moog valve. The electronic control system, supplied by Gilmore Industries, Inc., allows displacement control of the bed with a maximum possible displacement ≈ 75 mm.[25]

Accelerations of the shake table and test model were measured with an accelerometer. Table displacements were recorded by a direct pen drive on a chart recorder. The relative displacements of the block to the table were measured using a linear transducer read by a strain indicator and sent to a voltmeter which controlled a second pen on the chart recorder. Figure 4-9 (page 99) shows the set-up of the instrumentation.

Shake table testing was done using sinusoidal excitations at a frequency of 2 Hz.

4.4.2 Test Results

Comparison of the results of shake table tests with the analysis is shown in Table 4-2.

Table 4-2 Shake Table Test Results - Pure Friction, f = 2 Hz

	FRICTION SURFACE	
	A.B.M. and H.C.M.	A.B.M. and T.S
$\ddot{x}_{gm}$ measured	0.3g	0.3g
$\ddot{x}_{bm}$ measured (μg)	0.22g 0.22g	* 0.035g
x_{gm} measured analysis	18 mm 18.7 mm	18 mm 18.7 mm
x_{br} measured analysis (Fig. 3-24)	3.5 mm 3.0 mm	15.1 mm 17.4 mm

* indicates no valid readings

As expected, a decrease in the coefficient of friction from 0.22 to 0.035 leads to an increase in the relative displacement. The results from shake table testing tally with the computed and analytical results [except for $\ddot{x}_{bm}$ of aluminum bronze, with teflon sheet in which the experimental value of $\ddot{x}_{bm}$ in this case was due to impact of the top and bottom walls of the friction base isolators].

4.5 Friction Base Isolators with Resilience

4.5.1 Resilient Constraints

The springs used in this study, supplied by Associated Spring-Barnes Group to the specifications given in Table 4-3, were of music wire, ASTM A 228, which is a preferred material because of its high yield strength, toughness, high fatigue life and ability to take severe bends.[26]

Table 4-3 Spring Specifications

SIZE	C0360-045-1750
OUTSIDE Ø [mm]	9.14
WIRE Ø [mm]	1.14
FREE LENGTH [mm]	44.45
SPRING CONSTANT, k_s [N/mm]	2.66

Table 4-4 gives the spring combinations to give selected values of f_s.

Table 4-4 Spring Combinations

NUMBER OF SPRINGS PER FRICTION BASE ISOLATOR	k_{TOT} [N/mm]	f_s [Hz]
2	10.64	0.32
4	21.28	0.45
6	31.92	0.56

To facilitate the incorporation and removal of different groups of springs in the friction base isolators, four wooden blocks of the shape shown in Figure 4-10 (page 100) were manufactured. These blocks fitted in the spaces available between the top and bottom portion of the friction base isolators (Figure 4-11, page 100). Each block could hold up to six spring. To prevent buckling, steel dowels were introduced to guide the springs, as shown in Figure 4-12 (page 101). Figure 4-13 (page 101) shows a wooden block installed in position in a friction base isolator.

4.5.2 Shake Table Studies on Friction Base Isolators with Resilient Constraints

Testing was done using sinusoidal excitation, with a frequency of 2 Hz.

Results of shake table testing for friction base isolators (A.B.M. and H.C.M.) with springs are compared to the results of the computer analyses in Table 4-5.

Table 4-5 Shake Table Test Results for Friction Base Isolators (A.B.M. and H.C.M. Surfaces) with Resilient Constraints, f = 2 Hz, $\mu = 0.22$

	4 SPRINGS / FRICTION BASE ISOLATOR $f_s = 0.45$	6 SPRINGS / FRICTION BASE ISOLATOR $f_s = 0.56$
$\ddot{x}_{gm}$ measured	0.3g	0.3g
$\ddot{x}_{bm}$ measured analysis (Fig. 3-24)	0.22g 0.22g	0.23g 0.224g
x_{gm} measured theory	18 mm 18.7 mm	18 mm 18.7 mm
x_{br} measured analysis (Fig. 3-24)	3.5 mm 3.0 mm	3.5 mm 3.5 mm

The measured and recorded results from shake table testing agree with the computed values. As expected, an increase in f_s lead to an increase in $\ddot{x}_{bm}$. The corresponding measured increase in x_{br} was too small to be detected.

The above tests were repeated for slip surface of A.B.M. and T.S. Table 4-6 compares the experimental results to those obtained from analyses.

Table 4-6 Shake Table Test Results for Friction Base Isolators (A.B.M. and T.S. Surfaces) with Resilient Constraints, f = 2 Hz, $\mu = 0.035$

	4 SPRINGS / FRICTION BASE ISOLATOR $f_s = 0.45$	6 SPRINGS / FRICTION BASE ISOLATOR $f_s = 0.56$
$\ddot{x}_{gm}$ measured	0.3g	0.3g
$\ddot{x}_{bm}$ measured analysis (Fig. 3-24)	* 0.055g	* 0.065g
x_{gm} measured theory	18 mm 18.7 mm	18 mm 18.7 mm
x_{br} measured analysis (Fig. 3-24)	15.0 mm 14.8 mm	15.0 mm 15.0 mm

* no valid readings obtained

The results of x_{br} from shake table testing agree with the computed values. The measured increase in x_{br} corresponding to an increase in f_s from 0.45 Hz to 0.56 Hz was too small to be detected.

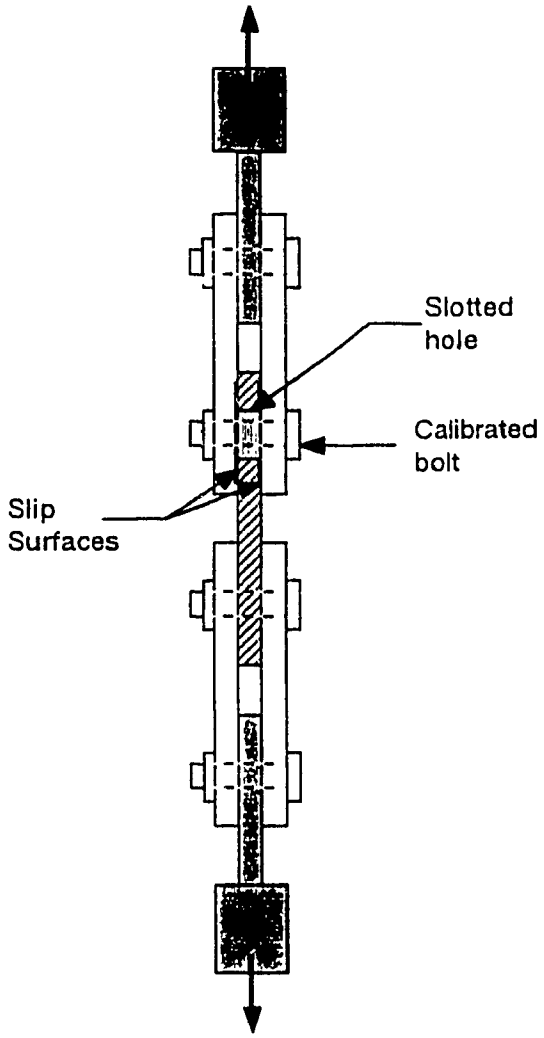

Figure 4-1 Assembly to Test for Coefficients of Friction

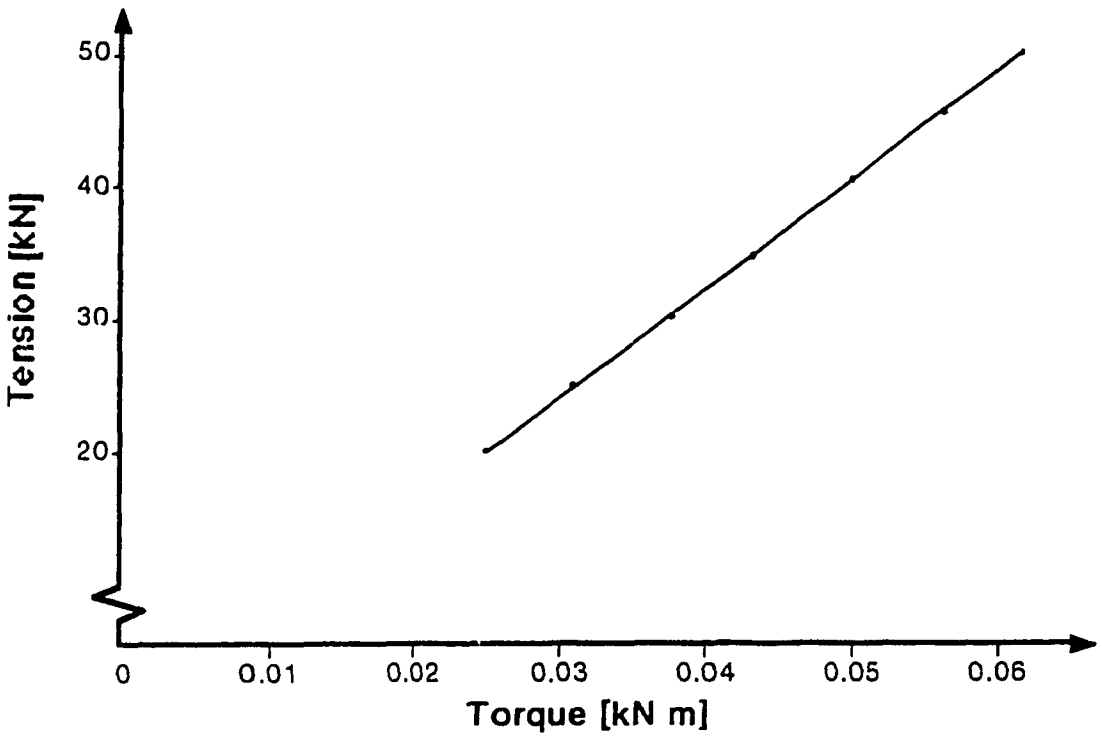

Figure 4-2 Load Calibration Curve

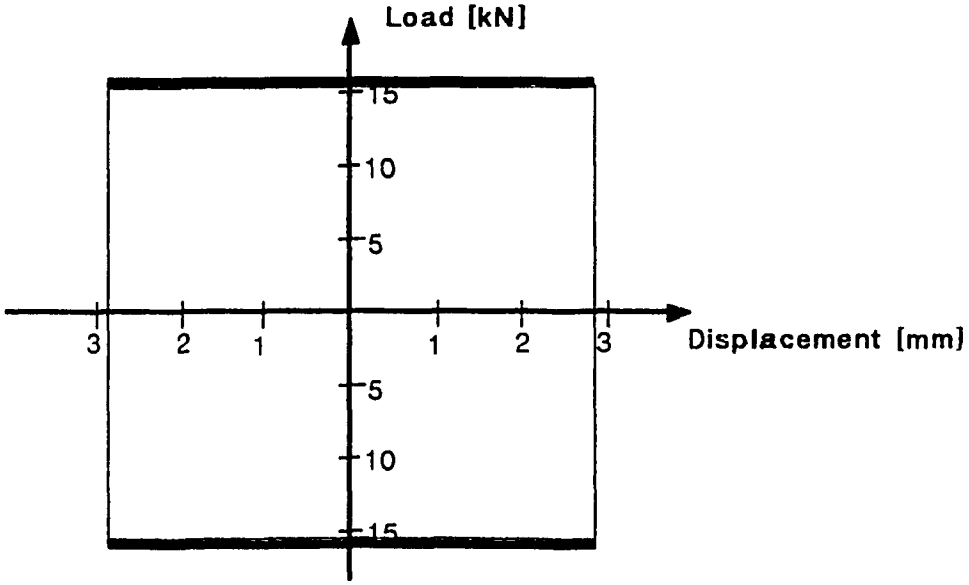

Figure 4-3 Hysteretic Loop - Slip Surface H.C.M. with A.B.M.

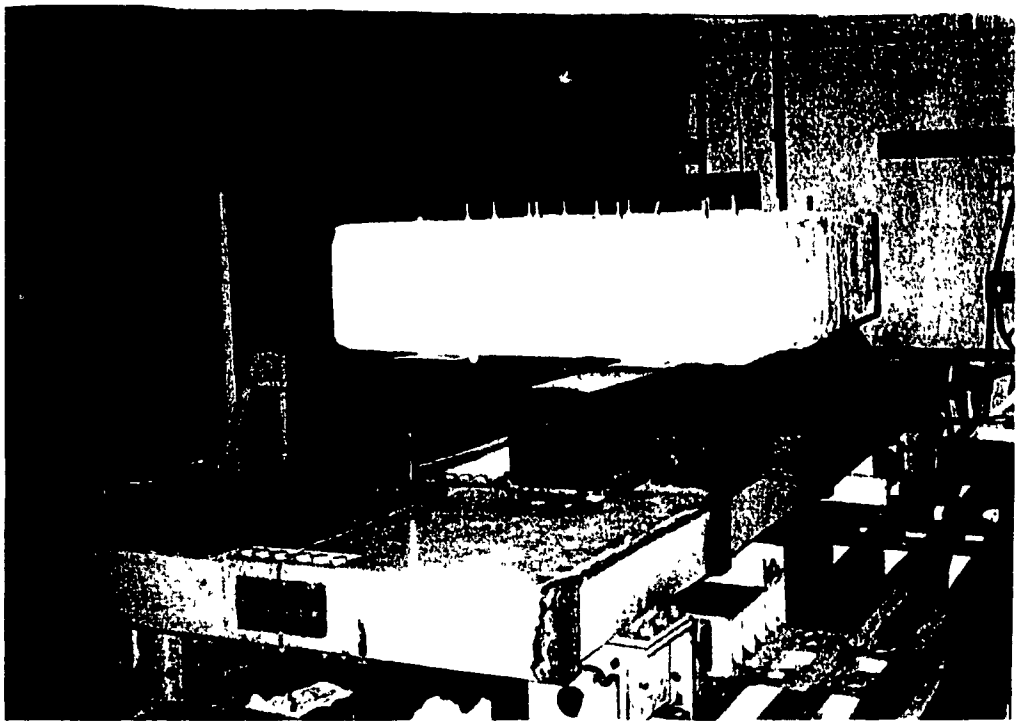

Figure 4-4 Model for Shake Table Tests

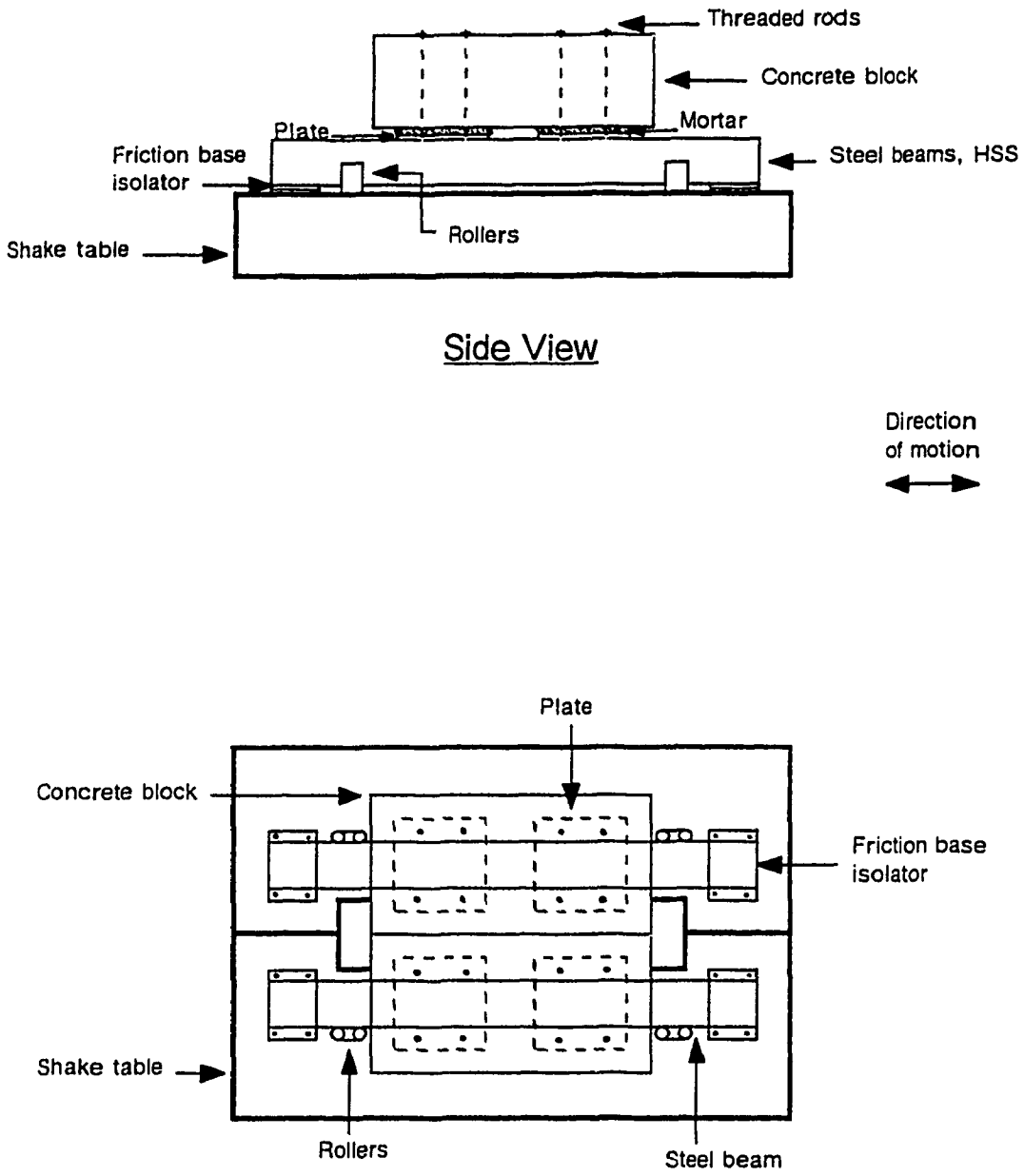

Figure 4-5 Model for Shake Table Tests - Side and Top View

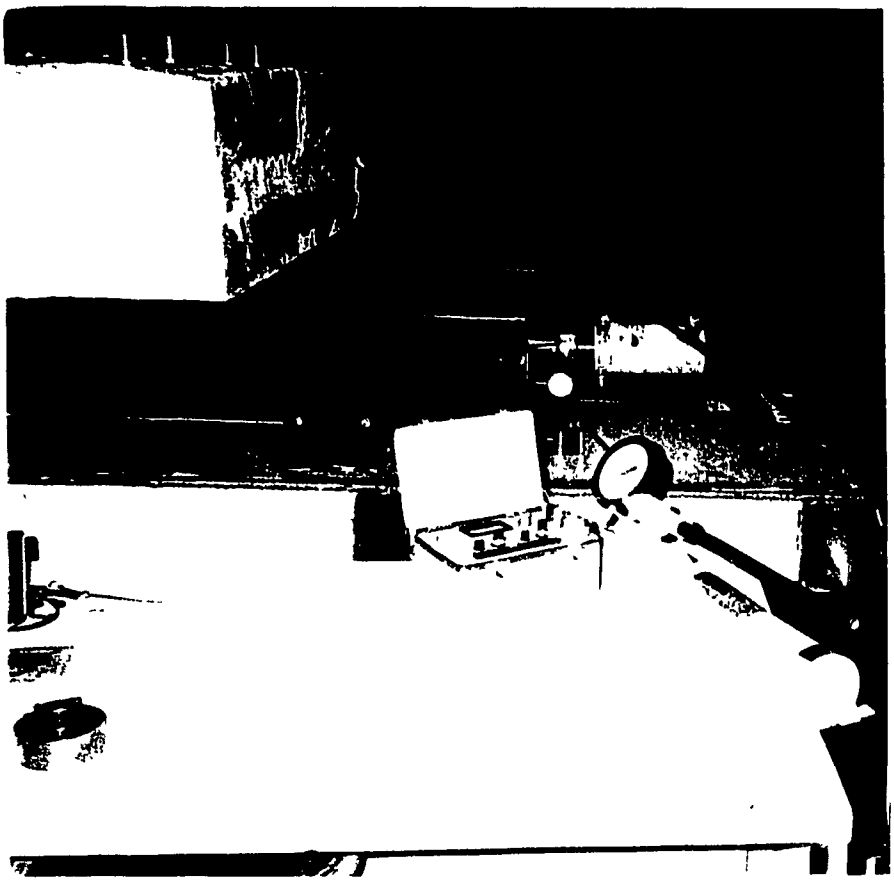

Figure 4-6 At Site Static Test Set-up

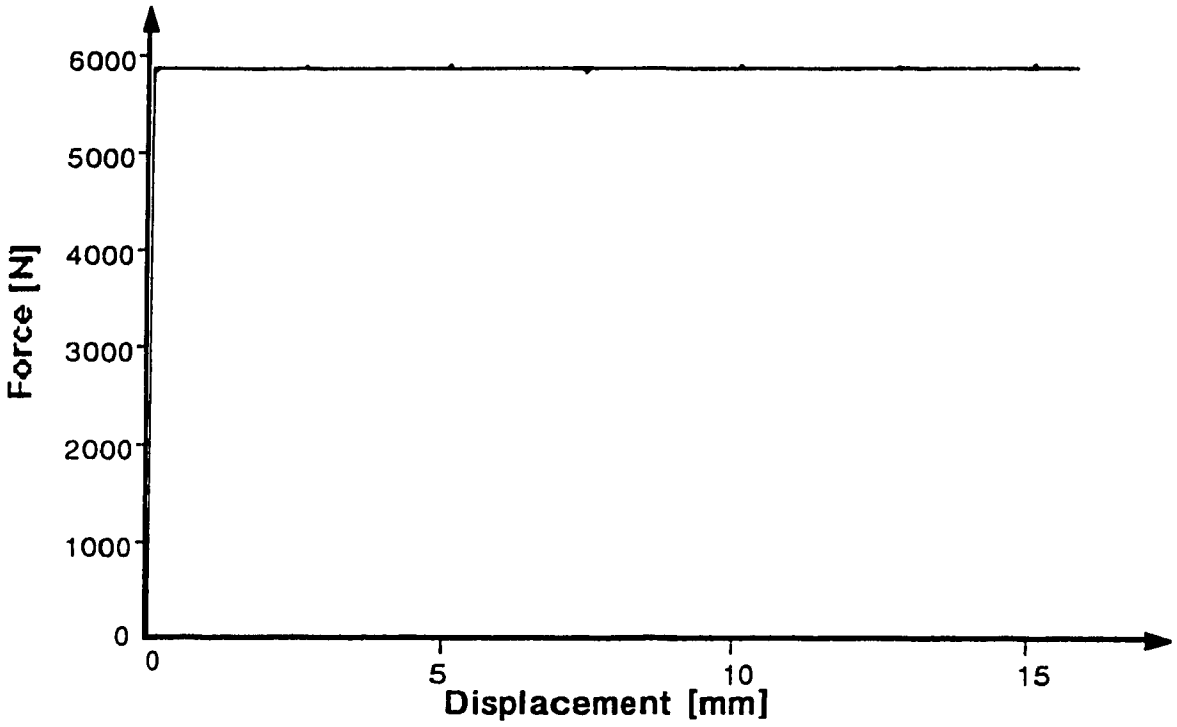

Figure 4-7 Force-Displacement Curve for A.B.M. and H.C.M.

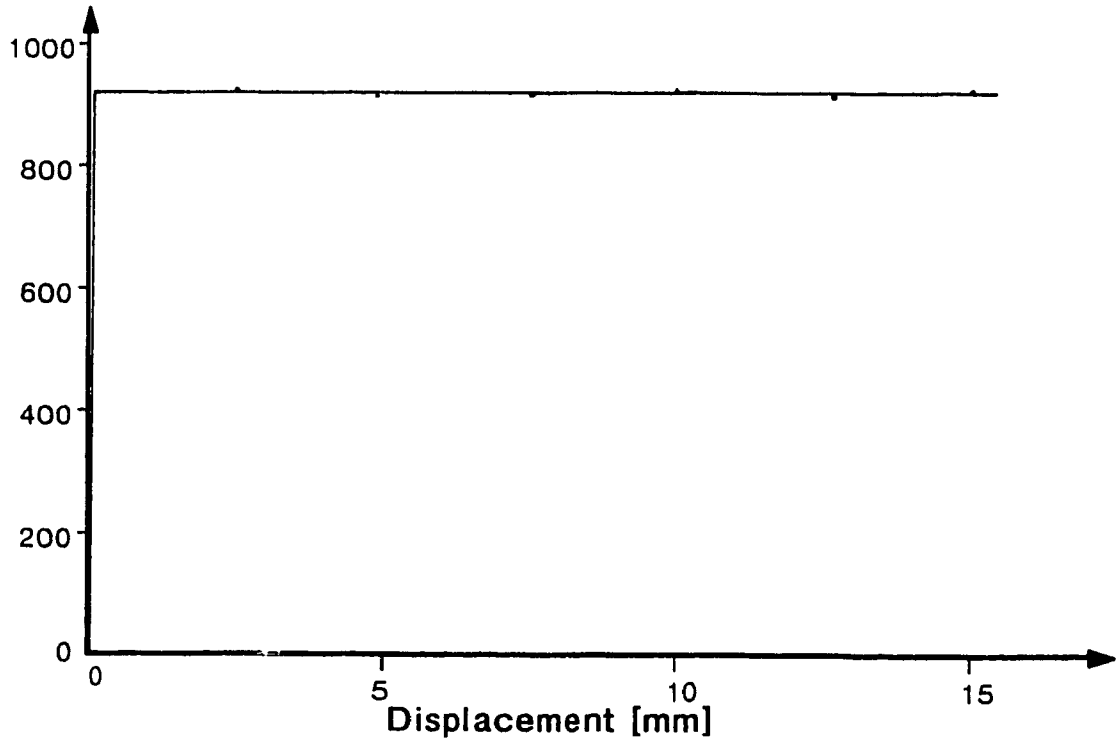

Figure 4-8 Force-Displacement Curve for A.B.M. and T.S.

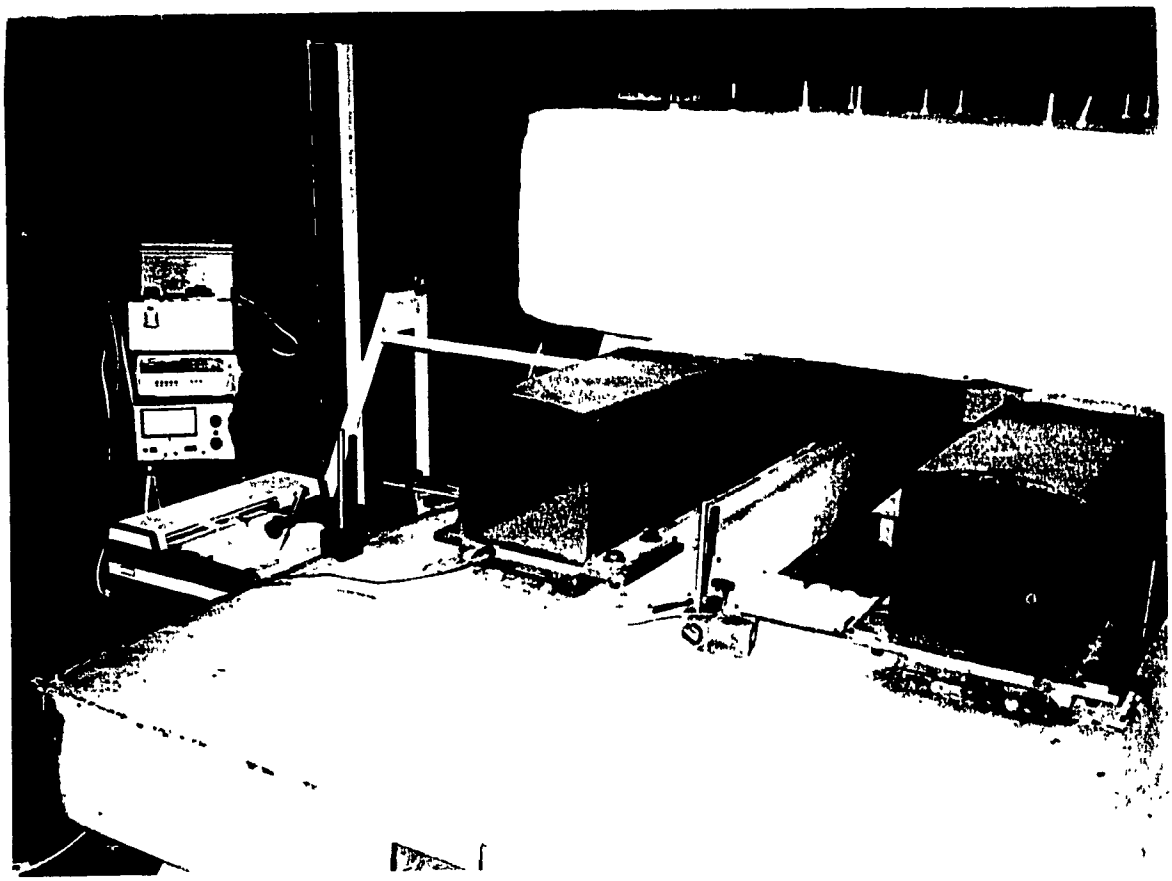

Figure 4-9 Instrumentation

Figure 4-10 Wooden Block

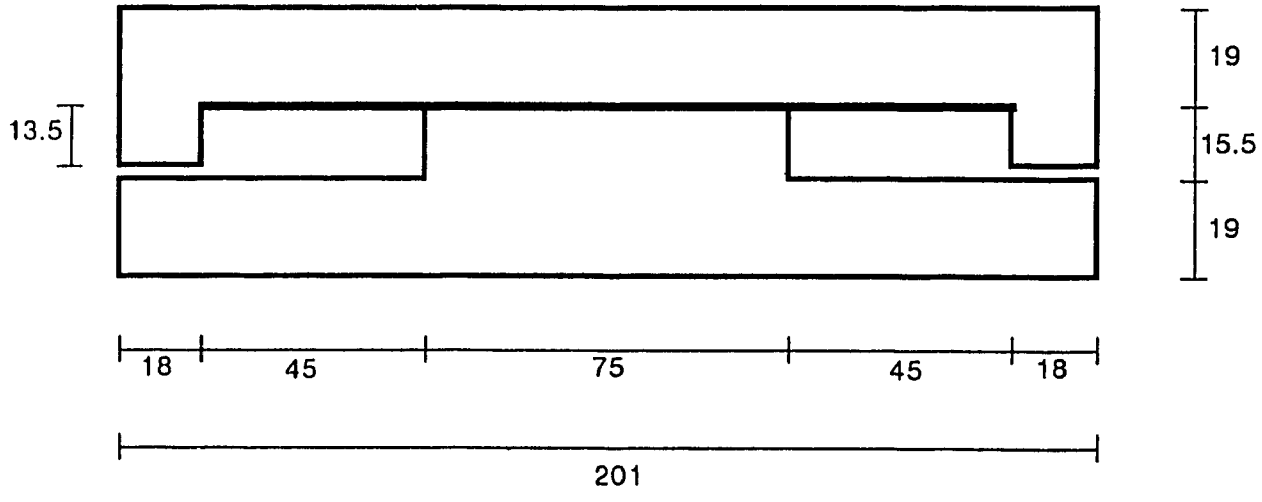

Figure 4-11 Cross-Section of Friction Base Isolator in Direction of Motion

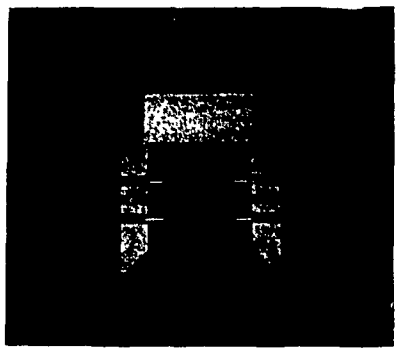

Figure 4-12 Wooden Block with Dowels in Springs

Figure 4-13 Wooden Block with Springs Positioned in Friction Base Isolator

5. CONCLUSIONS

5.1 General

The relationships between the coefficient of friction, wind force, the aspect ratio of a building and the resilient constraint have been established. To resist wind in the Montreal region, a minimum coefficient of friction of 0.10 is required for a typical wood stud / brick veneer construction. To prevent uplift at the base of the structure during earthquakes, the height should not be greater than the depth/3μ for a structure with a large number of base isolators located in a line. These considerations set the minimum and maximum values of the coefficient of friction.

With pure friction base isolators, an increase in the coefficient of friction leads to a decrease in relative displacements and an increase in accelerations. It has been shown that for an earthquake intensity of $\ddot{x}_{gm}$=0.2g, a coefficient of friction of 0.1 will halve the maximum acceleration of the body and reduce the maximum relative displacement to 13%, 31% and 11% of the amplitude of the ground displacement for El Centro, Olympia and N.B.K. earthquakes, respectively.

By adding resilient constraints the unrestricted progressive displacement of the building is prevented,

and the maximum relative displacements are significantly reduced, while the accelerations of the body increase only marginally. It was observed that, for a given earthquake, as the natural frequency of the spring/mass system increased, the relative displacement decreased until the natural frequency reached an optimum value, beyond which the displacement increased as the system frequency moved towards the value of the predominant ground frequency. As the response is sensitive to the relationship between the natural frequency of the spring/mass system and the frequency spectrum of the ground motion it is important to carry out analyses for site specific ground motions.

Shake table studies confirmed the results of the analysis for sinusoidal excitations.

The qualities of friction base isolators, with and without resilient constraints, are compared to different base isolators in Appendix E. Friction base isolators are shown to provide an effective approach to the design of low-rise structures to resist earthquakes and to control damage to the building and its contents.

5.2 Recommendations for Future Studies

In this research, the shake table motion was limited to sinusoidal motion. In future studies, experimental work with typical earthquake time-histories on multi-degree-of-freedom structures should be considered.

REFERENCES

1. Supplement to National Building Code of Canada, 1990, Commentary B and J, pp. 141-171, pp. 202-220.
2. Tarics, A.G., "Earthquake - Are We Ready?", The Military Engineer, September-October, 1987, pp. 486-490.
3. State of California Assembly Concurrent Resolution No. 55 - Relative to Seismic Safety, Filed with Secretary of State September 20, 1985.
4. Pall, A., Verganelakis, V., Marsh, C., "Friction Dampers for Seismic Control of Concordia University Library Building", Proceedings, Fifth Canadian Conference on Earthquake Engineering, Ottawa, Ontario, 1987, p.191-200.
5. Kelly, J., "State-of-the-Art and State-of-the-Practice in Base Isolation", Proceedings of Seminar on Seismic Isolation, Passive Energy Dissipation, and Active Control; Applied Technology Counci.., San Francisco, California, 1993, pp. 9-28.
6. Kelly, J.,"Progress and Prospects in Seismic Isolation", Proceedings of Seminar on Base Isolation and Passive Energy Dissipation; Applied Technology Council, San Francisco, California, 1986, pp. 29-38.
7. Elsesser, E., "A Survey of Seismic Structural Systems and Design Implications", Proceedings of Seminar on Base Isolation and Passive Energy Dissipation; Applied Technology Council, San Francisco, 1986, pp. 51-62.

8. Vaidya, R., Plichon, C., "On the Concept of Base Isolation Design in France", Proceedings of Seminar on Base Isolation and Passive Energy Dissipation; Applied Technology Council, San Francisco, 1986, pp. 175-184.

9. Mostaghel, N., "Resilient Friction Base Isolator", Proceedings of Seminar on Base Isolation and Passive Energy Dissipation; Applied Technology Council, San Francisco, California, 1986, pp. 221-230.

10. Su, L., Goodarz, A., Tadjbakhsh, I., "Performance of Sliding Resilient-Friction Base Isolation System", ASCE Journal of Structural Engineering, Vol. 117, No. 1, January 1991, pp. 165-181.

11. Zayas, V., Low, S., Stephen, M., "The FPS Earthquake Resisting System - Experimental Report", Report No. UCB/EERC-87/01, University of California, Berkeley, California, June 1987, pp. 1-3.

12. Pall, A.S., Pall, R., "Friction Base Isolated House in Montreal", Proceedings, Sixth Canadian Conference on Earthquake Engineering, Toronto, June, 1991, pp. 375-382.

13. Hadijian, A., Tseng, W., "A Comparative Evaluation of Passive Seismic Isolation Schemes", Proceedings of Seminar on Base Isolation and Passive Energy Dissipation; Applied Technology Council, San Francisco, California, 1986, pp. 291-304.

14. Martelli, A., Parducci, A., Forni, M., "State-of-the-Art on Development and Application of Seismic Design

Innovative Seismic Design Techniques in Italy", Proceedings of Seminar on Seismic Isolation, Passive Energy Dissipation, and Active Control; Applied Technology Council, San Francisco, 1993, pp. 401-412.

15. Palfalvi, B., Amin, N., Mokha, A., Fatehi, H, Lee, P., "Implementation Issues in Seismic Isolation Retrofit of Government Buildings", Proceedings of Seminar on Seismic Isolation, Passive Energy Dissipation, and Active Control; Applied Technology Council, San Francisco, California, 1993, pp. 257-264.
16. Vagliente, V., "Age-Hardening of Elastomeric Bearing Pads", Proceedings of Seminar on Base Isolation and Passive Energy Dissipation; Applied Technology Council, San Francisco, California, 1986, pp. 323-330.
17. Tabor, D., "Friction - The Present State of Our Understanding", Journal of Lubrication Technology, Vol. 103, April 1981, pp. 169-178.
18. Beer, F. "Mechanics for Engineers - Statics and Dynamics", McGraw-Hill Inc., Fifth Edition, 1989, pp. 301-309.
19. Westermo, B., Udwadia, F., "Periodic Response of a Sliding Oscillator System to Harmonic Excitation", Earthquake Engineering and Structural Dynamics, Vol. 11, 1983, pp. 135-145.
20. Kanaan, A.E., Powell, G.H., "DRAIN-2D, A General Purpose Computer Program of Dynamic Analysis of Inelastic Plan

Structures", University of California, Berkeley, California, 1973.

21. Tan, M., "A Study on Friction-Damped-Frames", Masters Thesis, Concordia University, Montreal, Quebec, 1992, pp. 27-62.

22. Blume, J., Newmark, N., Corning, L., "Design of Multistory Reinforced Concrete Buildings for Earthquake Motions", Portland Cement Association, Chicago, Illinois, 1961, pp. 2.

23. Shenton, H., "Draft Guideline for Testing and Evaluation of Seismic Isolation Systems", Proceedings of Seminar on Seismic Isolation, Passive Energy Dissipation, and Active Control; Applied Technology Council, San Francisco, California, 1993, pp. 349-354.

24. Mokha, A., Constantinou, M., Reinhorn, A., "Verification of Friction Model of Teflon Bearings Under Triaxial Load", Journal of Structural Engineering, Vol. 119, No. 1, January 1993, pp. 240-261.

25. Pekau, O., Marsh, C., Hradil, H., "Simulation of Earthquake Effects on Buildings", Proceedings, Third International Symposium on Lower-Cost Housing Problems, Concordia University, Montreal, Quebec, May 1974, pp. 996-1004.

26. Carlson, A., "Springs - Troubleshooting and Failure Analysis", Marcel Dekker Inc., New York, 1980, pp. 3-45.

APPENDIX A STATE OF CALIFORNIA ASSEMBLY RESOLUTION

"This measure would request the State Architect to give full consideration to new technology that can mitigate the effects of a major earthquake on new or existing public buildings, personnel, equipment, data systems, and other elements of vital concern to the state that are at risk from seismic events, would request the State Architect to report back to the Legislature within 120 days on the actions taken to effect the use of new seismic technology in new building design or retrofitted into existing buildings, and would request that the State Architect take whatever action is permitted under existing law to incorporate new seismic technology into state and other publicly owned, operated, or licensed buildings to mitigate the negative effects of earthquakes.

WHEREAS, There are now whole new parameters of consideration to be taken into account as buildings now contain extremely sensitive and costly equipment that has become vital in education, business, commerce, and health, among others, and records which are kept electronically must be protected; and

WHEREAS, Most of the above requirements cannot be met through past seismic design approaches which were directed toward survival of the building structure itself, and it is now necessary to protect the structure and the building contents; and

WHEREAS, There are emerging new technologies, such as base isolation, that can be incorporated into new building design or retrofitted into existing buildings which will protect both the building and its contents during a seismic event; and

WHEREAS, The officers of the state have a duty and responsibility for the protection of the property of the state, for the lives of the citizens of the state, and the prevention of the breakdown of the infrastructure of society in the aftermath of a major earthquake, and there is also a need to provide for uninterrupted operation of hospitals, rescue services, schools, and communications, as well as the necessity for the protection of public records in connection with social services and insurance; now, therefore, be it

Resolved by the Assembly of the State of California, the Senate thereof concurring, that the State Architect is hereby requested to give full consideration to new technology, including but not limited to base isolation, that can mitigate the effects of a major earthquake on new or existing public buildings, personnel, equipment, data systems, and other elements of vital concern to the state that are at risk from seismic events".

APPENDIX B - BASE ISOLATED BUILDINGS IN THE UNITED STATES

Table B-1 Some Base Isolated Buildings in United States[3]

BUILDING	OWNER	TOTAL COST OF PROJECT million ($US)	ISOLATION SYSTEM USED
Foothills Communities Law and Justice Center (California)	County of San Bernard	36	HDR *
Aircraft Simulator Manufacturing Facility (Utah)	Evans and Sutherland Corp.	8	LRB **
University of Southern California Hospital (California)	U.S.C.	50	LRB
Fire Command and Control Facility (California)	County of Los Angeles	6.3	HDR
Titan Solid Rocket Motor Storage (California), near completion	U.S. Air Force	----	HDR
Kaiser Computer Center (California)	Kaiser Foundation Health Plan	32	LRB, HDR
Salt Lake City and County Building (Utah), retrofit	Salt Lake City Corp.	30	LRB
Mackay School of Mines (Nevada), retrofit	University of Nevada	7	HDR

*HDR = High-damping rubber bearings

**LRB = Lead rubber bearings

APPENDIX C - SINMOT

```
C          COMPUTER PROGRAM SINMOT  -   by Rashmi Pall
C
c      program to solve for relative displacements and
c      absolute accelerations of body using equations of
c      motion.
c
c      ab      = absolute acceleration of body
c      abr     = relative acceleration of body
c      ag      = ground acceleration
c      agm     = peak ground acceleration
c      Deltat = time step interval
c      f       = frequency of ground motion
c      fs      = natural frequency of the spring-mass system
c      I       = # of time step
c      mu      = coefficient of friction
c      T       = time
c      vb      = absolute velocity of body
c      vbr     = relative velocity of body
c      vg      = ground velocity
c      xbr     = relative displacement of body
c
       integer k(510),v
       real ab(510),abr(510),ag(510),agm,deltat,f,fs,
      +g,maxaccp,maxaccn,maxdisp,maxdisn,mu,mug,negmug,
      +pi,t(510),time,vb(510),vbr(510),vg(510),xbr(510)
c
c      read input data pertaining to friction base
c      isolators and ground motion
c
        open (unit=6,file='sinmot.out',status='new')
        print *,'enter coefficient of friction, mu'
        read *, mu
        print *,'enter natural freq. of spring-mass system, fs
       +     [Hz]'
```

```
      read *, fs
      print *,'enter freq. of ground motion, f [Hz]'
      read *, f
      print *,'enter peak ground acceleration / g, agm'
      read *, agm
      print *,'enter time step interval, deltat'
      read *, deltat
      print *,'enter total # of time step intervals, tott'
      read *, tott
c
      write (6,2) mu,fs,f,agm,deltat,tott
2     format (//,'  coefficient of friction, mu = ',f5.3,/,
     +'  natural freq. of spring-mass system, fs [Hz] =
     +',f5.3,/,
     +'  freq. of ground motion, f [Hz] = ',f5.3,/,
     +'  peak ground acceleration / g, agm = ',f5.3,/,
     +'  time step interval, deltat = ',f6.4,/,
     +'  total # of time step intervals, tott = ',f6.1,//)

c
      print (6,5)
5     format ('Time [sec]',2x,'xbr [m]',2x,
     + 'vg [m/s]',2x,'vb [m/s]',2x,'ag [m/s^2]',2x,
     + 'abr [m/s^2]',2x,'ab [m/s^2]')
c
      pi=3.14159
      g=9.81
      mug=mu*g
      negmug=-1*mug
      agm=agm*g
c
      i=1
      k(i)=0
      t(i)=0.0
      time=t(i)
      abr(i)=mu*g-agm
      vbr(i)=0.0
```

```
      xbr(i)=0.0
      vg(i)=(agm/(2*pi*f))*sin(2*pi*f*time)
      vb(i)=vbr(i)+vg(i)
      ag(i)=agm*cos(2*pi*f*time)
      ab(i)=abr(i)+ag(i)
c
      i=i+1
      k(i)=0
      t(i)=deltat
      time=t(i)
      abr(i)=abr(i-1)
      vbr(i)=abr(i-1)*deltat
      xbr(i)=0.5*mu*g*(deltat)**2-0.5*agm*(deltat)**2
      vg(i)=(agm/(2*pi*f))*sin(2*pi*f*time)
      vb(i)=vbr(i)+vg(i)
      ag(i)=agm*cos(2*pi*f*time)
      ab(i)=abr(i)+ag(i)
c
      do 10 j=1,tott
        i=i+1
        t(i)=deltat*(i-1)
        time=t(i)
        xbr(i)=2*xbr(i-1)-xbr(i-2)+abr(i-1)*(deltat)**2
        vbr(i-1)=(xbr(i)-xbr(i-2))/(2*deltat)
        vg(i)=(agm/(2*pi*f))*sin(2*pi*f*time)
        vb(i-1)=vbr(i-1)+vg(i-1)
        v=vb(i-1)*1000-vg(i-1)*1000
          if (v .eq. 0) then
              print (6,11) v,vg(i-1),vb(i-1),t(i-1)
11            format (' v=',i3,'  vg(i-1)=',f8.4,
     +        '  vb(i-1)=',f8.4,' t=',f5.4)
          end if
        ag(i)=agm*cos(2*pi*f*time)
         if (vb(i-1) .ge. vb(i-2)) then
              abr(i)=mu*g-(2*pi*fs)**2*xbr(i)-ag(i)
                if (v .eq. 0) then
                    abr(i)=-1*mu*g-(2*pi*fs)**2*xbr(i)-ag(i)
```

```
                else
                    abr(i)=mu*g-(2*pi*fs)**2*xbr(i)-ag(i)
                end if
            else
                abr(i)=-1*mu*g-(2*pi*fs)**2*xbr(i)-ag(i)
                if (v .eq. 0) then
                    abr(i)=mu*g-(2*pi*fs)**2*xbr(i)-ag(i)
                else
                    abr(i)=-1*mu*g-(2*pi*fs)**2*xbr(i)-ag(i)
                end if
            end if
          ab(i)=abr(i)+ag(i)
10      continue
c
        maxaccp=0.0
        maxaccn=0.0
        maxdisp=0.0
        maxdisn=0.0
        do 30 i=1,tott
          if (maxaccp .le. ab(i)) then
              maxaccp=ab(i)
          end if
          if (maxaccn .ge. ab(i)) then
              maxaccn=ab(i)
          end if
          if (maxdisp .le. xbr(i)) then
              maxdisp=xbr(i)
          end if
          if (maxdisn .ge. xbr(i)) then
              maxdisn=xbr(i)
          end if
          print (6,20) t(i),xbr(i),vg(i),vb(i),ag(i),
     +          abr(i),ab(i)
20        format (2x,f5.3,4x,f7.4,4x,f7.4,4x,f7.4,4x,
     +          f7.4,4x,f7.4,4x,f7.4)
30      continue
        print (6,40)
```

```
40     format ('Time [sec]',2x,'xbr [m]',2x,
     + 'vg [m/s]',2x,'vb [m/s]',2x,'ag [m/s^2]',2x,
     + 'abr [m/s^2]',2x,'ab [m/s^2]')

       print (6,50) maxaccp,maxaccn,maxdisp,maxdisn
50     format (/,'  max. ab=',f7.4,'  min. ab=',f8.4,' m/s^2',
     +/'  max. xbr=',f7.4,'  min. xbr=',f8.4,' m')
c
       stop
       end
```

APPENDIX D - ACCEL

```
C          COMPUTER PROGRAM ACCEL  -   by Rashmi Pall
C
C      PROGRAM TO READ TIME-DVA.LST FILE OF DRAIN-2D
C      TO CALCULATE ABSOLUTE VELOCITIES AND ACCELERATIONS
C      OF A NODE AT EACH TIME STEP.
C
C      I = time step
C      4000 = # of integration time steps
C      ABSACC = absolute nodal acceleration
C      GRACC = ground acceleration
C      RELDIS = relative nodal displacement
C      RELACC = relative nodal acceleration
C
       REAL TIME(4000),RELDIS(4000),RELACC(4000),GRACC(4000),
      +ABSACC(4000),MAXPOS,MAXNEG
C
       OPEN (UNIT=5,FILE='TIME-DVA.LST',STATUS='OLD')
       OPEN (UNIT=6,FILE='ACCEL.DAT',STATUS='NEW')
C
C      Access DRAIN 2D's input ground accelerations:
       DO 20 I=1,4000
         READ (5,*) GRACC(I)
10       FORMAT (5X,F10.6)
20     CONTINUE
C
C      Access calculated relative displacements
C      and accelerations:
       DO 40 I=1,4000
         READ (5,*) TIME(I),RELDIS(I),RELACC(I)
30       FORMAT (4X,F8.5,5X,F10.6,5X,F10.6)
40     CONTINUE
C
C      To calculate absolute nodal accelerations:
       DO 60 I=1,4000
```

```
        ABSACC(I)=RELACC(I)+GRACC(I)
60      CONTINUE
C
        WRITE (6,70)
70      FORMAT (13X,'RELAT',7X,'GROUND',7X,'ABSOL')
        WRITE (6,80)
80      FORMAT ('TIME',9X,'DISP',9X,'ACCEL',7X,'ACCEL')
        DO 100 I=1,4000
          WRITE (6,90) TIME(I),RELDIS(I),GRACC(I),
     +    ABSACC(I)
90        FORMAT (1X,F8.5,1X,F10.6,2X,F10.6,2X,F10.6)
100     CONTINUE
C
C       To find peak absolute nodal accelerations:
        MAXPOS=0.0
        MAXNEG=0.0
        TIMEPOS=0.00
        TIMENEG=0.00
C
        DO 110 I=1,4000
          IF (MAXPOS .LE. ABSACC(I)) THEN
              MAXPOS=ABSACC(I)
              TIMEPOS=TIME(I)
          END IF
          IF (MAXNEG .GE. ABSACC(I)) THEN
              MAXNEG=ABSACC(I)
              TIMENEG=TIME(I)
          END IF
110     CONTINUE
        WRITE (6,120) MAXPOS,TIMEPOS
120     FORMAT (/'MAX.POS.ABSOL.ACCELER=',F10.6,'m/s^2 AT
+    TIME=',F9.6,'s')
        WRITE (6,130) MAXNEG, TIMENEG
130     FORMAT (/'MAX.NEG.ABSOL.ACCELER=',F10.6,'m/s^2 AT
+    TIME=',F9.6,'s')
        stop
        end
```

APPENDIX E - COMPARISON OF BASE ISOLATED SYSTEMS

Table E.1 shows the ratings for cost and technical performance of different base isolation systems for El Centro.

Table E-1 Comparison of Base Isolation Systems ($\ddot{x}_{gm}$ = 0.4g).
Rating: ■ ■■ ■■■ ■■■■
----------→ Best

CRITERIA	RUBBER/ RUBBER + LEAD	FRICTION + RUBBER	FPS	FRICTION BASE ISOLATOR	
				WITH RESILI ENCE	PURE FRICT ION
Cost of isolators.	■	■	■■	■■■	■■■■
Secondary costs. (foundations, service connections, wind restraint)	■	■■	■■	■■■■	■■■■
Durability. (effects of temperature, aging)	■	■■	■■■	■■■	■■■■
Relative displacement [mm]	■ >300	■■ >200	■■ >200	■■■■ 45, μ=0.1 25, μ=.15	■■■■ 25, μ=.22
Acceleration (% of $\ddot{x}_{gm}$)	■■■■ (10%)	■■■ (20%)	■■■■ (15%)	■■ (25%) μ=0.1 (37%) μ=.15	■ (50%) μ=.22
Permanent offset [mm]	■■■■	■■	■■■	■■ 1	■ 4

This table provides a guide for system selection when cost, displacement and accelerations are to be considered. Rubber pad and other types of isolators are expensive and, for this reason, have found use mainly in important public buildings. Friction base isolators provide a good degree of protection against damage and their low cost of suggests a wide application in low-rise buildings, including residential houses.